Η αλληλεπίδραση μεταξύ των μηχανισμών της γήρανσης, της ρευματοειδούς αρθρίτιδας και των σχετιζόμενων συννοσηροτήτων

Ηράκλειο, 2019

Πανεπιστήμιο Κρήτης, Ιατρική Σχολή

The interplay between mechanisms involving Aging, Rheumatoid Arthritis and related comorbidities

Διδακτορική Διατριβή

Επιβλέπων καθηγητής:

Καθ. Χρήστος Τσατσάνης

Λυδία Ντάρη

Στοιχειά ταυτότητας της διδακτορικής διατριβής

Ημερομηνία αιτήσεως της υποψηφίας: 4/7/2014

Ημερομηνία ορισμού 3μελούς Συμβουλευτικής Επιτροπής: 15/7/2014

Ημερομηνία ορισμού του Θέματος:15/7/2014

Ημερομηνία τροποποίησης Τίτλου: 27/3/2018

Ημερομηνία κατάθεσης της διδακτορικής διατριβής: 6/11/2019

Συμβουλευτική επιτροπή

Χρήστος Τσατσάνης ***(Επιβλέπων Καθηγητής)*****,**
Καθηγητής Κλινικής Χημείας, Ιατρικής Σχολής Πανεπιστημίου Κρήτης

Γεώργιος Γαρίνης,
Καθηγητής Βιολογίας, Βιολογικής Σχολής Πανεπιστημίου Κρήτης

Πρόδρομος Σιδηρόπουλος**,**
Αναπληρωτής Καθηγητής Ρευματολογίας, Ιατρικής Σχολής Πανεπιστημίου Κρήτης

7 μελής επιτροπή (επιπλέον μέλη)

Γεώργιος Κόλλιας,
Ακαδημαϊκός Καθηγητής Πειραματικής Φυσιολογίας, Ιατρικής Σχολής Εθνικού και Καποδιστριακού Πανεπιστημίου Αθηνών

Γεώργιος Μπερτσιάς,
Επίκουρος Καθηγητής Ρευματολογίας/Κλινικής Ανοσολογίας, Ιατρικής Σχολής Πανεπιστήμιο Κρήτης

Ελένη Παπαδάκη,
Καθηγήτρια Αιματολογίας, Ιατρικής Σχολής Πανεπιστήμιο Κρήτης

Γεώργιος Κοχιαδάκης,
Καθηγητής Καρδιολογίας, Ιατρικής Σχολής Πανεπιστήμιο Κρήτης

Όρκος του Ιπποκράτη

Ὄμνυμι Ἀπόλλωνα ἰητρὸν, καὶ Ἀσκληπιὸν, καὶ Ὑγείαν, καὶ Πανάκειαν, καὶ θεοὺς πάντας τε καὶ πάσας, ἵστορας ποιεύμενος, ἐπι ωτελέα ποιήσειν κατὰ δύναμιν καὶ κρίσιν ἐμὴν ὅρκον τόνδε καὶ ξυγγραφὴν τήνδε. Ἡγήσασθαι μὲν τὸν διδάξαντά με τὴν τέχνην ταύτην ἴσα γενέτῃσιν ἐμοῖσι, καὶ βίου κοινώσασθαι, καὶ χρεῶν χρηίζοντι μετάδοσιν ποιήσασθαι, καὶ γένος τὸ ἐξ ωὐτέου ἀδελφοῖς ἴσον ἐπικρινέειν ἄῤῥεσι, καὶ διδάξειν τὴν τέχνην ταύτην, ἢν χρηίζωσι μανθάνειν, ἄνευ μισθοῦ καὶ ξυγγραφῆς, παραγγελίης τε καὶ ἀκροήσιος καὶ τῆς λοιπῆς ἁπάσης μαθήσιος μετάδοσιν ποιήσασθαι υἱοῖσί τε ἐμοῖσι, καὶ τοῖσι τοῦ ἐμὲ διδάξαντος, καὶ μαθηταῖσι συγγεγραμμένοισί τε καὶ ὡρκισμένοις νόμῳ ἰητρικῷ, ἄλλῳ δὲ οὐδενί. Διαιτήμασί τε χρήσομαι ἐπ' ὠφελείῃ καμνόντων κατὰ δύναμιν καὶ κρίσιν ἐμὴν, ἐπὶ δηλήσει δὲ καὶ ἀδικίῃ εἴρξειν. Οὐ δώσω δὲ οὐδὲ φάρμακον οὐδενὶ αἰτηθεὶς θανάσιμον, οὐδὲ ὑφηγήσομαι ξυμβουλίην τοιήνδε. Ὁμοίως δὲ οὐδὲ γυναικὶ πεσσὸν φθόριον δώσω. Ἁγνῶς δὲ καὶ ὁσίως διατηρήσω βίον τὸν ἐμὸν καὶ τέχνην τὴν ἐμήν. Οὐ τεμέω δὲ οὐδὲ μὴν λιθιῶντας, ἐκχωρήσω δὲ ἐργάτῃσιν ἀνδράσι πρήξιος τῆσδε. Ἐς οἰκίας δὲ ὁκόσας ἂν ἐσίω, ἐσελεύσομαι ἐπ' ὠφελείῃ καμνόντων, ἐκτὸς ἐὼν πάσης ἀδικίης ἑκουσίης καὶ φθορίης, τῆς τε ἄλλης καὶ ἀφροδισίων ἔργων ἐπί τε γυναικείων σωμάτων καὶ ἀνδρῴων, ἐλευθέρων τε καὶ δούλων. Ἃ δ' ἂν ἐν θεραπείῃ ἢ ἴδω, ἢ ἀκούσω, ἢ καὶ ἄνευ θεραπηίης κατὰ βίον ἀνθρώπων, ἃ μὴ χρή ποτε ἐκλαλέεσθαι ἔξω, σιγήσομαι, ἄῤῥητα ἡγεύμενος εἶναι τὰ τοιαῦτα. Ὅρκον μὲν οὖν μοι τόνδε ἐπιτελέα ποιέοντι, καὶ μὴ ξυγχέοντι, εἴη ἐπαύρασθαι καὶ βίου καὶ τέχνης δοξαζομένῳ παρὰ πᾶσιν ἀνθρώποις ἐς τὸν αἰεὶ χρόνον. παραβαίνοντι δὲ καὶ ἐπιορκοῦντι, τἀναντία τουτέων.

This research has been conducted in two collaborating research laboratories. The first is the *Research and Development* department of Biomedcode Hellas SA, which is located in the Biomedical Sciences Research Center (BSRC), “Alexander Fleming”, campus in Vari, Athens. This work was supported by the European Union within the 7th framework program (GA 31354 (CodeAge) FP7 PEOPLE-2011-ITN). The research was then continued in the laboratory of Prof. George Kollias in the Institute of Immunology, Biomedical Sciences Research Center (BSRC), “Alexander Fleming”, Vari, and it was supported by the IMI project BTCure (GA no. 115142-2), the Advanced ERC grant MCs-inTEST (340217), and a “Research Project for Excellence IKY/Siemens” to George Kollias. In addition, InfrafrontierGR Infrastructure (co-funded by the ERDF and Greek NSRF 2007-2013) supported the mouse hosting and the phenotyping facilities, including histopathology, flow cytometry and advanced microscopy.

Ευχαριστίες

Η παρούσα έρευνα εκπονήθηκε κυρίως στην Biomedcode Hellas ΑΕ, καθώς και στο εργαστήριο του Καθηγητή κ. Γεωργίου Κόλλια στο Ερευνητικό Κέντρο ΕΚ.Ε.ΒΕ «Αλέξανδρος Φλέμινγκ», υπό την επίβλεψη του ιδίου και του Καθηγητή κ. Χρήστου Τσατσάνη, καθώς και των Δρ. Νίκη Καραγιάννη και Δρ. Μαρία Δένη.

Θα ήθελα αρχικά να ευχαριστήσω θερμά τον καθηγητή κ. Γεώργιο Κόλλια για την συνεχή υποστήριξη, έμπνευση και καθοδήγηση, αλλά και να εκφράσω την ευγνωμοσύνη μου για την εμπιστοσύνη που μου έδειξε όλα αυτά τα χρόνια. Ευχαριστώ θερμά τον επιβλέποντα καθηγητή κ. Χρήστο Τσατσάνη για τη συνεχή καθοδήγηση και έμπρακτη βοήθεια και υποστήριξη του, όπως και τον Καθηγητή κ. Ιορδάνη Μουρούζη για την καταλυτική του βοήθεια και την όμορφη συνεργασία. Θα ήθελα επίσης να ευχαριστήσω τους καθηγητές της τριμελούς επιτροπής κ. Γεώργιο Γαρίνη και κ. Πρόδρομο Σιδηρόπουλο για τη βοήθεια τους, όπως και τα μέλη της επταμελούς επιτροπής, τους καθηγητές κ. Γεώργιο Μπερτσιά, κ. Ελένη Παπαδάκη και κ. Γεώργιο Κοχιαδάκη.

Ιδιαίτερα θα ήθελα να ευχαριστήσω τις Νίκη Καραγιάννη και Μαρία Δένη για τη συνεχή επίβλεψη και καθοριστική καθοδήγησή τους, την πρακτική αλλά και ηθική υποστήριξή τους στις δύσκολες στιγμές όλων αυτών των χρόνων, τις ανεκτίμητες συμβουλές και την υπομονή τους. Επίσης, ευχαριστώ ολόψυχα τα μέλη των δύο αυτών εργαστηρίων τα οποία, εκτός από την άψογη συνεργασία τους, τη βοήθειά τους και το ευχάριστο κλίμα, με τίμησαν με την αγάπη και τη φιλία τους.

Κλείνοντας, θα ήθελα να ευχαριστήσω την οικογένεια μου και ιδιαίτερα τη μητέρα μου και τη γιαγιά μου για την αμέριστη υποστήριξή τους, καθώς και τους δικούς μου ανθρώπους και ιδιαίτερα την καλύτερή μου φίλη για τη συμπαράσταση, ανοχή και υπομονή τους κατά τη διάρκεια αυτών των χρόνων.

List of contents

Όρκος του Ιπποκράτη 2

Ευχαριστίες 4

Table of figures 8

Table of tables 10

Abbreviations 11

Summary 16

Περίληψη 18

Significance statement 20

Introduction 21

1. Rheumatoid Arthritis 21

1.1. The aetiopathogenesis of RA 21

1.2. The pathophysiology of RA 23

1.2.1. The role of Tumor Necrosis Factor (TNF) 24

1.2.2. The role of mesenchymal cells -Synovial Fibroblasts (SFs) 30

1.3. Animal mouse models 33

1.3.1 Tg-huTNF model of RA (Tg197) 37

1.3.2. Col6a1-Cre (ColVI-Cre) mouse 38

1.4. Extraarticular RA-related manifestations/ comorbidities 39

1.4.1. RA-related heart diseases 40

1.4.2. The role of TNF in heart diseases 44

1.4.3. The role of mesenchymal cells- Valve Interstitial cells (VICs)- in heart diseases 46

2. Aging 49

2.1. The aetiopathogenesis of aging 49

2.2. DNA Damage Response (DDR) 53

2.2.1. Nucleotide Excision Repair (NER) 55

2.3. Animal mouse models of aging 60

2.3.1. Excision Repair Cross Complementation Group 1 (ERCC1) deficiency 62
3. RA and aging 66
3.1. TNF and aging 66
3.2. Premature aging in RA 67
3.3. Aging in mesenchymal cells 67
Aims 68
Materials and methods 69
Mice 69
Clinical and histopathological arthritic assessment 69
Collagen Antibody Induced Arthritis 70
Antibodies 70
Immunohistochemistry and immunofluorescence 70
Genotyping PCR 71
Quantification of valvular thickness 72
Echocardiography and Electrocardiography 72
Isolation and culturing of SFs and VICs 72
Fluorescence activated cell sorting (FACS) 73
Proliferation assay 73
ELISA 73
Wound-healing assay 73
3' RNAseq and deep sequencing 74
RNA seq analysis 74
Statistical analysis 75
Results: Part I 76
Systemic *Ercc1* deficiency does not spontaneously induce RA-like symptoms in *Ercc1*$^{\Delta/-}$ mice 76
Systemic *Ercc1* deficiency does not affect RA-like symptoms in Tg197 mice 78

Mesenchymal-specific *Ercc1* deficiency causes slight cachexia, without inducing RA-like symptoms 80

Mesenchymal-specific *Ercc1* deficiency ameliorates arthritis symptoms in CAIA-induced arthritis 82

Mesenchymal-specific *Ercc1* deficiency does not affect RA-like symptoms in Tg197 mice 82

Discussion: Part I 84

Results: Part II 86

TNF-dependent left-sided heart valve pathology develops as a comorbid condition in the Tg197 arthritis model 86

Heart valve pathology leads to left ventricular dysfunction in the Tg197 animals . 88

Hypertrophic valves of Tg197 mice consist mainly of activated Valve Interstitial Cells (VICs) 94

TNFR1 signaling in mesenchymal cells is necessary and sufficient for the development of Tg197 heart valve pathology 96

Ex vivo-derived Tg197 VICs exhibit an activated phenotype 98

Tg197 VICs express common pathogenic signatures with Tg197 SFs 100

Discussion: Part II 105

Results: Part III 109

Systemic, but not mesenchymal-specific, *Ercc1* deficiency ameliorates heart valve pathology of Tg197 109

Discussion: Part III 110

Conclusion and future perspectives 112

References 114

Appendix (Publication) 127

Table of figures

Figure 1. Pathophysiology of RA.. 23
Figure 2. Signaling modalities and bioactivities downstream of TNF receptors. 27
Figure 3. The role of TNF-α in the pathogenesis of joint damage in Rheumatoid Arthritis. 29
Figure 4. The role of FLS in RA. 31
Figure 5. Prevalence of evaluated comorbidities in RA patients 39
Figure 6. The role of TNF-α in the pathogenesis of comorbidities in Rheumatoid Arthritis 44
Figure 7. Schematic depiction of the role of VICs in valvular pathology. 48
Figure 8. The Hallmarks of Aging. 50
Figure 9. Main DNA lesions and corresponding DNA damage repair pathways. 54
Figure 10. **Nucleotide excision repair.** 56
Figure 11. **Systemic *Ercc1* deficiency does not spontaneously induce RA-like symptoms.** 77
Figure 12. **Systemic *Ercc1* deficiency does not affect RA-like symptoms in Tg197 mice.** 79
Figure 13. **Mesenchymal-specific *Ercc1* deficiency causes cachexia and amelioration of CAIA arthritis.** 81
Figure 14**. Mesenchymal-specific *Ercc1* deficiency does not affect RA-like symptoms in Tg197 mice.** 83
Figure 15**. Tg197 arthritis model develops TNF-dependent left-sided heart valve disease which leads to LV dysfunction**. 87
Figure 16. **Peripheral vessel wall of the arteries appears unaffected in Tg197 animals.** 90
Figure 17. Tg197 heart valve pathology progresses with time. 91
Figure 18. **Inflammation has a minimal contribution to the heart valve disease phenotype of Tg197 mice.** 91
Figure 19. **Treatment of Tg197 animals with the anti-TNF Infliximab (Remicade) results in the amelioration of the heart valve pathology.** 92
Figure 20. **Valvular regurgitation detected in Tg197 animals by echocardiographic screening.** 93

Figure 21. **Kaplan Meier survival curve of WT and Tg197 mice.** 93
Figure 22. **Heart valve disease of Tg197 mice is caused by accumulation of activated mesenchymal Valve Interstitial Cells (VICs).**..... 95
Figure 23. **TNF signaling on VICs is required and sufficient for the development of heart valve disease of Tg197 animals.** 97
Figure 24. **Activated phenotype of Tg197-derived VICs *ex vivo*.** 99
Figure 25. **Tg197 VICs exhibit common pathogenic molecular signatures with Tg197 SFs at 8 weeks of age.** 101
Figure 26. **Further functional enrichment analysis of the overlapping upregulated/downregulated genes in Tg197 VICs and SFs isolated at 8 weeks of age.** 103
Figure 27. **TgA86 SpA model develops TNF-dependent left-sided heart valve pathology.**..... 108
Figure 28. Systemic, but not mesenchymal-specific, Ercc1 deficiency ameliorates heart valve pathology of Tg197. 109

Table of tables

Table 1. Action of TNF on various cells in Rheumatoid Arthritis. 28
Table 2. Characteristics of selected induced models of RA. 35
Table 3. Characteristics of selected spontaneous mouse models of RA. 36
Table 4. Key comorbidities in Rheumatoid Arthritis 40
Table 5. Parameters evaluated in echocardiography assessment 43
Table 6. Classification of VIC markers and functions into five phenotypes. 47
Table 7. Clinical and cellular features of nucleotide excision repair disorders 58
Table 8. Principal features of Cockayne syndrome and related NER-deficient mice 61
Table 9. Table listing the symptoms of aging-related phenotypes observed in Ercc1$^{-/-}$ mice at 4 weeks of age, Ercc1$^{\Delta/-}$ mice at 28 weeks of age and normal human aging at >120 years old. 63
Table 10. Primer sequences for genotyping of the mouse lines used 71
***Table 11.* Echocardiographic parameters in Tg197 and WT mice at 12 weeks of age.** 89

Abbreviations

Abbreviation	*Meaning*
ACPAs	Anti-Citrullinated Protein Antibodies
ADAM	A disintegrin and metalloproteinase
ADAMTs	A disintegrin and metalloproteinase with thrombospondin motifs
AGT	O6-Alkylgouanine-DNA alkyltransferase
ALP	Alkaline Phosphatase
AMP	Adenosine Monophosphate
AMP	AMP-activated kinase
Ao	Aorta
AoV	Aortic Valve
AP-1	Activator-protein 1
ATM	Ataxia Telangiectasia Mutated
ATP	Adenosine Triphosphate
AV	Aortic Velocity
AV	Aortic Valve
aVICs	Activated Valve Interstitial Cells
AVR	Aortic Valve Root
BER	Base Excision Repair
BMP	Bone Morphogenic Protein
BrdU	Bromodeoxyuridine
BW	Body Weight
CAIA	Collagen Antibody-Induced Arthritis
CAVD	Calcific Aortic Valve Disease
CCL	Chemokine (C-C motif) ligand
CCP	Cyclin Citrullinated Peptide
CIA	Collagen-Induced Arthritis
CO	Cardiac Output
COFs	Cerebro-oculo-facio-skeletal syndrome
CRP	C-Reactive Protein
CS	Cockayne Syndrome
CVD	Cardiovascular Disease
CXCL	Chemokine (C-X-C motif) ligand

DAB	3,3′-Diaminobenzidine
DAMPs	Damage-associated Molecular Patterns
DDB	Damage-Binding Protein
DDR	DNA Damage Response
DEGs	Deregulated Expressed Genes
DMARDs	Disease-Modifying Anti-Rheumatic Drugs
DNA	Deoxyribonucleic acid
DR	Direct Repair
DSBs	Double Strand Break Repair
DVD	Cardiovascular Disease
ECG	Electrocardiogram
ECM	Extracellular matrix
EF	Ejection Fraction
ELISA	Enzyme-linked Immunosorbent Assay
EndMT	Endothelial-to-mesenchymal Transformation
Ercc1	Excision repair cross-complementation group 1
FACS	Fluorescence-activated cell sorter
FADD	Fas-associated protein death domain
FBS	Fetal Bovine Serum
FGF	Fibroblast Growth Factor
FLS	Fibroblast-like Synoviocytes
FS	Fractional Shortening
G6PI	Glucose-6-phoshate isomerase
GFP	Green Fluorescent Protein
GG-NER	Global Genome NER
GWAS	Genome-wide associated studies
H/E	Haematoxylin /Eosin
HF	Heart Failure
HLA	Human Leukocyte Antigen
HR	Heart Rate
HR	Homologous Recombination
huTNF/hTNF	Human TNF
HVD	Heart Valve Disease
HW	Heart weight
IBD	Inflammatory Bowel Disease

ICAM	Intercellular Adhesion Molecule 1
ICLs	Interstrand Crosslinks
IFN	Interferon
IKK	Inhibitor of nuclear factor kappa-B kinase
IL	Interleukins
IL1Ra	IL1 Receptor antagonist
IMCs	Intestinal Mesenchymal Cells
IVSd	End-diastolic interventricular septal thickness
JNK	Jun N-terminal kinase
kDa	Kilo-Daltons
KEGG	Kioto Encyclopedia of Genes and Genomes
KI	Knock In
KO	Knock Out
LA	Left Atrium
LPS	Lipopolysaccharide
LV	Left Ventricle
LVEDd	Left Ventricular end-diastolic diameter
LVEDs	Left Ventricular end-systolic diameter
LVEDV	Left Ventricle end diastolic volume
LVESV	Left Ventricle end systolic volume
LVLd	Left Ventricular length in diastole
LVPWd	Left Ventricular end-diastolic posterior wall thickness
MAPK	Mitogen-activated protein kinases
MCP1	Monocyte Chemoattractant Protein
MHC	Major Histocompatibility Complex
MLKL	Mixed lineage kinase domain-like protein
MMP	Metalloproteinase
mRNA	Messenger RNA
mTNF	Mouse TNF
MV	Mitral Valve
NER	Nucleotide Excision Repair
NF-κB	Nuclear Factor Kappa-light-chain-enhancer of activated B cells
NHEJ	Non-Homologous End Joining
obVICs	Osteoblastic Valve Interstitial Cells
OCT	Optimal cutting temperature

OD	Optical Density
PBS	Phosphate-buffered Solution
PCNA	Proliferating Cell Nuclear Antigen
PCR	Polymerase Chain Reaction
PDGF	Platelet-derived Growth Factor
PV	Pulmonary Valve
pVICs	Progenitor Valve Interstitial Cells
qVICs	Quiescent Valve Interstitial Cells
RA	Rheumatoid Arthritis
RANKL	Receptor Activator of Nuclear Factor-κB Ligand
RANTES	Regulated on Activation, Normal T Cell Expressed and Secreted
RASFs	Rheumatoid Arthritis Synovial Fibroblasts
RF	Rheumatoid Factor
RIP1	Receptor interacting protein 1
RNA	Ribonucleic acid
RNA-seq	RNA sequencing
ROS	Reactive Oxygen Species
RV	Right Ventricle
SASP	Senescence-associated secretory phenotype
SCID	Severe Combined Immunodeficiency
SEM	Standard error of the mean
SF	Synovial fibroblast
SNP	Single Nucleotide Polymorphism
SpA	Spondyloarthritis
SSBR	Single Strand Break Repair
SV	Stroke Volume
SVPW	Systolic Velocity of the posterior wall
TACE	TNF-α converting enzyme
TC-NER	Transcription Coupled NER
TFIIH	Transcription Factor II Human
Tg	Transgenic
TGF-β	Transforming Growth Factor beta
TLR	Toll-like Receptor
TNF	Tumor Necrosis Factor
TNFR1	TNF Receptor 1

TRADD	TNFR1-associated death domain
TRAF	TNFR1-associated factor
TTD	Trichothiodystrophy
TTP	Tristetraprolin
UV	Ultraviolet
VCAM	Vascular cell adhesion protein 1
VE	Vascular Endothelial
VEC	Valve Endothelial Cell
VEGF	Vascular Endothelial Growth Factor
VIC	Valve Interstitial Cell
WT	Wild type
XP	Xeroderma Pigmentosum
α-SMA	Alpha smooth muscle antibodies

Summary

Patients with rheumatoid arthritis and spondyloarthritis show higher mortality rates, mainly caused by cardiac comorbidities and premature aging of their immune system. The TghuTNF (Tg197) arthritis model develops tumor necrosis factor (TNF)-driven and mesenchymal synovial fibroblast (SF)-dependent polyarthritis. Here, we investigate whether this model develops, similarly to human patients, comorbid heart pathology and we explore the cellular and molecular mechanisms linking arthritis to cardiac comorbidities. We also investigate whether these pathologies are affected by premature aging which is caused by accumulation of DNA damage in the synovium and in the heart valve.

For these reasons, we used the TghuTNF (Tg197) arthritis model, which overexpresses huTNF and develops chronic polyarthritis, as well as systemic or tissue-specific *Ercc1* KO mice, which lack *Ercc1* protein and develop a premature aging phenotype. Furthermore, synovial fibroblasts (SFs) and Valve interstitial cells (VICs) were targeted by mice carrying the *ColVI-Cre* transgene. Clinical and histopathological evaluation of arthritis features were performed in the above animals and echocardiographic evaluation of cardiac function was performed in the Tg197 model. *In vitro* analysis of cultured SFs and VICs was also performed to investigate possible similarities of these two mesenchymal cellular populations. *Tnfr1*$^{fl/fl}$ and *Tnfr1*$^{cneo/cneo}$ mutant mice were used to explore the role of mesenchymal TNF signaling in the development of heart valve disease. Pathogenic VICs and SFs were further analysed by comparative RNA-sequencing analysis.

The pathology of Tg197 was not affected by either systemic loss of *Ercc1* or mesenchymal-specific ablation of the protein. Similarly, the arthritogenic phenotype of SFs derived from these mice was not affected by the premature aging phenotype. Interestingly, mesenchymal-specific *Ercc1* deletion caused muscle atrophy leading to reduced body weight of *ColVI-Cre Ercc1f*$^{/-}$ mice compared to their littermates. It also ameliorated induced arthritis.

Furthermore, Tg197 mice were found to develop left-sided heart valve disease, characterised by valvular fibrosis with minimal signs of inflammation. Thickened valve areas consisted almost entirely of hyperproliferative *ColVI*-expressing mesenchymal VICs. Development of pathology resulted in valve stenosis and left ventricular dysfunction, accompanied by arrhythmic episodes and, occasionally, valvular

insufficiency. TNF dependency of the pathology was indicated by disease modulation following pharmacological inhibition or mesenchymal-specific genetic ablation or activation of TNF/TNFR1 signaling. Tg197-derived VICs exhibited an activated phenotype ex vivo, reminiscent of the activated pathogenic phenotype of Tg197-derived SFs. Significant functional similarities between SFs and VICs were revealed by RNA-seq analysis, demonstrating common cellular mechanisms underlying TNF-mediated arthritides and cardiac comorbidities. Interestingly, heart-valve pathology of Tg197 mice was completely abolished by systemic *Ercc1* ablation, but not by mesenchymal-specific *Ercc1* deletion. This has to be due to additional mechanisms which are beyond the scope of this study.

In conclusion, comorbid heart valve disease and chronic polyarthritis are efficiently modelled in the Tg197 arthritis model and share common TNF/TNFR1-mediated, mesenchymal cell-specific aetiopathogenic mechanisms. Chronic polyarthritis was not affected by premature aging phenotype, suggesting that the mechanisms driving the pathology of Tg197 act independently of the DNA damage caused by *Ercc1* deletion.

Περίληψη

Οι ασθενείς με ρευματοειδή αρθρίτιδα και σπονδυλοαρθρίτιδα παρουσιάζουν υψηλότερα ποσοστά θνησιμότητας, που προκαλούνται κυρίως από καρδιακές συννοσηρότητες και πρόωρη γήρανση του ανοσοποιητικού τους συστήματος. Το μοντέλο αρθρίτιδας TghuTNF (Tg197) αναπτύσσει πολυαρθρίτιδα εξαρτώμενη από τον παράγοντα νέκρωσης όγκου (TNF) και από τους μεσεγχυματικούς ινοβλάστες (SF). Στην παρούσα μελέτη, εξετάζεται εάν σε αυτό το μοντέλο αναπτύσσεται, όπως και στους ανθρώπους, συνυπάρχουσα καρδιακή νόσος και διερευνώνται κυτταρικοί και μοριακοί μηχανισμοί που συνδέουν την αρθρίτιδα με τις καρδιακές συννοσηρότητες. Εξετάζεται, επίσης, εάν αυτές οι παθήσεις επηρεάζονται από την πρόωρη γήρανση, λόγω συσσώρευσης βλαβών στο DNA του αρθρικού υμένα και της καρδιακής βαλβίδας.

Για αυτούς τους σκοπούς χρησιμοποιήθηκε το ανθρωποποιημένο μοντέλο αρθρίτιδας TghuTNF (Tg197) ποντίκι, το οποίο υπερεκφράζει τον huTNF και αναπτύσσει χρόνια πολυαρθρίτιδα, όπως και ποντικοί με ολική ή ιστοειδική αποσιώπηση της πρωτεΐνης *Ercc1*, τα οποία αναπτύσσουν φαινότυπο πρόωρης γήρανσης. Για τη στόχευση των αρθρικών ινοβλαστών (SFs) και των κύτταρων της βαλβίδας (VICs) χρησιμοποιήθηκαν ποντικοί που έφεραν το *ColVI-Cre* διαγονίδιο. Τα παραπάνω ζώα αξιολογήθηκαν κλινικά και ιστοπαθολογικά ως προς τα χαρακτηριστικά της αρθρίτιδας, ενώ στο μοντέλο Tg197 ελέγχθηκε η καρδιακή λειτουργία μέσω ηχοκαρδιογραφικής αξιολόγησης. Επιπροσθέτως, διεξήχθη *in vitro* ανάλυση των κυττάρων SFs και VICs με σκοπό τη διερεύνηση πιθανών ομοιοτήτων των δύο αυτών μεσεγχυματικών κυτταρικών πληθυσμών. Οι διαγονιδιακοί ποντικοί *Tnfr1*$^{fl/fl}$ και *Tnfr1*$^{cneo/cneo}$ χρησιμοποιήθηκαν για να διερευνηθεί ο σηματοδοτικός ρόλος του μεσεγχυματικού TNF στην ανάπτυξη της καρδιακής βαλβιδοπάθειας. Τα παθογόνα κύτταρα VICs και SFs αναλύθηκαν περαιτέρω με ανάλυση αλληλουχίας RNA.

Σύμφωνα με τα ευρήματα της μελέτης, η συστημική ή ιστοειδική (στα μεσεγχυματικά κύτταρα) απαλοιφή της πρωτεΐνης *Ercc1*, δεν επηρέασε την παθολογία των Tg197 ποντικών . Ομοίως, ο αρθριτογόνος φαινότυπος των SFs που προέρχονται από αυτά τα ποντίκια δεν επηρεάστηκε από το φαινότυπο της πρόωρης γήρανσης. Είναι ενδιαφέρον το γεγονός ότι η εξάλειψη της *Ercc1* από τα μεσεγχυματικά κύτταρα βελτίωσε την επαγόμενη αρθρίτιδα, ενώ ταυτόχρονα προκάλεσε μυϊκή ατροφία

οδηγώντας σε μειωμένο σωματικό βάρος των ποντικών *ColVI-Cre Ercc1*$^{fl/-}$ σε σύγκριση με τους ποντικούς μάρτυρες.

Επιπλέον, οι ποντικοί Tg197 ανέπτυξαν ασθένεια καρδιακής βαλβίδας αριστερής πλευράς, που χαρακτηρίζεται από βαλβιδική ίνωση με ελάχιστα σημάδια φλεγμονής. Οι περιοχές των βαλβίδων που έχουν υποστεί βλάβη συνίστανται σχεδόν εξ' ολοκλήρου από υπερ-πολλαπλασιαστικά μεσεγχυματικά VICs που εκφράζουν το διαγονίδιο *ColVI-Cre*. Η ανάπτυξη της παθολογίας έχει σαν αποτέλεσμα τη στένωση βαλβίδας και τη δυσλειτουργία της αριστερής κοιλίας, συνοδευόμενη από αρρυθμικά επεισόδια και, περιστασιακά, βαλβιδική ανεπάρκεια. Η φαρμακολογική αναστολή του TNF, όπως και η μεσεγχυματική γενετική απαλοιφή του σηματοδοτικού του μονοπατιού μέσω του υποδοχέα του, TNFR1, οδηγούν σε βελτίωση της νόσου, γεγονός που υποδεικνύει την άμεση σχέση της παθολογίας αυτής με τον TNF. Τα VICs που προέρχονται από τα Tg197 ποντίκια εμφάνισαν ενεργοποιημένο φαινότυπο ex νίνο, που θυμίζει τον ενεργοποιημένο παθογόνο φαινότυπο των SFs που προέρχονται από τα ίδια ποντίκια. Σημαντικές λειτουργικές ομοιότητες μεταξύ των SFs και των VICs προέκυψαν μετά από ανάλυση RNA-seq, αποδεικνύοντας κοινούς κυτταρικούς μηχανισμούς που ελέγχουν την αρθρίτιδα, όπως και τις καρδιακές συννοσηρότητες με τη μεσολάβηση του TNF.

Ενδιαφέρον παρουσιάζει το γεγονός ότι η παθολογία των καρδιακών βαλβίδων των ποντικών Tg197 βελτιώθηκε πλήρως μέσω της συστημικής απαλοιφής της πρωτεΐνης *Ercc1*, αλλά δεν επηρεάστηκε από την ιστοειδική απαλοιφή της στα μεσεγχυματικά κύτταρα. Αυτό οφείλεται σε επιπρόσθετους μηχανισμούς που δεν εμπίπτουν στο πεδίο εφαρμογής της παρούσας μελέτης.

Συμπερασματικά, προκύπτει ότι η συνυπάρχουσα ασθένεια της καρδιακής βαλβίδας και η χρόνια πολυαρθρίτιδα μοντελοποιούνται αποτελεσματικά στο μοντέλο αρθρίτιδας Tg197. Επίσης, μοιράζονται κοινούς αιτιοπαθογόνους μηχανισμούς που σχετίζονται με τους μεσεγχυματικούς κυτταρικούς πληθυσμούς των συγκεκριμένων οργάνων και τα μοριακά μονοπάτια που ενεργοποιούνται διαμέσου του TNF και του υποδοχέα του (TNFR1). Τέλος, η χρόνια πολυαρθρίτιδα δεν επηρεάστηκε από τον πρόωρο φαινότυπο γήρανσης, υποδηλώνοντας ότι η παθολογία του Tg197 δρα ανεξάρτητα από τις βλάβες του DNA που προκαλούνται από τη διαγραφή της πρωτεΐνης *Ercc1*.

Significance statement

Cardiovascular conditions, such as heart valve disease, present as the most prevalent comorbidities in patients with Rheumatoid arthritis (RA) and Spondyloarthritis (SpA) and their common mechanistic basis is not well understood. Here, we provide novel evidence that TNF signaling in the mesenchymal valve interstitial cells (VICs) drives RA-related comorbid cardiac pathology, eventually leading to fatal left ventricular dysfunction. Considering previous evidence, demonstrating that TNF-targeted mesenchymal synovial fibroblasts are sufficient drivers of the arthritogenic process in the Tg197 model, we propose that joint diseases and valvular comorbidities in human patients may be explained by common mechanisms associated with TNF signaling in mesenchymal cells. Interestingly, ex vivo cellular assays and gene expression analyses of Tg197-derived SFs and VICs, showed that both cell types share common pathogenic molecular and functional profiles, which could be of value for the design of future commonly targeted therapeutic strategies.

We also show that TghuTNF arthritis is not affected by premature aging. However, the induction of another type of arthritis, with greater involvement of the immune compartment, was ameliorated due to accumulation of DNA damage specifically in mesenchymal SFs. This result could contribute to our understanding of the interplay between aged stromal cells and immune compartment under inflammatory conditions. Additionally, we found that mesenchymal-specific DNA damage in muscles led to muscle atrophy and reduced body weight. Therefore, we suggest that this mouse, if further studied, could be potentially used as a model of muscular aging.

Introduction

1. Rheumatoid Arthritis

Rheumatoid arthritis (RA) is a chronic inflammatory disease primarily associated with articular inflammation and synovial hyperplasia, eventually leading to bone destruction and cartilage damage. RA affects approximately 1% of the general population, with women to show two to three-fold higher predisposition compared to men (1). Although the main cause of the disease is yet unknown, the evolution of the field during the last two decades has greatly improved our understanding of RA risk factors and pathophysiology (2).

1.1. The aetiopathogenesis of RA

There are several risk factors that pose a predisposition for the development of RA, which include genetics, environmental factors, gender and microbes. These aetiopathogenic determinants act synergistically to contribute to the development of such a multifaceted disease.

There are several **genetic** loci that show significant involvement in the susceptibility to RA, with most of relevant Single Nucleotide Polymorphisms (SNPs) being associated with immune and inflammatory pathways (3). The most significant genetic risk factor for RA is variations of the human leukocyte antigen (HLA; mostly known as major histocompatibility complex-MHC) loci that encodes for MHC molecules (4), which cause immune deregulation. More specifically, genome-wide association studies (GWAS) have identified that variations of *HLA-DRB1* loci are the most significantly RA-associated loci (5). **Epigenetic** mechanisms, such as DNA methylation and histone acetylation in the MHC region have also been found to be potential mediators of RA genetic risk (6). These post-translational modifications are induced by **environmental factors**, which raise the risk for RA. For example, smoking is associated with high levels of pro-inflammatory cytokines and is one of the most essential environmental risk factor for RA development (7). Environmental factors and a specific lifestyle can also cause **altered microbiome,** which is another RA risk factor (8). Oral dysbiosis characterized by the existence of pathogenic

microbes such as *Porphyromonas gingivalis* and *Aggregatibacter actinomycetemcomitans,* that are associated with the pathogenesis of periodontitis, raises RA risk (9,10). Moreover, RA patients have often intestinal dysbiosis, where high levels of pathogens, such as *Clostridrium* and *Escherichia coli*, are found in their gut (11).

1.2. The pathophysiology of RA

Although RA etiology is still unclear, there has been a great advance in understanding disease pathogenesis. As mentioned above, RA starts with a high-risk genetic background that, in combination with an epigenetic mark, leads to a cascade of events inducing dysregulated cytokine networks and thus synovitis, chondrocyte and osteoclast activation which ultimately lead to chronic destructive arthritis (12). The hypertrophic inflamed synovium is the main target of the dysregulated immune pathways in RA. RA synovial tissue is characterized by hyperplasia of the synovium lining layer, mainly composed of hyperproliferative stromal cells [**Fibroblast-like Synoviocytes (FLS)** (discussed below)] and accumulating inflammatory cells, such as T and B lymphocytes, plasma cells, macrophages, neutrophils, antigen-presenting dendritic cells, macrophages, $CD38^+$ mast cells and natural killer cells (13), as shown in Figure 1. The recruitment of the $CD3^+$,4^+ and $CD8^+$ T cells to the affected joint is facilitated by the neoangiogenesis occurring in the inflamed joint (2). B and T cells have been observed to form aggregates, which potentially produce Rheumatoid Factor (RF) and Anti-Citrullinated Protein Antibodies (ACPAs) that are widely used as RA biomarkers (14).

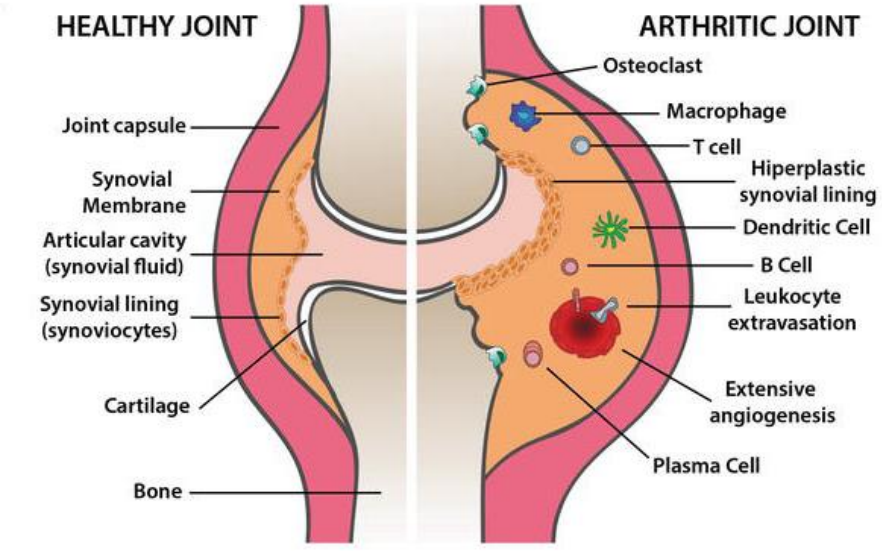

Figure 1. **Pathophysiology of RA.** In a healthy synovial joint (left), a thin layer of SFs restricts the joint capsule. By contrast, in RA (right), SFs form an invasive synovial lining and leukocytes, such as T and B cells, macrophages, dendritic cells and plasma cells infiltrate the synovial membrane. “Pannus” is developed with the

help of neoangiogenesis, and osteoclasts drive later the bone destruction (modified by 15).

Various studies have suggested the pivotal role of cytokines and chemokines in both the homeostasis of the synovium, but also in the development of RA, as they can possess anti- and pro-inflammatory properties. Pro-inflammatory cytokines/chemokines are highly expressed in the inflamed synovium by various cell types, such as lymphocytes, stromal cells, macrophages and neutrophils (16). **Tumor Necrosis Factor** (**TNF**-discussed below), IL6, IL1α and β, IL17, CXCL8, CXCL1, IFNs and MCP1/CCL2 are some of the most important cytokines/chemokines affecting hallmarks of RA pathology, such as cellular activation, adhesion, migration, neoangiogenesis, cell-extracellular matrix interactions, cytoskeleton reorganization and additional inflammatory properties which lead to the progressive cartilage and bone destruction (17,18). Clinical studies of drugs successfully ameliorating RA pathology by targeting some of these molecules in patients have validated their causal role in the disease (2).

Once inflamed synovium invades into adjacent articular structures, namely cartilage and bone, there are several pathways activated driving progressive cartilage destruction and bone erosion, mainly by the release of the aforementioned cytokines, as well as Matrix Metalloproteinases (MMPs), such as collagenases (19). Cartilage destruction is mainly caused by aggressive invasion of the activated FLS (20), while bone erosion occurs mainly due to maturation and activation of the bone-resorbing cells, osteoclasts. These cells are activated by the receptor activator of nuclear factor-κB ligand (RANKL), which is highly produced by the inflammatory and stromal cells of the inflamed synovium, and degrade the bone matrix by releasing proteases (21). These events result in joint dysfunction and disability in patients with RA.

1.2.1. The role of Tumor Necrosis Factor (TNF)

TNF plays a leading pathogenic role in RA pathology as supported by animal work and clinical findings which show the high efficiency of anti-TNF therapy in TNF-driven RA models and RA patients respectively (22–24). A small overview on TNF and its signaling will follow:

TNF was initially found to be produced upon immune system activation and was able to exert significant cytotoxicity on many tumor cells lines and to cause tumor necrosis

in certain animal model systems, hence its name (25). It was then found to play a significant role in cachexia and endotoxin-induced septic shock (26). Studies of the last two decades have implicated TNF signaling in various organismal and cellular responses, including lymphocyte and leukocyte activation and migration, cell proliferation, differentiation and apoptosis, inflammatory and immunoregulatory responses, antiviral responses, growth inhibition and cell death (27,28). Further biochemical and molecular analysis revealed that TNF is comprised by 233 amino acids and is synthesized as a nonglycosylated transmembrane protein of ~26 kDa, of which a soluble 17 kDa fragment is proteolytically cleaved from the plasma membrane by the metalloprotease TNF-alpha converting enzyme (TACE), which belongs to the ADAMs family of disintegrins (29). In the soluble form, TNF monomers assemble and circulate as a stable 51 kDa homotrimer, consisting of 157 amino acid (30).

The biological actions of TNF depend on the response of the target cell, which is mediated by two distinct surface receptor subtypes, **TNF-R1 (p55)** and **TNF-R2 (p75)**, with molecular weights of 55-60 kDa and 70-80 kDa respectively (31). In the vast majority of cells, TNFR1 appears to be the key mediator of TNF signaling, as it is constitutively expressed in most cell types, while TNF signaling through TNFR2 plays a role in the lymphoid tissue, as it is highly regulated and found only in specific cells, such as immune cells, but also in neurons and endothelial cells (32). One explanation of the restrictive role of TNFR2 is that it can be fully activated only be transmembrane TNF (33).

The two cell receptors have similar extracellular TNF-binding structures, but their distinct intracellular domains define the response of each cell to TNF. As shown in Figure 2, TNFR1 which is expressed by all cells including tumor and endothelial cells, is considered to have a dual role. TNFR1 can either recruit **complex I** which consists of the receptor-interacting protein (RIP1) and TNF-receptor-associated factor 2 (TRAF2) and promotes the activation of two of the main TNF effectors, activator protein-1 (AP-1) and NF-κB as well as the activation of inhibitor of nuclear factor kappa-B kinase (IKK) and mitogen-activated protein kinases (MAPKs), such as Jun N-terminal Kinase (JNK) and p38 (28). Thus, induction of signaling complex I leads to expression of NF-κB and AP1 target genes that are important in inflammation, host defense as well as cell proliferation and survival (34). TNFR1 can also promote a pro-apoptotic signaling, as it contains a protein-protein interaction domain, called death domain, which –once activated- recruits the TNFR1 **complex II** which consists

of TNFR1-associated death domain (TRADD), Fas-associated death domain (FADD) as well as its downstream caspases, such as caspase 8 and eventually leads to programmed cell death via caspase-dependent apoptosis or/and necroptosis (35–37). TNFR2 is considered anti-apoptotic, meaning TNF signaling though TNFR2 is pro-survival, and its occupancy by TNF results in direct recruitment of TRAF2, which in turn recruits TRAF1 and they eventually activate MAPKs, NF-κB as well as AKT (38). Overall, TNF receptor complexes are thought to serve a beneficial physiological role as a buffer against the potentially damaging acute effects of TNF, but may also impose a detrimental impact as a source of prolonged cytokine activation (31).

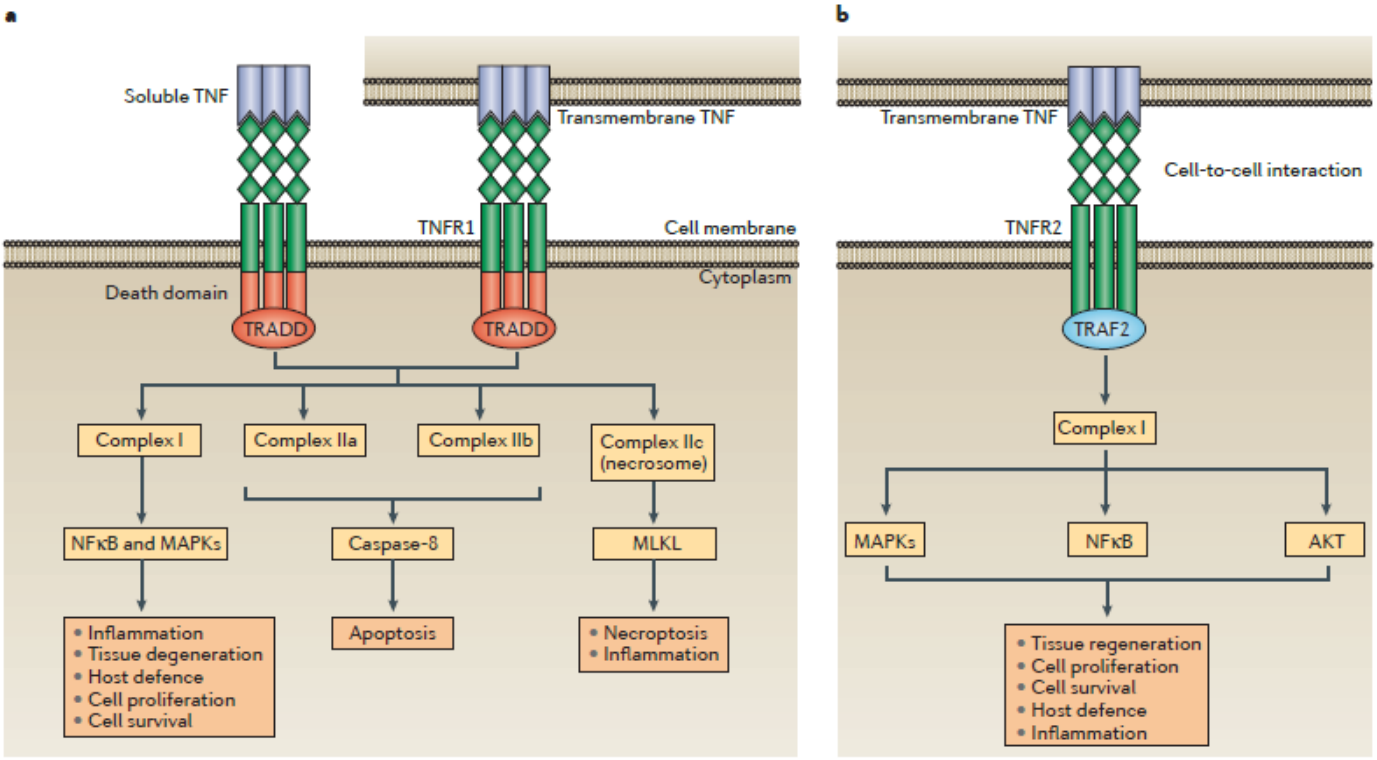

***Figure 2*. Signaling modalities and bioactivities downstream of TNF receptors**.

(a) TNF receptor 1 (TNFR1) signaling is activated by both soluble and transmembrane TNF. TNFR1 bears a death domain that recruits the adaptor protein TNFR1-associated death domain protein (TRADD). Ligation of TNFR1 by soluble TNF or transmembrane TNF leads initially to the assembly of complex I, which activates nuclear factor κB (NF-κB) and mitogen-activated protein kinases (MAPKs). TNFR1–complex I signaling induces inflammation, tissue degeneration, cell survival and proliferation and orchestrates the immune defense against pathogens. Alternative signaling modalities, associated with programmed cell death, can also be activated downstream of TNFR1. The formation of the complexes IIa and IIb (also known as ripoptosome) results in apoptosis, whereas complex IIc (necrosome) induces necroptosis and inflammation. [MLKL, mixed lineage kinase domain-like protein]

(b) TNFR2 is proposed to be fully activated primarily by transmembrane TNF, in the context of cell-to-cell interactions. TNFR2 recruits TNFR-associated factor 2 (TRAF2) via its TRAF domain, triggering the formation of complex I and the downstream activation of NF-κB, MAPKs and AKT. TNFR2 mediates primarily homeostatic bioactivities including tissue regeneration, cell proliferation and cell survival. This pathway can also initiate inflammatory effects and host defense against pathogens. (34).

The key inflammatory cascade of RA includes overproduction and overexpression of TNF which is found in high concentrations both in the synovium, as well as in the serum of RA patients (39,40). TNF is mainly produced by monocytes, macrophages, B- and T-cells as well as fibroblasts and it acts as an autocrine stimulator, as well as a potent paracrine inducer of the inflammatory cytokines, such as IL-6, IL-1 and IL-8 (41). In Table 1, the effect of TNF on various crucial cells in RA is outlined.

Cell type	TNF-α action
Macrophages	Increases proliferation, increases cytokine production
Activated T-cell	Enhances proliferation, increases interleuken (IL)-2 receptor
B-cell	Increases proliferation, increases differentiation
Synovial lining cell	Induces proliferation, induces synthesis of IL-1, granulocyte monocyte-colony stimulating factor, stromelysin, collagenase, prostaglandins
Endothelial cells	Induces expression of intracellular adhesion molecule 1, vascular cell adhesion molecule 1, endothelial leucocyte adhesion molecule-1 (ELAM-1), IL-8

***Table 1*. Action of TNF on various cells in Rheumatoid Arthritis** (41)**.**

TNF plays a significant role on all three main hallmarks of RA, that is synovial fibroblasts activation/proliferation, cartilage destruction and bone erosion. As shown in Figure 3, TNF induces the production of adhesion molecules from synovial fibroblasts in order to attract leucocytes into the affected joints, as well as MMPs that destroy cartilage (42) [Further analysis on the role of TNF in the RA-SFs is found in the next section]. Apart from the significant impact that TNF has on SFs, it also causes decrease in proteoglycan production by chondrocytes, which eventually leads to cartilage destruction. In addition, bone erosion in RA is highly driven by TNF, as TNF enhances the differentiation of osteoclast precursor cells into mature osteoclasts, overexpressing RANKL, hence leading to bone destruction (21). The essential role of TNF is also confirmed by the considerable positive impact of anti-TNF therapy on clinical symptoms of RA patients (43). More specifically, anti-TNF therapy significantly reduces neovascularization and synovial hyperplasia, as well as fibrosis and additional cytokine levels, such as IL-1β and IL-6 (44,45). Once TNF is blocked, SFs lose their activated/transformed phenotype and osteoclast maturation is also reduced. Overall, TNF plays a significant role in both the initiation and the development of RA symptoms, although the exact mechanisms of its effect on this multifaceted disease are not completely unraveled yet (46).

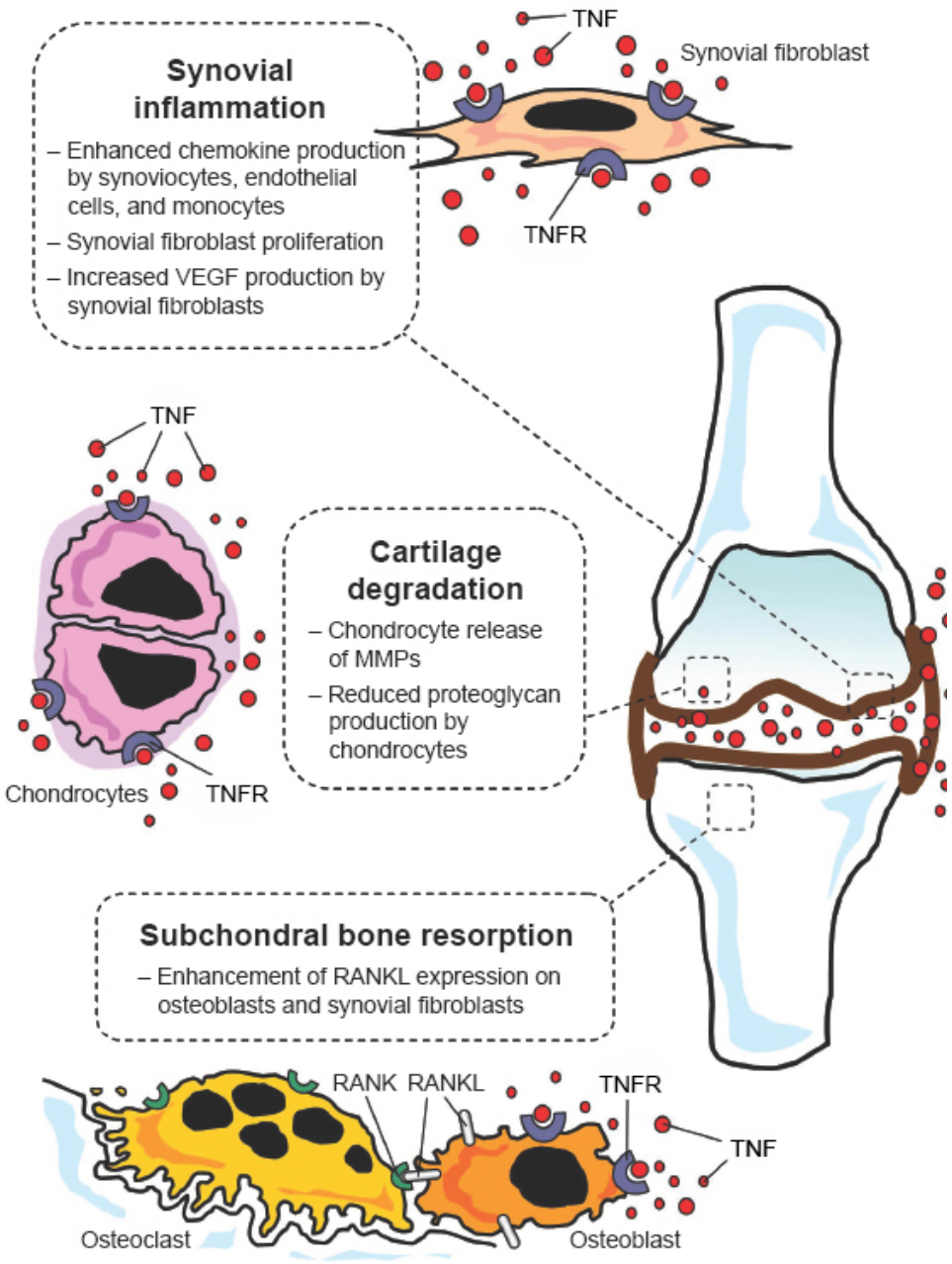

Figure 3. **The role of TNF-α in the pathogenesis of joint damage in Rheumatoid Arthritis.** TNF: Tumor Necrosis Factor; TNFR: Tumor Necrosis Factor Receptor (modified by 47).

1.2.2. The role of mesenchymal cells -Synovial Fibroblasts (SFs)

Mesenchymal cells are active participants in the structure and function of almost all tissues and contribute to their homeostasis (48). The mesenchymal cells of the joint are the Fibroblast-like Synoviocytes (FLSs), also named **Synovial Fibroblasts (SFs)** (49,50). SFs are located in the intimal lining layer of the synovial membrane of the joints and are required for the constant supply of various proteins which help in maintaining proper joint function and lubrication, as well as tissue repair and wound healing when required (51). These proteins are Vimentin, proteoglycans, extracellular matrix components, such as collagens and hyaluronic acid, as well as lubricin, VCAM-1, ICAM-1, IL-6, IL-1, cadherins, podoplanin, RANTES, MMPs etc (52). SFs is one of the main constitutive cellular population of the stromal compartment of the joint and together with tissue-resident macrophages, endothelial cells, nerves, vessels and ECM, they form the healthy joint (53).

Although immune cells, such as T and B-cells have been widely associated with the development of RA, several studies have implicated SFs as the key pathogenic orchestrators of the disease, capable of driving the development of joint pathologies both in mouse models and human patients (20,24,54). It was recently shown that depending on their location, either throughout different joints (55) or within the same joint -lining or sublining (56)- SFs can have unique characteristics, but they all acquire an aggressive arthritogenic phenotype in RA. More specifically, SFs are able to initiate and further develop RA symptoms, independently of inflammation in the synovium (51). Further knowledge regarding their role in the disease has derived from studies performed *in vitro,* as SFs can grow as a monolayer and easily expand displaying mostly fibroblastic morphology and properties (52).

As discussed above, SFs of RA patients actively contribute not only to the synovial hyperplasia due to their activation and production of inflammatory cytokines, but also to the subsequent joint destruction due to their involvement in matrix degradation, hence in cartilage and bone destruction (57). As shown in Figure 4, the arthritogenic phenotype of RASFs is characterized by unique features of aggressiveness and high capacity to invade into ECM, thus resembling the transformed phenotype of tumor cells. Another unique feature of RASFs is their resistance to intrinsic apoptosis pathway due to several factors which trigger imbalanced ratio between anti- and pro-apoptotic molecules (52). For example, highly activated NF-κB or/and Akt

phosphorylation provide a strong pro-survival signal which links inflammation with decreased apoptosis (58).

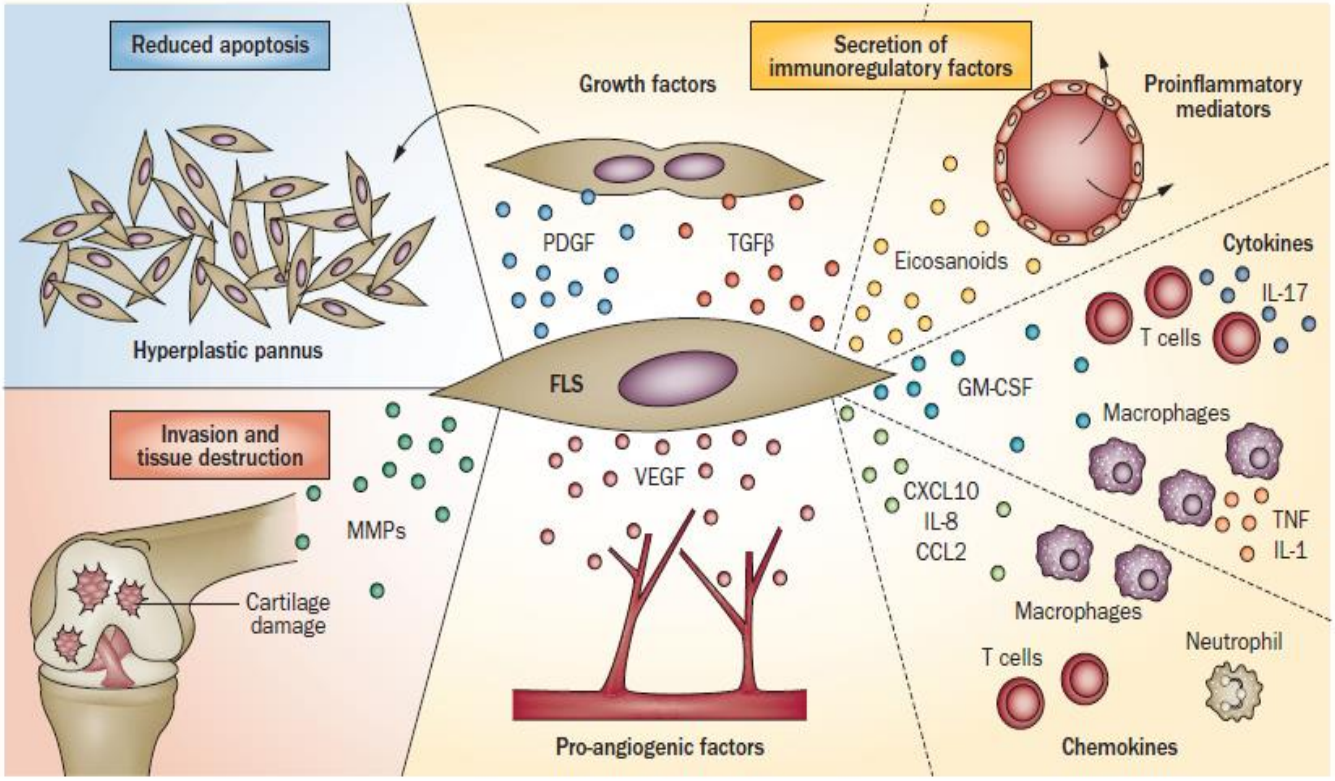

Figure 4. **The role of FLS in RA.** FLS contribute to RA pathology through a reduced ability to undergo apoptosis, the production of proteases that degrade the ECM and their ability to invade cartilage. FLS produce factors that potentiate growth, inflammation, angiogenesis and immune cell recruitment (modified by 59).

RASFs activation is induced by various stimuli, such as adhesion molecules (integrins, cadherins, fibronectin) derived from the synovial ECM, growth factors (FGF, TGF-β, PDGF) released by synovial macrophages, inflammatory factors (TNFα, IL-6, IL-1β, IFNγ, IL-17) released by immune cells, proto-oncogenes and tumor suppressor genes (p53, p21, c-Myc), though the main factors leading to their activation are still unknown (57). Once stimulated, RASFs enhance the production of inflammatory factors, such as VEGF, TNFα, various ILs, adhesion molecules (ICAM-1, VCAM-1), MMPs, adipokines, thus sustaining synovitis and a chronic inflammatory milieu together with the continuous influx of innate immune cells which eventually altogether contribute to ECM destruction (50). They also release chemokines, such

as CCL2, CCL4, CCL5, CCL8, CXCL8, CXCL12 and IFNβ (53). The expanded or thickened synovial tissue, called “pannus”, which behaves like a local invasive tumor, consists mainly of activated and invasive SFs and osteoclasts which can erode the interface of cartilage and bone (12).

RASFs adhere to cartilage, with the help of ICAM-1 and mostly VCAM-1, where they control and potentiate MMP, ADAMT and cathepsin expression (59). Involvement of cadherins and specifically cadherin-11 in invasion into ECM-like matrices is also evident from *in vitro* studies (20). The production of these proteins by RASFs is induced by pro-inflammatory factors (59). Once RASFs invade cartilage, they start damaging the adjacent bone, by mainly producing high levels of RANKL and myostatin –a TGFβ family member-, which directly promote osteoclastogenesis (42).

1.3. Animal mouse models

Despite the improvements in unraveling the pathophysiological mechanisms of RA, the actual pathways driving the initiation of the disease remain unclear, which hinders effective drug development. Although we have gained essential knowledge from studying the human SFs, animal models that recapitulate aspects of human disease provide an invaluable tool to understand the basic biological mechanisms and to potentially target pathways implicated in the disease by future therapeutic agents (60).

As reviewed in Table 2, there is a wide variety of agents that can induce different types of experimental arthritis which mimic specific or multiple aspects of the human disease. Although most of them show high variability within the experimental groups, the advantage of working with induced models of RA is that they are applicable to genetically engineered mice, such as knockout (KO) or knockin (KI) mice, which allows the examination of specific genes of interest in the context of RA (61).

Additionally, several genetically engineered, mutated and congenic mice have been generated to develop spontaneous RA-like pathology, as shown in Table 3. Mainly by targeting inflammatory factors or immune mediators, there are many models of RA that have helped in elucidating the drivers of human disease and further translating this knowledge into clinic (62). Most of the induced and the genetically modified RA models can recapitulate the basic characteristics of RA disease, such as synovial hyperplasia, cartilage destruction and bone erosion, as well as the interplay between SFs and immune cells, such as T and B cells, neutrophils and macrophages (63).

Although all of these models have been proven essential for studying pathways associated with human RA, it is necessary to focus on their targeted identification and validation. The correlation of animal models with the human disease could be improved by precise phenotyping and characterization of the models and by acquiring publicly available large-scale profiling and metadata integration. These advances would allow a more efficient exploitation of animal models in the development and assessment of new and more reliable therapeutics, which would also be improved if more humanised models are generated (60).

Induced Models								
Model	***Spe-cies***	***Induction***	***Characteristics of Pathology developed***	***Similarity to Human Disease***	***Dura-tion***	***Adva-ntages***	***Disadva-ntages***	***Refe-rences***
Collagen-Induced Arthritis (CIA)	Mouse, rat, rabbit, non-human primate	Active immunizatio n by inoculation with type II heterologou s Collagen	Acute monophasic erosive polyarthritis, antibody and Th17-cell response	Presence of RF and ACPAs, chronic relapsing arthritis resembling human remission	Onset within 12-15 days, peak is at ~30 days, lasting up to 2 months	Easy to perform	1)Only inducible in susceptible strains of rodents, such as DBA/1 2)Variable incidence, severity and inter-group inconsistency	(64,65)
Collagen Antibody -Induced Arthritis (CAIA)	Mouse	1) Passive immunizatio n by inoculation with a commerciall y available cocktail of monoclonal antibodies against various epitopes of Collagen Type II 2) Serum transfer from an immunized mouse 3) Serum transfer from RA patients	Self-limiting polyarthritis in 100% animals, macrophage and polymorphonuclear cell involvement, no T- and B-cell involvement	RA-like symptoms, CAIA can provide insight into separate roles of innate and adaptive immune response in RA	Onset within 48 h, with peak at ~7 days, lasting for 1 month	1) Can be induced in any mouse strains 2) High degree of synchroni city 3) 100% penetran ce	1)Due to its independency from T and B cells, it does not recapitulate the immune compartment of human RA 2)High incidence of variability in different LOTs of the induction antibodies mixture	(66,67)
Zymosan -Induced Arthritis	Mouse, rat	Inoculation with intra-articular injection of Zymosan (a polysacchari de from the cell wall of *Saccharomy ces cerevisiae)*	Proliferative inflammatory monoarthritic pathology, synovial hypertrophy, pannus formation, TLR-2 dependency	RA-like symptoms	Onset within 3 days, lasting for 7 days, relapsing after ~25 days	Inducible in multiple strains of mice	High degree of technical ability to perform intra-articular injection in mice	(68,69)

Model	*Spe-cies*	*Induction*	*Characteristics of Pathology developed*	*Similarity to Human Disease*	*Dura-tion*	*Adva-ntages*	*Disadva-ntages*	*Refe-rences*
Antigen-Induced Arthritis	Mouse, rat	Inoculation with intra-articular injection of antigen	Arthritis, which is followed by the emergence of auto-reactivity to collagen, followed by T cell-mediated responses	Presence of RF		Inducible in multiple strains of mice	1) High degree of technical ability to perform intra-articular injection in mice 2) It does not recapitulate the human characteristic of endogenous breach of tolerance	(70,71)
Pristane-Induced Arthritis	Mouse, rat	Inoculation with a single injection of pristine (a natural saturated terpenoid alkane)	T-cell dependent acute severe inflammation with edema formation and infiltration of mononuclear and polymorphonuclear cells, followed by a chronic relapsing phase	RA-like symptoms, it can provide insight into pathways leading to non-responsiveness of some RA patients to TNFα inhibitors	It includes a chronic relapsing disease course	Inducible in multiple strains of mice	It does not recapitulate RA TNF-dependency	(72,73)
Serum-Induced Arthritis	Mouse	Serum transfer from K/BxN (see Table 3)	Severe and destructive polyarthritis	Presence of anti-G6PI antibodies, TNF and IL1 involvement	Onset within 2 days, peak at 6-14 days, wane by day 18-21	Inducible in multiple strains of mice	Variability in different mouse strains	(74,75)
Human/ SCID chimeric mice	Mouse	Implantation of human synovial tissue from RA patients as xenografts in SCID mice	RA-like symptoms with cartilage invasion and destruction, mediated by SFs	Activated synovium and cartilage destruction	At day 35, focal erosion starts appearing, at day 105 activated SFs invade the cartilage	Human-derived cells can be studied	1) High degree of technical ability is needed 2) High incidence of variability	(76)

Table 2. **Characteristics of selected induced models of RA** (60–63)**.**

Spontaneous Models							
Model	***Genetic Modification***	***Characteristics of Pathology developed***	***Similarity to Human Disease***	***Duration***	***Adva-ntages***	***Disadva-ntages***	***References***
TNF$^{\Delta ARE/+}$	Deletion of AU-rich elements, which leads to persistent elevation of TNF levels	Chronic inflammatory polyarthritis, the mice also develop intestinal inflammation	TNF-dependency, SFs activation	Onset at 6 weeks of age, peak at 16 weeks of age	100% penetrance	Systemic cachexia/ growth retardation	(24,77)
Tg-huTNF	Overexpression of human TNF	Chronic inflammatory erosive polyarthritis	TNF-dependency, SFs activation	Onset at 3 weeks of age, peak at 8 weeks. Mice die at 11-12 weeks	1)100% penetrance 2) humanised model where anti-human TNF treatment can be tested	Mice die within 12 weeks of age because of the extreme TNF-driven cachexia	(23,24,78)
ILRa $^{-/-}$	Systemic ablation of natural inhibitor of IL-1 receptor, which leads to high levels of IL-1	Chronic arthritis with T cell-dependent pathology	Presence of RF, autoantibodies to double-stranded DNA and type II Collagen, IL-1, TNF, IL-6 and IL-17 are elevated	Onset at 5 weeks of age, peak at 16 weeks of age	100% penetrance	Spontaneous arthritis only develops in the inflammatory-susceptible mouse strains, such as Balb/C, DBA/1	(79)
K/BxN	Transgenic T-cell receptor *KRN* that recognizes a peptide of G6PI as an autoantigen in the context of MHC-II	Severe and destructive polyarthritis, activation and mast cell degranulation, sustained T cell activation leads to high affinity antibodies against G6PI; TNF- and IL1-driven pathology	Presence of anti-G6PI antibodies, TNF and IL-1 involvement	Onset at day 15, peak at day 60	Usefulness for the study of initial events of RA	Presence of anti-G6PI antibodies in RA patients is still controversial	(80,81)
SKG	Point mutation in ZAP-70, which alters thymic T-cell selection	Inflammatory arthritis, T-cell driven pathology	Presence of RF	Onset at 2 months, peak at 8 months of age	Useful for studying how T-cells stimulate SFs	Absent in germ-free mice	(82)
DNaseII $^{-/-}$ IFN-IR$^{-/-}$	Induced deletion of the DNase II gene	Inflammatory polyarthritis	TNF involvement, presence of anti-CCP and RF	Early onset, peak at 12 months	Useful for studying how macrophages stimulate SFs	Long protocol	(83)

Table 3. **Characteristics of selected spontaneous mouse models of RA** (60–63)**.**

1.3.1 Tg-huTNF model of RA (Tg197)

A successful paradigm of a humanised animal model of RA that has been widely widely in preclinical studies, is the human TNF transgenic mouse, **Tg-huTNF,** or Tg197. As discussed earlier, TNF is a mediator of RA pathology and its critical role has been proved by the highly positive clinical responses of human patients to anti-TNF therapies (43,84). The pathogenic role of TNF and the reversal of disease progression by its inhibition was originally demonstrated in the Tg-huTNF mouse (23) and recently validated in therapies with more than one anti-huTNF agents (85). This model is characterized by deregulated expression of human TNF, which leads to the spontaneous development of chronic, erosive and symmetrical polyarthritis with histological features that highly resemble the ones of human RA. This mouse model has catalytically contributed to our knowledge on the mechanisms that control the development and progression of RA, highlighting the key role of TNF in the pathology of the disease (23). It has also provided an essential tool for studying the role of the mesenchymal compartment in the development of RA, as Tg-huTNF-derived SFs show a TNF-driven transformed phenotype mainly characterized by increased proliferative and migratory capacity and production of inflammatory cytokines (86–88), resembling the one of RASFs which was discussed earlier. In addition, it has been proven that Tg-huTNF mice can develop arthritis even in the absence of adaptive immune system and that the key cellular orchestrator of the disease is SFs (24,89). Arthritogenic SFs of Tg-huTNF mice have been recently found to exhibit a distinct expression profile mimicking the one of human RASFs (90), which can be reversed by anti-TNF therapy (85).

Overall, this RA mouse model has been widely used to study the role of TNF as well as the role of TNF-driven activation of SFs in the pathology of RA, strongly recapitulating the human disease.

1.3.2. Col6a1-Cre (ColVI-Cre) mouse

Apart from the genetically engineered mice that permit studying of RA mechanisms, the use of the Cre-LoxP system and various *Cre* lines have also been a valuable tool to study the role of specific cells in the disease. More specifically, by using the Cre-LoxP system, one can (in)activate genes in specific genes in the tissue of interest (91). By using ***Col6a1-Cre (ColVI-Cre)*** mouse, which targets the mesenchymal cells of joints, small intestine, skin, skeletal muscle cells (24) and additional tissues (92), the role of TNF and its main receptor (TNFR1) in SFs was further investigated in the Tg-huTNF mice.

Our lab generated mice whose TNFR1 signaling was activated specifically in the SFs (***ColVI-Cre Tnfr1*$^{cneo/cneo}$ mice**) (93), as well as mice whose TNFR1 signaling was ablated specifically in the SFs (***ColVI-Cre Tnfr1*$^{flox/flox}$**) (94). When these two mice strains were crossed with the Tg-huTNF mice, it was proven that TNFR1 signaling on SFs is not only required for the disease, as mice with ablation of TNF signaling in their SFs showed amelioration of chronic polyarthritis (95), but also sufficient to initiate the disease, as mice with ablated TNF signaling in every cell but their SFs developed chronic polyarthritis (24).

Overall, the engineered mice Tg-huTNF in combination with the *ColVI-Cre* mice, have been used to study the driving role of TNF in RA pathology as well as its effects on the SFs of the animal.

In addition, a more advanced version of the Cre-LoxP system is the use of reporter mice of *Cre* activity which are important for defining the spatial and temporal extent of *Cre*-mediated recombination. An example is the ***Rosa26*$^{mT/mG}$** mouse, a double-fluorescent Cre reporter mouse that expresses membrane-targeted tandem dimer Tomato (mT) prior to *Cre*-mediated excision and membrane-targeted green fluorescent protein (mG) after excision, meaning that upon *Cre* recombination with a *Cre* line, Cre^{+} cells are stained with green fluorescence and the rest of the cells (Cre^{-}) are stained with red fluorescence. Both membrane-targeted markers outline cell morphology, highlight membrane structures, and permit visualization of fine cellular processes (96).

1.4. Extraarticular RA-related manifestations/ comorbidities

Although the main features of RA are joint inflammation and damage, the notion that RA is a multisystemic syndrome, affecting not only the joints, but also additional organs has been recently gained momentum (97). Due to its multifactorial nature and complexity, the clinical picture of RA patients is highly heterogeneous with several different subsets of RA being manifested in patients (60) and with many patients showing increased mortality compared to the general population (98,99). The different subsets of patients may involve different types of RA, such as RF positive or negative, but they may also include different extraarticular manifestations, which are broadly collected together as co-morbidities leading to increased disability and shortened life expectancy (100).

Unfortunately, comorbidities are not well managed in RA patients and many clinicians prefer to simply record the presence of comorbid pathologies, but not to use standardized indexes, such as Charlson index, which assess their pathology stage, rendering the record of incidence and prevalence of these condition challenging (97). In Figure 5, the prevalence of most common RA-related comorbidities is depicted.

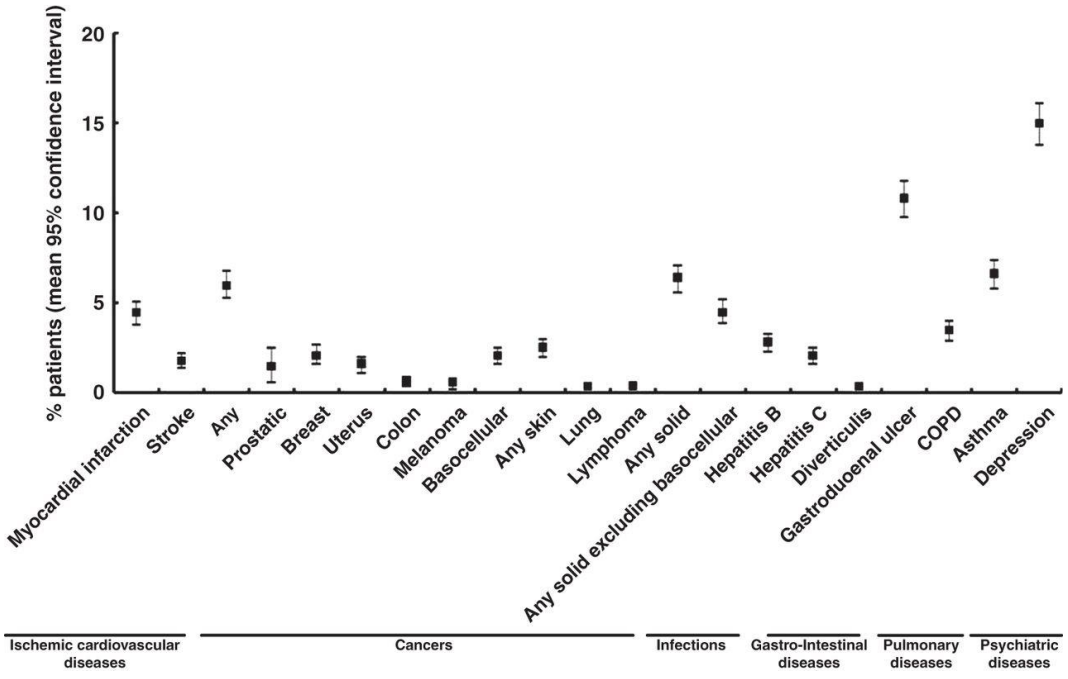

Figure 5. **Prevalence of evaluated comorbidities in RA patients** (97).

Some comorbidities, such as cancers, do not have a causal association with RA, although their incidence is higher in RA. The most dominant theory about these types of comorbidities is that patients are predisposed to develop non-causal comorbidities due to chronically active inflammation (97). Nevertheless, some comorbidities are causally associated with RA, as their frequency and impact are increased in RA patients. The most common causally associated comorbidities are cardiovascular diseases, osteoporosis, periodontal diseases, gastrointestinal and lung disorders (100), as summarized in Table 4.

Type of co-morbidity	Specific examples
Cardiac	Ischaemic Heart Disease and Cardiac failure
Lung disease	Interstitial lung disease
Gastrointestinal Disease	Upper gastrointestinal ulcers, hepatitis
Osteoporosis	Fracture
Oral disease	Periodonitis
Infection	Bacterial sepsis
Cancer	Lymphoma

Table 4. **Key comorbidities in Rheumatoid Arthritis** (modified by 100).

1.4.1. RA-related heart diseases

Cardiovascular disorders are one of the most common and most important arthritis-related comorbidities as they are highly responsible for the increased mortality rates observed in RA patients (97,101). Cardiac disease manifestations are detected in 70-80% of Rheumatoid arthritis (RA) and Spondyloarthritis (SpA) patients and symptoms can vary greatly, including ischemic and congestive heart failure, pericarditis, cardiomyopathy, arrhythmias, as well as valvular diseases, such as valve insufficiency and stenosis (102,103).

Coronary artery disease, or otherwise ischemic heart disease or cardiovascular disease (CVD), is characterized by accumulation of atherosclerotic plaques in the arteries of the patients, which poses high risk for myocardial infarction. In ~14% of RA patients, accelerated atherosclerosis begins around the same time-onset of RA symptoms and may cause myocardial infarction and hospitalization with the need of surgical intervention (104). CVD can be diagnosed via resting electrocardiography and echocardiography, which may indicate Left Ventricular hypertrophy, an

established feature of RA (105), and arrhythmias or by cardiac catheterization and angiogram, where the width of the arteries and hence the presence of atheromatous plaques can be evaluated (106). Coronary plaques of RA patients are more frequent, more severe and more prone to rupture compared to the general population, hence RA patients have worse outcomes after myocardial infarction, with earlier relapse and increased mortality (107). This indicates that CVD diagnosed in RA patients differs from the non-RA patients and this could be attributed to the different microenvironment of the patients (101). Chronic high-grade inflammatory state of RA patients could cause these differences, as both RA and atherosclerosis have an inflammatory basis. In fact, formation, progression and high levels of proinflammatory factors, such as TNF, IL-1β and IL-6 found in plaques, are also found in the synovial membrane of RA patients. Therefore, it could be suggested that proinflammatory factors can be transferred from pathogenic synovium of RA patients to distant tissues through blood, thus generating a spectrum of proatherogenic changes, such as insulin resistance, prothrombotic effects, pro-oxidative stress and endothelial dysfunction in these patients (108).

Apart from a higher risk to develop ischemic heart disease, RA patients have also an increased risk to develop **heart failure (HF)**, with a two-fold higher incidence (109). Cardiomyocyte hypertrophy, the hallmark of myocardial remodeling, which is enhanced during HF, is evident in RA patients (105). Heart failure can be diagnosed via resting electrocardiography and echocardiography, which may indicate left ventricular diastolic dysfunction, hypertrophy and fibrosis as well as impairment in contractility (110). Not only do RA patients with HF present differently from those without HF, but their prognoses are also worse, with significantly higher mortality (111).

Moreover, in RA patients without evident cardiovascular or heart failure disease, there could be findings of **valvular involvement**, such as valvular calcifications, thickening, insufficiency, stenosis, prolapse or a combination of two or more co-existing valvular pathologies (112). In fact, meta-analysis data combining findings of several studies, have shown that RA patients have three-to-five times increased risk to develop mitral/aortic valvular insufficiency, aortic valve stenosis and mitral/aortic valve thickening/calcification (103). These pathologies are clinically defined as “silent rheumatoid heart disease”, as they may not present with clinical symptoms until they are very progressed, which intensifies the importance of echocardiographic assessment in RA patients (113). They can be diagnosed by anatomic evaluation

combining short- and long- echocardiography axis to describe the valvular leaflet mobility, thickness and calcification. Continuous-wave Doppler can also detect severe valvular stenosis jet, by measuring the maximum velocity and color Doppler analysis can detect possible regurgitation jet and –in combination with imaging- it can also determine the level of any valvular obstruction (114). The effects of a chronic valvular abnormality on cardiac function can be also evaluated using echocardiography assessment in patients, evaluating parameters outlined in Table 5. Left ventricular volume, as well as other chambers' volume and function can be measured by 3D echocardiography, which also permits measurements of chamber dimensions and filling volumes which altogether allow the calculation of Ejection Fraction (EF) volume, a measurement of the percentage of blood leaving the heart each time it contracts, using the Simpson equation. Contractility efficiency, evaluated by measurements like systolic velocity of the posterior wall (SVPW), can be measured by 2D M-Mode measurements (115).

The increased prevalence of heart diseases in RA patients could be attributed to several pathologies observed in RA patients that pose as risk factors for heart diseases, such as hypertension, dyslipidemia, diabetes, obesity as well as insulin resistance (104). However, besides the correlation between RA inflammation and cardiovascular disease analyzed above, the mechanisms mediating the co-occurrence of cardiac comorbidities in patients with chronic inflammatory joint diseases remain unknown.

Echocardiography methods	Measurements	Description
2D	**LVEDd**	Left ventricular end diastolic diameter
	LVEDs	Left ventricular end systolic diameter
	LA	Left atrium
	LVLd	Left ventricular end diastolic length
	LVPWd	LV posterior wall thickness in diastole
	IVSd	LV interventricular septal wall thickness in diastole
M-mode	**HR**	Heart beat per minute
	SVPW	Systolic velocity of the posterior wall
Color Doppler	**AoV**	Aortic valve velocity
	MV E and A	Mitral valve velocity
	PV	Pneumonic valve velocity
Calculated measurements	**LVEDV**	Left Ventricle end diastolic volume
	LVESV	Left Ventricle end systolic volume
	FS	Fractional shortening (degree of shortening of the left ventricular diameter between end-diastole and end-systole = LVEDd – LVEDs/LVEDd * 100%)
	SV	Stroke volume (volume of blood pumped from the left ventricle per beat=LVEDV-LVESV)
	CO	Cardiac Output (volume of blood being pumped by the heart per unit of time = HR*SV)
	EF	Ejection fraction (the volumetric portion of the total blood ejected from the heart, with each heartbeat =[SV/LVEDV]*100; Simpson’s equation)

***Table 5*. Parameters evaluated in echocardiography assessment**

1.4.2. The role of TNF in heart diseases

As discussed above, chronic exposure to high-grade inflammation renders RA patients prone to develop extra-articular manifestation. Therefore, the involvement of several proinflammatory factors, such as TNF, IL-1β, IL-6 and IL-8 may play an important role in RA-related comorbidities. Here we are going to focus on the role of TNF as it appears to play the most important role in RA and possibly in comorbidities, most specifically in RA-related heart pathologies (Figure 6). Elevated circulating levels of inflammatory cytokines, have been associated with cardiovascular disease, as well as HF, myocardial dysfunction and valvular diseases (116).

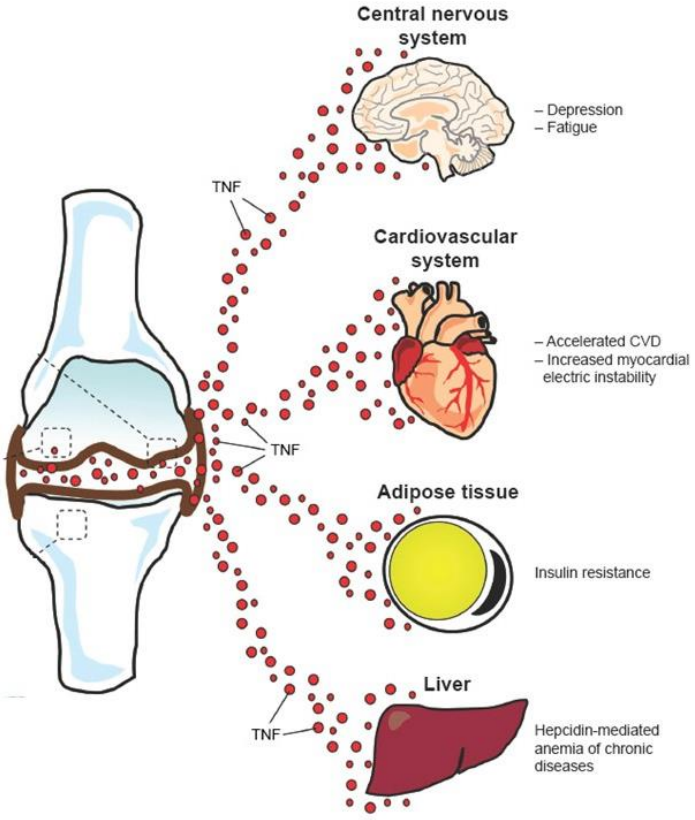

Figure 6. **The role of TNF-α in the pathogenesis of comorbidities in Rheumatoid Arthritis** (modified by 47).

In fact, high serum levels of circulated TNF (117) as well as high myocardial protein levels of TNF and its receptors -TNFR1 & 2- (118) are detected in patients with severe chronic heart failure and associated cachexia, as well as in patients with CVD (119,120). Additionally, recent clinical and experimental studies have noted that

increased release of TNF can contribute to LV myocardial remodeling, the milestone in the progression of HF, by inducing cardiomyocytes hypertrophy (121), which leads to LV dilation (31). The involvement of TNF in HF mechanisms has also been underscored by various studies in transgenic mice. More specifically, mouse models that overexpress TNF in a cardiac-specific manner develop cardiac dysfunction, while the systemic deregulation of TNF expression results in aortic/mitral valve inflammation (122–124). Overall, these findings in both mouse models and humans, have suggested that not only circulating TNF and TNFR levels can be used as biomarkers and as prognostic predictors for HF, but they could also be targeted therapeutically in HF patients (125,126). Unfortunately, recent clinical trials that used anti-TNF biologics in patients with HF showed that TNF inhibition had no or even adverse effects in their clinical outcome (127). However, in case of RA patients, anti-TNF therapy seemed beneficial regarding the increased risk of these patients to develop HF or CVD (128). It, therefore, appears that anti-TNF therapy, in certain instances, confers protection against HF and/or CVD, but in case of RA-related cardiac manifestations, medications should be prescribed very carefully as there is a variety of possible explanations for the failure of anti-TNF therapy, which ends up being controversial (129). Further randomized controlled trials are required to determine the therapeutic potential of different anti-TNF agents and different therapeutic regimens in the management of HF.

Apart from its pivotal, if not causal, role in the pathogenesis of heart failure, TNF also exerts an important role in heart valvular diseases. TNF has been mainly associated with the pathogenesis of Calcific Aortic Valve Disease (CAVD), which is characterized by aortic valve inflammation, fibrosis and calcification progressing to aortic stenosis (130). Valve Interstitial Cells (VICs) –see below- which are the main components of the human heart valves are induced by TNF and hence acquire an activated osteoblastic phenotype which contributes to the progression of calcification in CAVD (131). In addition, elevated serum TNF levels have been found in patients with aortic stenosis and mitral regurgitation, suggesting an association of TNF levels with hemodynamic pressure and cardiac volume overload (132). The driving role of TNF in the development of valvular pathologies has also been shown through studies in mouse models. TNF overexpression by the myeloid cells in BPSM1 mice has led to the development of aortic root aneurism, as well as mitral and aortic valve disease (133). Moreover, TNF-dependent valvulitis has been found in two additional knockout mice, IL-1Ra-/- and TTP-/-, further strengthening the association of TNF with valvular

diseases (134,135). However, further studies are needed to elucidate the underestimated role of TNF in valvular diseases.

Overall, given that TNF is mediating both RA and cardiac diseases, which are manifested in RA, it may commonly underlie arthritis and arthritis-related cardiac manifestations in human patients, which could also explain the amelioration of both of these comorbidities in patients treated with anti-TNF biologics (136).

1.4.3. The role of mesenchymal cells- Valve Interstitial cells (VICs)- in heart diseases

Cardiac valves are mainly composed of **Valve Interstitial Cells (VICs)** that are enclosed by two thin layers of Valve Endothelial Cells (VECs) (137). VICs is the most prevalent cell type in the heart valves and is responsible for the maintenance of the valve integrity by adapting to homeostatic and pathogenic conditions, as dictated by the ECM, mechanical force and other factors in the valve (138). Numerous studies have shown that VICs have a heterogeneous population, but their main characteristics are the fibroblastic nature and the mesenchymal origin, confirmed by their capacity to multi-lineage differentiation, their fibroblastic morphology *in vitro*, as well as their expression profile of known mesenchymal markers, such as Vimentin, α-SMA, CD90, CD73, CD105 and their negative expression of hematopoietic markers (CD34, CD45) and endothelial markers (CD31, VEGF, VE-Cadherin) (139–141). However, they could be distinguished into five phenotypes, as outlined in Table 6, based on their cellular functions in normal valve physiology, as well as in pathological processes.

Cell type	Location	Function
Embryonic progenitor endothelial/mesenchymal cells	Embryonic cardiac cushions	Give rise to resident qVICs, possibly through an activated stage. EMT can be detected by the loss of endothelial and the gain of mesenchymal markers
qVICs	Heart valve leaflet	Maintain physiologic valve structure and function and inhibit angiogenesis in the leaflets
pVICs	Bone marrow, circulation, and/or heart valve leaflet	Enter valve or are resident in valve to provide aVICs to repair the heart valve, may be CD34-, CD133-, and/or S100-positive
aVICs	Heart valve leaflet	α-SMA-containing VICs with activated cellular repair processes including proliferation, migration, and matrix remodeling. Respond to valve injury attributable to pathological conditions and abnormal hemodynamic/ mechanical forces
obVICs	Heart valve leaflet	Calcification, chondrogenesis, and osteogenesis in the heart valve. Secrete alkaline phosphatase, osteocalcin, osteopontin, bone sialoprotein

Table 6. **Classification of VIC markers and functions into five phenotypes.** [qVICs : quiescent VICs, pVICs: progenitor VICs, aVICs: activated VICs, obVICs: osteoblastic VICs] (142).

More specifically, embryonic progenitor endothelial/mesenchymal cells undergo endothelial-to-mesenchymal transformation (EndMT) during fetal development giving rise to quiescent VICs (qVICs) resident in the normal heart valve, which maintain normal valve physiology. When qVICs are subjected to a stimulus, they become activated, giving rise to myofibroblastic activated VICs (aVICs) that participate in valvular repair and remodeling by acquiring activated features, such as increased migration, proliferation and ECM synthesis. In fact, the interplay between qVICs and aVICs is thought to be the cornerstone of valve homeostasis (143). Another source of aVICs has been suggested to be the progenitor VICs (pVICs), which include bone-marrow derived cells, circulating cells and resident valvular progenitor cells, but this is still under research. qVICs can also undergo osteoblastic differentiation into osteoblastic VICs (obVICs) in the presence of osteogenic and chondrogenic factors or, generally, under conditions that promote valvular classification (142).

Recent in vitro studies have suggested that **TNF** is a very important stimulus of VICs activation as it can activate qVICs into myofibroblastic aVICs, hence inducing their pathogenic contribution to heart valve diseases (144). In addition, TNF is capable of inducing qVICs differentiation into obVICs and expressing markers such as Runx2, BMP2, ALP, Osteocalcin and Osteopontin thus actively contributing to the

development of valvular pathologies, such as CAVD (140), a progressed stage of aortic stenosis (Figure 7). In fact, strong evidence indicate that VICs derived from CAVD patients show a greater sensitivity to TNF induction, as TNF activates NF-κB in qVICs, accelerating their transformation (131). As VICs are able to synthesize matrix components, such as collagen, elastin, proteoglycans, growth factors, cytokines, chemokines as well as MMPs, they can interact with each other and with the valvular ECM to produce a fibro-calcific remodeling of the valve that can cause restriction of blood flow, which can potentiate deterioration of valvular function (145).

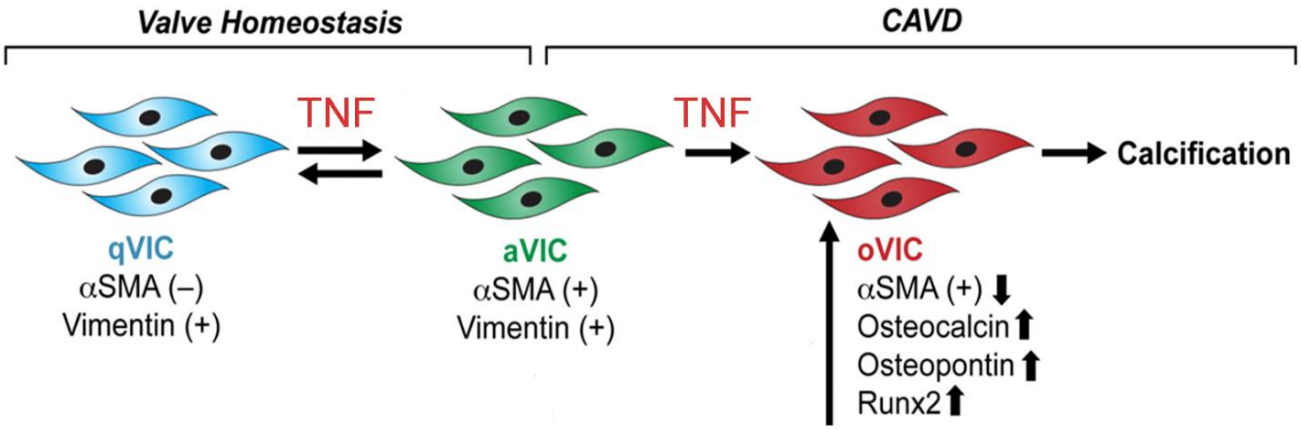

Figure 7. **Schematic depiction of the role of VICs in valvular pathology**. Quiescent VICs (qVICs) differentiate into activated myofibroblast-like VICs (aVICs), responsible for functional remodeling of the heart valve ECM. Upon TNF stimulation, aVICs can further differentiate into osteoblastic VICs (oVICs), which are responsible for calcium deposition in CAVD (modified by 146).

2. Aging

Aging has been defined as the progressive decline of functional capacity in multiple cells, tissues and organs associated with increased risk of morbidity and mortality. This deterioration is the primary risk factor for major human pathologies, such as cancer, diabetes, cardiovascular disorders and neurodegenerative diseases (146). Age-related loss of function is a feature of virtually all organisms that age, ranging from single-celled creatures to large, complex animals. In mammals, age-related degeneration gives rise to well-recognized pathologies such as sarcopenia, atherosclerosis, heart failure, osteoporosis, macular degeneration, pulmonary insufficiency, renal failure, neural degeneration and prominent neurodegenerative diseases such as Alzheimer's and Parkinson's diseases, and many more age-related pathologies (147). The mechanisms underlying the aging process are beginning to be unravelled at the molecular level, yet there is clear evidence that the rate of aging differs significantly between members of the same animal species, including humans.

2.1. The aetiopathogenesis of aging

Aging research has experienced an unprecedented advance over recent years, mostly due to the recent findings of genetic pathways and biochemical processes driving the pathogenesis of aging, as shown in Figure 8. In fact, scientists studying the molecular and cellular processes that govern these changes and their variation in individuals have identified nine interconnected "hallmarks of aging", that will be outlined here.

Numerous studies have reported that aging is characterized by increased **genomic instability**, mainly due to increase in somatic mutations and other forms of DNA damage, suggesting that impairment of DNA repair mechanisms is a determinant of aging (148). Causal evidence for the link between genomic damage and aging has risen from studies in cells, mice and humans in whom deficiencies in DNA repair mechanisms cause accelerated aging (149). Another additional hallmark of aging is the **telomere attrition** due to the decreased production of the enzyme called telomerase, eventually leading to decline in cellular division capacity which even further deteriorates upon increased levels of stress (150,151). In fact, telomerase

deficiency in humans is associated with premature development of diseases, such as pulmonary fibrosis, anemia and many others, which collectively comprise a single syndrome spectrum defined by the “short telomere defect” (152). Similar to many molecular processes and defects, **epigenetic alterations**, including histone modifications, alterations in DNA methylation and transcription, as well as chromatin remodeling, render as age-associated markers. More specifically, histone and DNA methylation are necessary for normal aging, which has been also associated with increased transcriptional changes (146).

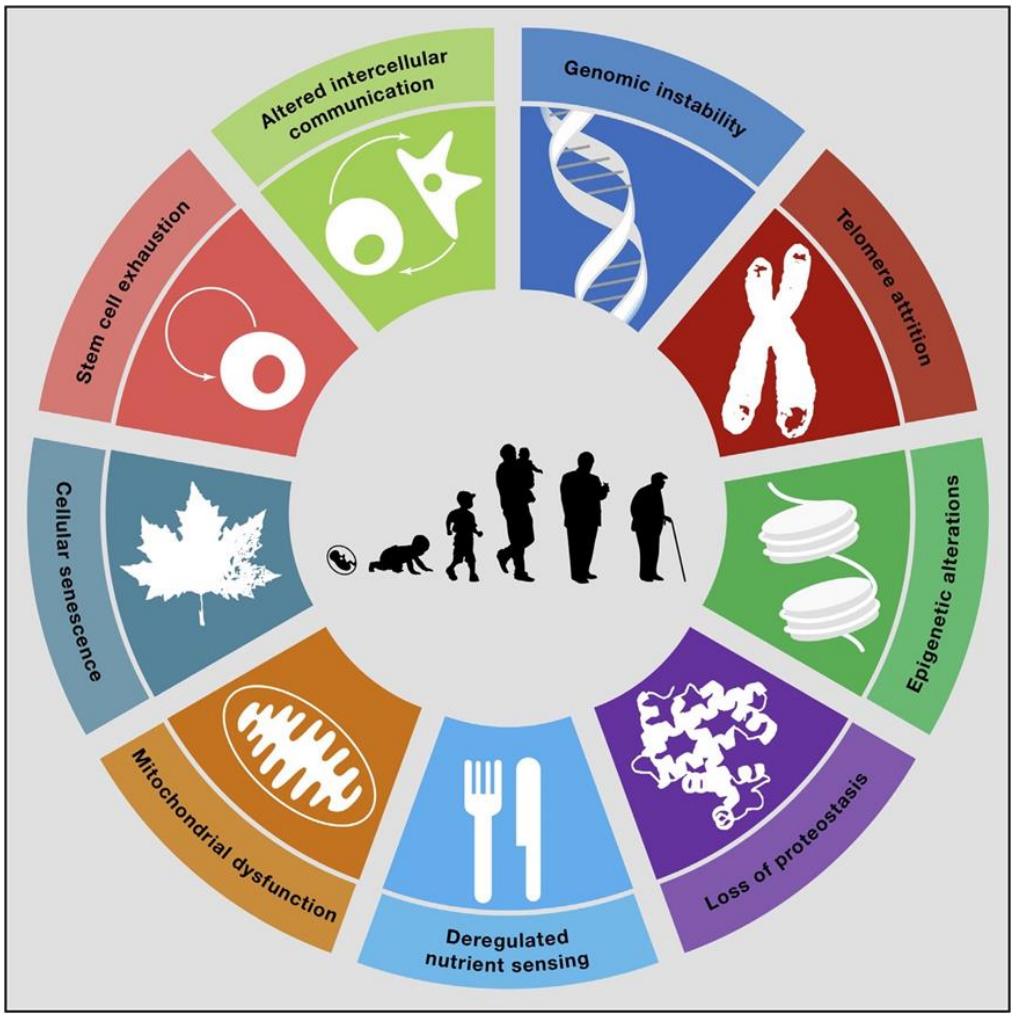

Figure 8. **The Hallmarks of Aging.** The scheme enumerates the nine hallmarks of aging, that is genomic instability, telomere attrition, epigenetic alterations, loss of proteostasis, deregulated nutrient sensing, mitochondrial dysfunction, cellular senescence, stem cell exhaustion and altered intercellular communication (146).

Moreover, aging is characterized by impaired **protein homeostasis**, namely proteostasis. During aging, the mechanisms which stabilize the correct folding of proteins and degrade the misfolded ones are disrupted, which results in chronic expression of unfolded, misfolded or aggregated proteins and contributes to the development of age-related diseases (153). The mechanisms mostly responsible for the correct proteolysis of these misfolded proteins, namely the autophagy-lysosomal system and the ubiquitin-proteasome system become deficient during aging (154). Additionally, **metabolic deregulations** through the somatotrophic axis, which consists of growth hormone, insulin-like growth factor, mechanistic target of rapamycin and AMPKs, contribute to the process of aging (155). The favorable role of metabolism in the natural process of aging has been further confirmed by studies on dietary restriction, which increases lifespan in mice (156). **Mitochondrial dysfunction** is another important contributor in the pathogenesis of aging, as the respiratory chain diminishes with aging, leading to decrease in ATP generation (146). The role of mitochondrial impairment in aging has been further strengthened by recent findings suggesting that when mitophagy, a selective type of autophagy targeting mitochondria for degradation, declines with aging, there is an accumulation of damaged mitochondria, leading to decreased lifespan (157).

Furthermore, **cellular senescence** has been suggested to be one of the most important hallmarks of aging. When cells undergo cellular senescence, they are characterized by permanent and irreversible growth arrest and resistance to apoptosis (158). Senescent cells are accumulating over the life span mainly due to extracellular and intracellular stress, such as telomeric dysfunction, mitochondrial deterioration, severe or irreparable DNA damage as well as oxidative stress (159). Recently, the senescent cell was more thoroughly described as metabolically active which ultimately develops a cellular phenotype, called senescence-associated secretory phenotype (SASP), that can alter its microenvironment. SASP is characterized by increased secretion of interleukins and inflammatory cytokines and chemokines, including IL-6 and TNF, proteases, such as MMPs, growth factors, as well as gene expression of cell-cycle inhibitors, such as $p16^{INK4a}$ and p21 (159). As senescent cells can affect the neighbor cellular proliferation, migration and differentiation, there is a controversy whether cellular senescence is a beneficial compensatory response to clear the tissues from damaged and potentially oncogenic cells or if it becomes deleterious and accelerates aging when tissues exhaust their regenerative capacity (146). This **stem cell exhaustion** plays a very essential role in

aging, as a deficient production of the necessary number of stem cells and the cell types that are differentiated to is observed and eventually leads to organ dysfunction. This renders stem cell exhaustion as the ultimate culprit of tissue and organismal aging (160). The process of aging also depends on the **altered intercellular communication**. One example is the so called “inflammaging”, that is a phenomenon combining the accumulation of a low-grade pro-inflammatory tissue damage, the dysfunction of the immune system (immunosenescence), the secretion of pro-inflammatory factors from senescence cells, the enhanced activation of the NF-κB transcription factor and the defective autophagy response observed in aging. These intercellular communication alterations result in an enhanced activation of the so-called inflammasome (a multiprotein oligomer responsible for the activation of inflammatory responses), which leads to increased production of IL-1β, TNF and IFNs (161). Interestingly, the involvement of inflammaging has been further supported by recent studies in which long-term administration of anti-inflammatory agents increased longevity (162). Beyond inflammation and its contribution to aging process, there are many findings on how aging-related changes in one tissue can lead to aging-specific deterioration of other tissues, which explains the inter-organ synchronized coordination of the aging phenotype in an organism (146). Apart from the inflammatory cytokines that can act in a paracrine manner to affect neighbor cells, senescent cells can induce senescence in neighboring cells via gap junction-mediated cell-cell contacts and processes involving ROS (163).

2.2. DNA Damage Response (DDR)

Preservation of genomic integrity is a prerequisite for proper cell function, but genomic stability can be insulted by various environmental factors or by the chemical properties of DNA itself, which eventually causes aging or cancer (164). In fact, increased genomic instability due to impairment of DNA repair mechanisms is one of the main characteristics of aging. DNA lesions can be caused by environmental agents, such as ultraviolet (UV) light and ionizing radiation, as well as numerous genotoxic chemicals, reactive oxygen species (ROS), generated by respiration and lipid peroxidation and spontaneous hydrolysis of nucleotide residues (165). Transcription and translation are dramatically affected by DNA lesions as replication over unrepaired DNA can induce mutations, which may initiate and propagate cancer or aging. Additionally, blockage of transcription by severe lesions can cause cellular senescence and hence accelerating aging (166). For these reasons, the organisms have developed a sophisticated network of DNA damage response (DDR) systems, including DNA repair mechanisms, damage tolerance processes and cell-cycle checkpoint pathways, whose impairment leads to age-related pathologies and severe cancer susceptibility (167).

The wide diversity of DNA lesion types necessitates multiple and largely distinct DNA-repair mechanisms, which are illustrated in Figure 9. In summary, in mismatch repair (MMR), the organism detects a mismatch or/and point insertion/deletion in a DNA strand and makes a single-strand incision in this place which is then acted upon by nuclease, polymerase and ligase enzymes (168); in base-excision repair (BER), a DNA glycosylase enzyme detects the damaged base and removes it before nuclease, polymerase and ligase proteins complete the repair, which they also perform in single-strand break repair (SSBR) (169,170). During double-strand break repair (DSBs), non-homologous end-joining (NHEJ) and homologous recombination (HR) mechanisms are used: in NHEJ, DSBs are recognized by kinases which recruit and activate end-processing enzymes, polymerases and DNA ligases, while HR is restricted to S and G2 phase because it uses sister-chromatid sequenced as the template to mediate accurate repair (171). The nucleotide excision repair (NER) system recognizes helix-distorting base lesions and excises the damaged lesion in a way that will be explained in the next section (172).

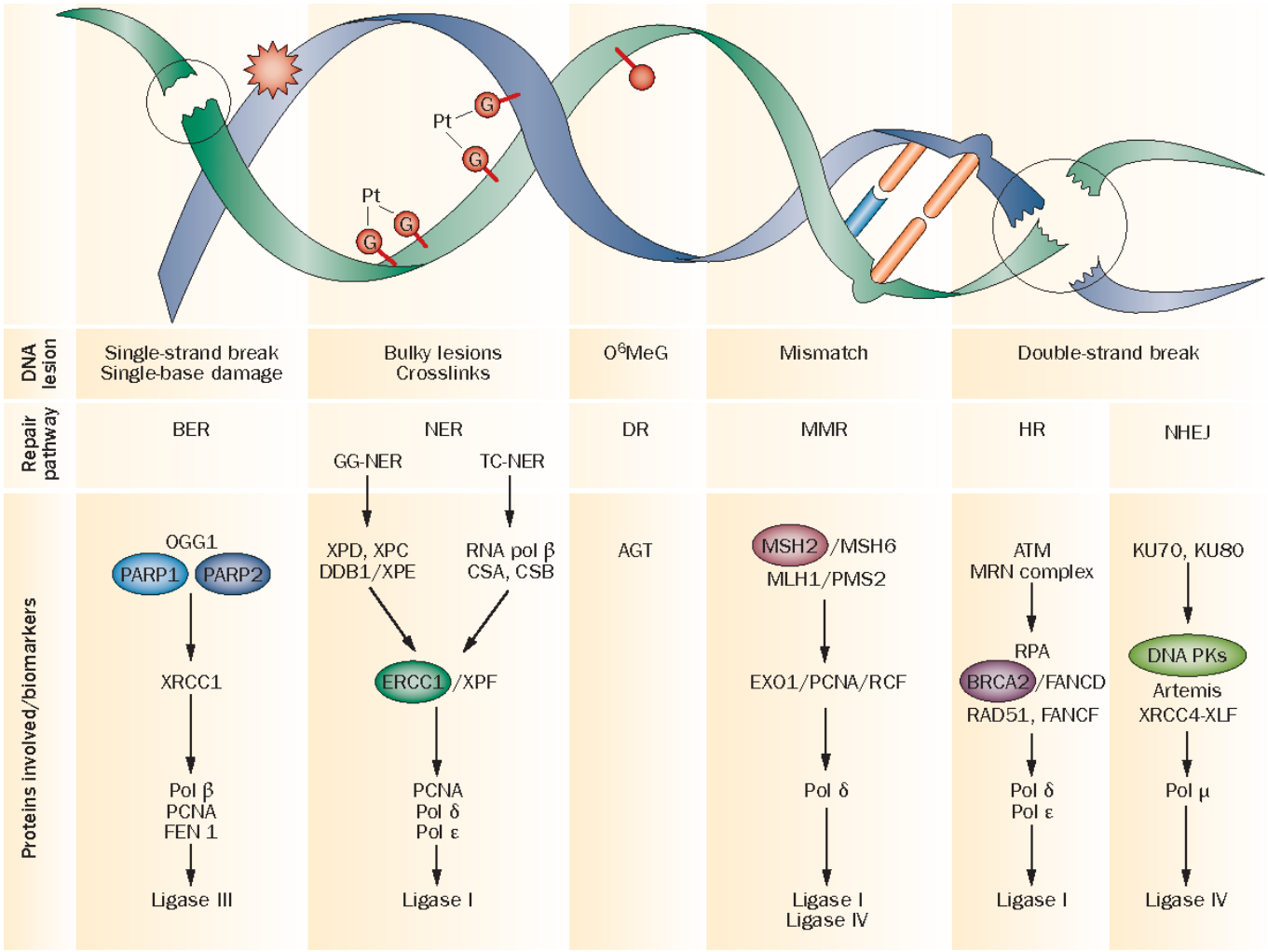

Figure 9. **Main DNA lesions and corresponding DNA damage repair pathways**. DNA lesions that affect a single strand without significantly disrupting the helical structure are generally repaired by BER, whereas DNA damage significantly distorting the DNA helix is repaired by NER. DR copes with small chemical changes affecting a single base, and MMR repairs mismatches in the pairing of DNA caused by replication errors. Finally, HR and NHEJ, although distinct pathways, are both involved in the repair of DNA double-strand breaks: HR allows 'error free' repair of the lesion whereas NHEJ is an 'error prone' mechanism that repairs DNA, but at the cost of introducing mutations into the genome. The selection of HR or NHEJ is primarily based on the phase of the cell cycle and the expression, availability and activation of DNA-repair proteins. [Abbreviations: AGT, O6-alkylguanine-DNA alkyltransferase; ATM, ataxia telangiectasia mutated; BER, base excision repair; DR, direct repair; GG-NER, global genome NER; HR, homologous recombination; 06MeG, O6-methylguanine; MMR, mismatch repair; NER, nucleotide excision repair; NHEJ, non-homologous end joining; TC-NER, transcription-coupled NER] (173).

2.2.1. Nucleotide Excision Repair (NER)

Among the plethora of DNA repair mechanisms, NER is the one responsible for the removal of bulky, helix distorting DNA adducts, as it senses the distortion caused to the DNA double helix and excises a short oligonucleotide spanning the lesion (174). The way NER recognises and eventually excises the area of the lesion is outlined in Figure 10 below. Briefly, once the damaged DNA strand is detected, a dual incision is performed, one on either side of the lesion so that the lesion-bearing oligonucleotide is removed. This is followed by the synthesis of a new DNA strand using the undamaged complementary strand as a template and it is eventually ligated to the contiguous strand (175). The correct activity of NER relies on the well-orchestrated activities of about 30 proteins, which participate in one or both of the different modes of NER, namely Global Genome NER (GG-NER) and Transcription-Coupled NER (TC-NER) (176). The basic difference between these two subpathways lies in the way of the detection of the lesion spot. In the GG-NER, the entire genome is examined for disturbed base-pairing associated with structural changes to nucleotides, while TC-NER is activated when RNA polymerase II is stalled during transcript elongation by a lesion in the template strand (177). Moreover, these two subpathways differ from each other in terms of the DNA point of correction, as GG-NER repairs damages to DNA not undergoing transcription, while TC-NER damages to the transcribed regions of DNA (178).

The essential role of NER is proven by the severity of NER deficiency syndromes, such as Xeroderma Pigmentosum (XP), Cockayne syndrome (CS) and Trichothiodystrophy (TTD), which systemically affect the organism, hence posing a devastating impact on human health. NER deficiencies can rise from germ-like mutations in genes encoding for any factor involved in the two subpathways, a fact that renders NER deficiencies inheritable (179). Although these genes have been identified, the reason why different molecular defects in the same pathway lead to such diverse pathologies remains unknown.

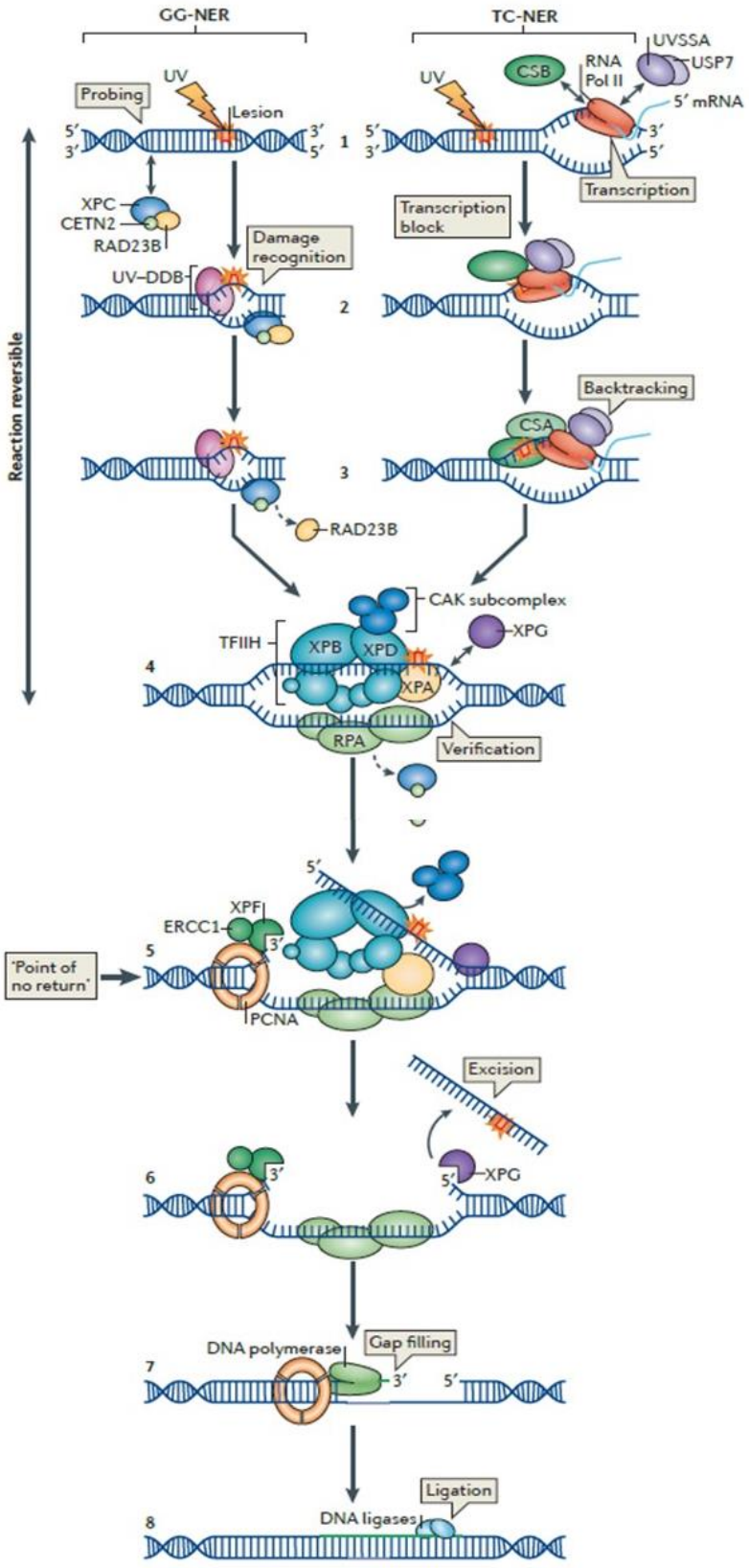

Figure 10. **Nucleotide excision repair.** In the global genome nucleotide excision repair (GG-NER; left) subpathway, the damage sensor XPC, in complex with UV excision repair protein RAD23 homologue B (RAD23B) and centrin 2 (CETN2), constantly probes the DNA for helix-distorting lesions (step 1, left), which are recognized with the help of the UV–DDB (ultraviolet (UV) radiation–DNA damage-binding protein) complex (step 2, left). Upon binding of the XPC complex to the damage, RAD23B dissociates from the complex (step 3, left). In the transcription-coupled NER (TC-NER; right) subpathway, damage is indirectly recognized during transcript elongation by the stalling of RNA polymerase II (RNA Pol II) at a lesion. During transcript elongation UV-stimulated scaffold protein A (UVSSA), ubiquitin-specific-processing protease 7 (USP7) and Cockayne syndrome protein (CSB) transiently interact with RNA Pol II (step 1, right). Upon stalling at a lesion, the affinity of CSB for RNA Pol II increases (step 2, right) and the Cockayne syndrome WD repeat protein CSA–CSB complex is formed, which probably results in reverse translocation (backtracking) of RNA Pol II (step 3, right) that renders the DNA lesion accessible for repair. RNA Pol II and the nascent mRNA transcript are not depicted further. After damage recognition, the TFIIH (transcription initiation factor IIH) complex is recruited to the lesion in both GG-NER and TC-NER (step 4). In NER, the XPG structure-specific endonuclease, either associated with TFIIH or separately,

binds to the pre-incision NER complex (step 4). Upon binding of TFIIH, the CAK (CDK-activating kinase) subcomplex dissociates from the core TFIIH complex. The helicase activity of TFIIH further opens the double helix around the lesion, and 5´–3´ unwinding of the DNA by the TFIIH basal transcription factor complex helicase subunit XPD verifies the existence of lesions with the help of the ATPase activity of the TFIIH XPB subunit and XPA, which bind to single-stranded, chemically altered nucleotides (step 4). In this step the single-stranded DNA binding protein replication protein A (RPA) is also recruited and coats the undamaged strand. XPA recruits a structure specific endonuclease -the XPF–ERCC1 heterodimer- which is directed to the damaged strand by RPA to create an incision 5´ to the lesion (step 5). Once this 'point of no return' is reached, XPG is activated and cuts the damaged strand 3´ to the lesion, which excises the lesion within a 22–30 nucleotide-long strand (step 6). The trimeric proliferating cell nuclear antigen (PCNA) ring, which is directly loaded after the 5´ incision by XPF–ERCC1, recruits DNA Pol δ, DNA Pol κ or DNA Pol ε for gap-filling DNA synthesis (step 7). Gap filling can begin immediately after the 5´ incision is made. The NER reaction is completed through sealing the final nick by DNA ligase 1 or DNA ligase 3 (step 8) (177).

In general, mutations that exclusively affect the GG-NER subpathway are associated with skin cancer, as in XP syndrome, whereas mutations exclusively affecting the TC-NER subpathway contribute to more complex developmental and neurological disorders, as in CS and TTD syndromes, which have mainly mutations of *CSA* or *CSB* proteins (180). The three main NER disorders are outlined in Table 7. Briefly, XP was the first human disease to be identified that is caused by a deficiency in NER (181) and it is a rare human, autosomal-inherited, skin and neurodegenerative disease in which exposure to sun can result in a high incidence of skin and basal cell carcinomas and melanomas (179). These symptoms begin in early life with the first exposure of the organism to the sunlight and the frequency of melanomas, anterior eye cancers and tongue cancers is increased by 1000-fold or more in patients with XP under 20 years old (182). Lifespan of XP patients is strongly dependent on accumulated sun exposure and quality of care, but these patients are also prone to developing neurological degeneration. On the other hand, CS is mainly a developmental and neurological disorder, as CS patients have dramatically reduced lifespan, but it is not linked to an increased incidence of cancer (183). The main characteristics of CS patients is cachectic dwarfism and growth retardation, retinopathy, microcephaly, deafness, neural defects, demyelination and ganglial calcifications (183). The average lifespan of these patients is only 10-12 years, which describes CS as a segmental progeroid disorder, although there have been reported

patients that have survived until their 40s (184,185). TTD is also a rare autosomal recessive disorder characterized by brittle, Sulphur-deficient hair and ichthyosis, with patients presenting an unusual facial appearance with protruding ears and receding chin, as well as with impaired mental abilities (180).

Characteristic*	Xeroderma pigmentosum (XP)	Trichothiodystrophy (TTD)	Cockayne syndrome (CS)
Genes	*XPA-V* and *XPV*	*XPB*, *XPD*, *TTDN1*[‡] and *TTDA*	*CSA*, *CSB*, *XPD* and *XPG*
Clinical features			
Cutaneous photosensitivity	++	– or +	+
Pigmentation disturbances	+	–	–
Corneal abnormalities	++	–	–
Oral abnormalities	+	–	–
Actinic keratoses	+	–	–
Skin cancer (basal, squamous and melanoma)	++	–	–
Neurological degeneration[§]	– or +	–[§]	++
Slow growth rate	– or +	++	++
Impaired sexual development	– or +	– or +	+
Sensorineural deafness	– or +	– or +	++
Mental retardation	– or +	++	++
Ichthyosis	–	– or +	–
Brittle (sulphur-deficient) hair	–	++	–
Peculiar facies	–	+[‖]	+
Retinopathy	–	–	++
Dental caries	–	+	++
Mental retardation	– or +	++	++
Ichthyosis	–	– or +	–
Brittle (sulphur-deficient) hair	–	++	–
Peculiar facies	–	+[‖]	+
Retinopathy	–	–	++
Dental caries	–	+	++
Lifespan	Reduced	6 yrs (median)[‖]	12.25 yrs (mean)[‖]
Cellular features			
Hypermutability	++	To be determined	To be determined
Global genome repair[¶]	++	– or +	–
Transcription-coupled repair[¶]	++	– or +	++
UV sensitivity	++	+	+
ROS sensitivity	–	Unknown	+

Table 7. **Clinical and cellular features of nucleotide excision repair disorders** (179).

2.2.1.1. Ercc1-XPF

Although GG-NER and TC-NER differ from one another in ways discussed in the previous section, once the damage is recognised, the repair reactions of these two sub-pathways are identical, namely the helix is locally unwound by the TFIIH complex and bound by XPA and RPA proteins which ensure correct positioning of two endonucleases, ERCC1-XPF and XPG (186). More specifically, ERCC1-XPF is a structure-specific endonuclease required to incise the damaged strand of DNA 5' to the lesion (187). This incision creates a 3' end that is used as a primer by the replication machinery to replace the excised nucleotide. For this, XPF is necessary to catalyse the activity with its conserved nuclease domain and ERCC1 is required for binding to DNA (188).

Apart from its essential role in NER, ERCC1-XPF structure also participates in additional DDR pathways, such as DSBs and DNA interstrand crosslinks (ICLs) (189). Moreover, a fraction of ERCC1-XPF is localized at telomeres, where it is implicated in the recombination of telomeric sequences and loss of telomeric overhangs at deprotected chromosome ends (190).

Deficiency of either ERCC1 or XPF in humans results in a variety of conditions, which include the skin cancer-prone disease Xeroderma Pigmentosum (XP), a progeroid syndrome of accelerated aging, or cerebro-oculo-facio-skeletal syndrome (COFS) (191). In fact, the first cases of human *ERCC1-XPF* deficiency were in 2006 (192), where the patient presented with dramatic progeroid symptoms due to a severe XPF mutations and 2007 (186), where the patient displayed a relatively mild impairment of NER due to low copy numbers of ERCC1, but with severe symptoms, including intrauterine growth retardation, microcephaly with premature closure of fontanels, bilateral microphthalmia, blepharophimosis, high nasal bridge, short filtrum, micrognathia, low-set and posterior-rotated ears arthrogryposis with rocker-bottom feet, flexion contractures of the hands and bilateral congenital hip dislocation. There was also mild hypoplasia of the kidneys, with normal structure and function. The patient died in early infancy.

These diseases are extremely rare in the general population and therefore mice with low levels of either ERCC1 or XPF as well as of other NER-associated proteins have been generated and studied extensively. These murine models clearly illustrate the importance of DNA repair in preventing aging-related tissue degeneration (191).

2.3. Animal mouse models of aging

To understand the biological significance of NER-associated proteins, a lot of genetically modified, mainly knock-out, mice have been generated. Their genetic modifications and their phenotype –with focus on the Cockayne-like pathology- are outlined below in Table 8.

Mutant mouse	NER-defect	Life span	Life span in absence of XPA	Principal features
CS				
Csa$^{-/-}$	TC-NER	>2 years	3 weeks	UV-hypersensitive skin and eyes, photoreceptor loss, increased sensitivity to γ-irradiation, mild neurodegenerative changes
Csb$^{m/m}$	TC-NER	>2 years	3 weeks	UV-hypersensitive skin and eyes, photoreceptor loss, increased sensitivity to γ-irradiation, mild neurodegenerative changes, mild age-related weight loss, reduced fat tissue
XP/CS				
Xpb^{XPCS}	Partial TC-NER partial GG-NER	>2 years	3–4 weeks to 2 years	UV-hypersensitive skin and eyes
Xpd^{XPCS}	TC-NER partial GG-NER	2 years	3 weeks	UV-hypersensitive skin and eyes, severe skin cancer predisposition, mild neurodegenerative changes, mild age-related weight loss, reduced fat tissue
Xpg$^{-/-}$	TC-NER GG-NER	3 weeks	ND	Severe post-natal growth deficiency (>50% reduced weight at 3 weeks), post-natal neurodegenerative changes, reduced size internal organs, absence of subcutaneous fat
Xpg$^{D811STOP/D811STOP}$	TC-NER GG-NER	4–5 weeks	ND	Post-natal growth deficiency (20–40% weight loss at 3 weeks), reduced size internal organs, absence of subcutaneous fat
Xpg$^{\Delta ex15/\Delta ex15}$	TC-NER GG-NER	>2 years	4–5 weeks	No changes reported
XP				
Xpa$^{-/}$	TC-NER GG-NER	>2 years	–	UV-hypersensitive skin and eyes, skin cancer predisposition, increased mutation frequencies; no or very mild nervous system changes
Xpc$^{-/-}$	GG-NER	>2 years	Unaltered	UV-hypersensitive skin and eyes, skin cancer predisposition, increased mutation frequencies; no or very mild nervous system changes
Xpg$^{D811A/D811A}$	Partial TC-NER partial GG-NER	>2 years	Unaltered	No change reported
Xpg$^{R791A/R791A}$	TC-NER GG-NER	>2 years	ND	UV-hypersensitive skin and eyes
TTD				
Xpd^{TTD}	Partial TC-NER partial GG-NER	≤2 years	3 weeks	TTD-like brittle hair, grey hair and hair loss, anemia, mild osteoporosis, signs of accelerated aging in multiple tissues, reduced weight
XFE				
Xpf$^{m/m}$	ND	3 weeks	ND	UV-hypersensitive skin and eyes, severe skin cancer predisposition, mild neurodegenerative changes, mild age-related weight loss, reduced fat tissue
Ercc$^{-/-}$	TC-NER GG-NER	3 weeks	ND	Severe growth deficiency (>50% reduced weight at 3 weeks), abnormalities in multiple tissues, absence of subcutaneous fat, progressive neurodegenerative changes and motor symptoms
Ercc1$^{-/-}$	TC-NER GG-NER	20–24 weeks	ND	Growth deficiency (40–50% reduced weight at 3 weeks), abnormalities in multiple tissues, reduced subcutaneous fat progressive neurodegenerative changes and motor symptoms
CS + CS				
Csa$^{-/-}$/*Csb*$^{m/m}$	TC-NER	>2 years	–	Same phenotype as single mutant *Csa*$^{-/-}$ and *Csb*$^{m/m}$
CS + XP				
Csb$^{m/m}$/*Xpa*$^{-/-}$ *Csb*$^{m/m}$/*Xpc*$^{-/-}$	TC-NER GG-NER	3 weeks	–	Severe post-natal growth deficiency (>50%), no subcutaneous fat, abnormalities in multiple organs, retinal degeneration, neurodegenerative changes and motor symptoms
XP/CS + XP				
Xpb^{XPCS}/*Xpa*$^{-/-}$	TC-NER GG-NER	3–4 weeks to 2 years	–	10% reduced weight, mild neurological abnormalities, premature kyphosis, loss of subcutaneous fat, no subcutaneous fat, abnormalities in multiple organs, retinal degeneration
Xpd^{XPCS}/*Xpa*$^{-/-}$	TC-NER GG-NER	3 weeks	–	Severe post-natal growth deficiency (>50%), no subcutaneous fat, abnormalities in multiple organs, neurodegenerative changes and motor symptoms
Xpg$^{\Delta ex15/\Delta ex15}$/*Xpa*$^{-/-}$	TC-NER GG-NER	4–5 weeks	–	Post-natal growth deficiency (20–40% weight loss at 3 weeks),
TTD + XP				
Xpd^{TTD}/*Xpa*$^{-/-}$	TC-NER GG-NER	3 weeks	–	Severe post-natal growth deficiency (>60% weight loss at 3 weeks), exacerbated skin and hair abnormalities; absence of subcutaneous fat; hypersensitivity to oxidative stress
XP/CS + TTD				
Xpd^{XPCS}/*Xpd*^{TTD}	TC-NER GG-NER	2 year	24 weeks	Attenuated TTD features of *Xpd*^{TTD} mice, attenuated skin cancer predisposition of *Xpd*^{XPCS}, attenuated growth deficiency and premature death of double mutant

Table 8. **Principal features of Cockayne syndrome and related NER-deficient mice** (modified by 194).

2.3.1. Excision Repair Cross Complementation Group 1 (ERCC1) deficiency

Mice with *Ercc1* deletion were generated, by interruption of exons leading to almost complete truncation of the protein (194,195). Weeda *et al.,* 1997, generated the second knock-out mouse by inserting a neomycin resistance cassette into exon 7 of ERCC1, which led to undetected ERCC1 mRNA in these mice, hence disrupting the helix-hairpin-helix motif required for the interaction of ERCC1 with XPF (194). Although *Ercc1* KO mice are viable in a mixed genetic background (FVB/C57BL/6J), they show postnatal growth retardation, weighing only 20% of their WT littermates' weight and premature death (before weaning). More specifically, the liver of *Ercc1*$^{-/-}$ mice is mainly affected showing symptoms of hepatic failure, namely hepatocellular polyploidy, hyperchromatic and enlarged hepatic nuclei as well as G2 arrest, which is the primary cause of premature death, as suggested by studies correcting *Ercc1* deletion specifically in the liver of these mice (196). *Ercc1*$^{-/-}$ mice also show progressive neurodegeneration, including ataxia and trembling (192), renal insufficiency (195) and dysfunction of various organs, such as skin, liver and bone marrow as well as loss of muscle mass and strength (sarcopenia), a hunchback spine (kyphosis) and on a cellular level, they suffer from premature replicative senescence and oxidative stress sensitivity (194). Overall, the phenotypes of this mouse, outlined in Table 9, are reminiscent of an aged organism and since they appear early on in life, this model is used to recapitulate progressive progeroid phenotypes. Interestingly, when *Ercc1* mutant mice were subjected to dietary restriction, their lifespan was extended, delaying aging, attenuating accumulation of genome-wide DNA damage and preserving transcriptional output, likely contributing to improved cell viability (156).

Symptom	*Ercc1*$^{-/-}$	*Ercc1*$^{-/\Delta}$	Human Aging
Loss of subcutaneous fat	+	+	+
Atrophic epidermis	+	+	+
Hearing loss	+	+	+
Visual impairment	+	+	+
Tremors	+	+	+
Ataxia	+	+	+
Cerebral atrophy	+	+	+
Hypertension	?	?	+
Renal acidosis	+	+	+
Bone marrow degeneration	+	+	+
Osteoporosis	+	+	+
Kyphosis	+	+	+
Dystonia	+	+	-
Sarcopenia	+	+	+
Frailty	+	+	+
Urinary Incontinence	?	+	+
Disc degeneration	+	+	+
Maximum Lifespan	4 weeks	28 weeks	120 years

Table 9. **Table listing the symptoms of aging-related phenotypes observed in *Ercc1*$^{-/-}$ mice at 4 weeks of age, *Ercc1*$^{\Delta/-}$ mice at 28 weeks of age and normal human aging at >120 years old.** (+) indicates presence and (−) indicates absence of the symptom (modified by 192).

To further investigate the DNA repair function of ERCC1 protein *in vivo,* the generation of a mouse model with *Ercc1* dysfunction, but prolonged lifespan compared to the one of *Ercc1*$^{-/-}$ mice, was needed. For this reason, a new mouse model was engineered in which a premature stop codon was inserted at position 292 of mouse ERCC1 protein, which caused a C-terminal deletion of the last 7 amino acids of the protein, hence leading to partial truncation of ERCC1 (194). Homozygous *Ercc1*^{*292} (also referred to as *Ercc1*$^{\Delta/\Delta}$) mice lived up to 6 months

showing similar defects to the ones of *Ercc1*$^{-/-}$ mice (194). Hypomorphic *Ercc1*$^{\Delta/-}$ mice were made by a combination of *Ercc1*$^{\Delta/\Delta}$ and *Ercc1*$^{-/-}$ mice and they have an even prolonged lifespan of 7 months in mixed genetic background (197). However, they still develop age-related phenotypes, such as tremors, kyphosis and ataxia, growth retardation, neurodegeneration, liver dysfunction as well as other symptoms outlined in Table 9, and reviewed in Dollé *et al,* 2011(156). Interestingly, *Ercc1*$^{\Delta/-}$ mice develop osteoporosis and intervertebral disc degeneration, characterized by reduced flexibility of the spine, pain, reduced mobility, loss of disc height and degenerative structural changes in the vertebral bodies mainly due to reduced matrix proteoglycans synthesis and enhanced osteoclastogenesis, as well as accumulation of apoptotic cells, DNA damage and senescence-associated secretory phenotype (198,199). However, there were no observations on symptoms resembling arthritis, despite findings showing an association between osteoarthritis and low levels of ERCC1 in patients (200).

To allow further dissection of the role of ERCC1 in the age-related pathology of *Ercc1*-mutant mice, mice with tissue-specific deletions have been generated, using the loxP-Cre system. More specifically, a floxed allele of ERCC1 was generated by inserting loxP sites in introns 2 and 5, so that Cre recombinase excises exons 3-5 of the ERCC1 locus (201). Several tissue-specific *Ercc1*-mutant mice have been reported. Skin-specific *Ercc1* deletion, using the K5Cre promoter which is specific for keratinocytes, led to dramatic hypersensitivity to UV-B irradiation-induced skin carcinogenesis (201). Hepatocyte-specific *Ercc1* deletion *in vitro* caused cytoplasmic lipid accumulation, damaged mitochondria as well as increased oxidative damage-induced apoptosis (202). Neural-specific *Ercc1* deletion in liver-corrected *Ercc1* knockouts, using the promoter of the neurofilament gene, nestin, showed no significance between the cerebellum development of *Ercc1*- deficient mice compared to WT, although these mice developed neurological defects, such as ataxia. However, the neural-specific *Ercc1* mutant mice developed uraemic encephalopathy, a brain disease resulting from kidney failure, suggesting that renal failure may trigger the neurological phenotype observed in *Ercc1* mutant mice (203). Melanocyte-specific *Ercc1* deletion caused unexpected colonic obstructive disorder, resembling late-onset Hirschsprung's disease, mainly because the promoter used, apart from the melanocytes precursors, is also expressed in additional neural crest lineages that differentiate into cells comprising the parasympathetic nervous system that innervates the gastrointestinal tract and control gut peristalsis (204). Neuron-specific

Ercc1 ablation, using the αCaMKII promoter which is specific for post-mitotic neurons, caused learning impairment, cognitive decline and neurodegeneration mainly due to age-dependent decrease in neuronal plasticity (205). Tissue-specific deletion of *Ercc1* in early and adult hematopoietic stem cells, using the Tie-2 promoter, revealed molecular mechanisms on how *Ercc1* deficiency leads to bone marrow deficiency (206). *Ercc1* ablation specifically from adipose tissue, using the aP2 promoter which targets adipocytes, led to steady loss of fat depots due to necrotic cell death and release of damage-associated molecular patterns (DAMPS) which eventually led to lipodystrophy (207). Interestingly, this study showed that the defective fat tissue secreted high levels of pro-inflammatory factors, such as TNF and IL-6, which were initiated by the deregulated adipocytes *per se* and not the activated macrophages, suggesting that persistent DNA damage triggers induction of pro-inflammatory cytokines and ultimately creates a microenvironment with chronic inflammation (207).

3. RA and aging

As discussed in the previous section, persistent DNA damage is thought to be a major contributor to cellular senescence and aging. Immune aging is a central component of advancing age and leads to the loss of immune system integrity, which causes higher predisposition to infections and a permanent risk for chronic inflammation and pathogenesis of autoimmune diseases (208). The link between RA and aging has been studied in the past, yet there are still various questions unanswered.

3.1. TNF and aging

Aging has been associated with increased levels of circulating cytokines, such as IL-6 that was initially found elevated in plasma/serum levels in elderly people (209). Some studies have even found that TNF is increased in elderly populations (210). More specifically, serum circulating levels of TNF have been found to be associated with mortality, indicating that TNF has specific effects in frail people (211). Although increases in inflammatory markers, such as IL-6, TNF and CRP are only 2- to 4-fold, hence the characteristic age-related low-grade inflammation, they still act as inflammatory markers and are strong predictors of all-cause mortality risk, as they possess specific biological activities (212). This low-grade inflammatory activity is caused by a dysregulated cytokine production, which is further exacerbated to be age-associated pathology (213).

Molecularly, NF-κB –which is directly associated with inflammatory conditions- is upregulated in aging in specific tissues and a shift occurs in the ratio of naive to memory T cells, with associated changes in the cytokine profile that favor increases in inflammatory cytokines such as TNF, IL-1, IL-6, IFNγ and TGF-β (214). The dependence of aging on inflammation is indicated by NF-κB deletion in mouse models of progeria (*Ercc1* KO mice), which showed significant delay in their age-related pathologies, mainly due to reduced oxidative stress and senescence (215). Moreover, there are findings suggesting an enhanced sensitivity to inflammation with aging (214) thus giving some explanations as to why older people could be prone to RA.

Interestingly, recent findings of Karakasilioti *et al*., 2013 (207) suggested the inter-relationship between persistent DNA damage and pro-inflammatory cytokines. More

specifically, DNA damage was sufficient to trigger, apart from the aging phenotype, the expression of pro-inflammatory cytokines via histone post-translational modifications, further suggesting that the transcriptional derepression of pro-inflammatory genes requires DDR signaling in adipocytes, a cellular population with mesenchymal origin (216). Ultimately, the gradual accumulation of irreparable DNA lesions leads to aging-like adipocyte degeneration which is related to chronic auto-inflammatory response (207).

3.2. Premature aging in RA

Rheumatoid Arthritis is characterized by premature aging mainly involving accelerated immunosenescence, shortened telomeres, DNA damage accumulation, as well as an excess of pro-inflammatory cytokines (217,218). In fact, RA patients have difficulties in maintaining genomic integrity due to accumulation of DNA lesions and impaired DNA repair mechanisms (219). A special focus has been given on T cells derived from RA patients, which on the one hand appear premature aged with shortened telomeres and accumulation of DNA damage, but on the other hand with accelerated growth due to their ability to reverse cell cycle arrest, which overall show a suppressed DDR pathway and a disrupted G2/M cell cycle checkpoint (220). Autoimmunity in RA has been proposed as a consequence of immunodegeneration associated with age-inappropriate remodeling of the T cell pool (221).

Although there have been a lot of findings in isolated T-cells derived from RA patients, our knowledge on possible aging of other key cellular players in RA or how aging could contribute to RA aetiopathogenesis is still poor.

3.3. Aging in mesenchymal cells

Mesenchymal cells, such as cells from umbilical cord blood, connective tissue, skin, synovium, fat and other organs have an aging-specific phenotype similar to other cell types derived from aged people (222). Aged mesenchymal cells are reportedly bigger *in vitro* than their younger counterparts, which is an indication of senescence (223). Moreover, they show no spindle-formed morphology in culture as well as diminished ability to proliferate and decreased telomeres (224). Regarding their secretion profile, aged mesenchymal cells secrete senescence markers *in vitro*, such as IL-6, IL-11, IL-7, BMP2/4, TGF-β, ICAM-2, and NFκ (222).

Aims

TNF drives pathways involved in the development of Rheumatoid Arthritis, Rheumatoid Arthritis-associated heart pathologies and aging. The aim of this research was to investigate the interplay between these pathologies in the TghuTNF (Tg197) arthritis model. Tissues of mesenchymal origin, that is synovial fluid and heart valve, have been suggested to adopt a common pro-inflammatory phenotype upon disease, which are highly conserved with fibroblast driving disease processes. For this reason, we mainly focused on the role of mesenchymal cells in the development of these three pathologies.

More specifically, we initially aimed to investigate possible correlations between the accumulation of genetic damages in DNA, due to deficits of DNA Damage Response, and specifically of NER (*Ercc1)*, and the development of RA-like pathology in the TghuTNF arthritis mouse model. Furthermore, we sought to study how mesenchymal-specific *Ercc1* deficiency would –and how- intervene in this pathology. Based on recent studies that have shown that accumulation of DNA damage in tissues of mesenchymal origin, and more specifically the adipose tissue, leads to chronic inflammation and lipodystrophy, we investigated whether accumulation of DNA damage in the synovial membrane, another tissue of mesenchymal origin, would cause chronic inflammation, hence RA-like symptoms.

Subsequently, we aimed to investigate whether TghuTNF mouse also develops, similarly to human RA patients, comorbid heart pathology. We further studied if mesenchymal compartment plays a role in the development of cardiovascular comorbidities, so we could explore cellular and molecular mechanisms linking arthritis to comorbid cardiac diseases. Finally, we investigated the interplay between mechanisms of aging and RA-related cardiovascular diseases in the TghuTNF arthritis model.

In summary, although little is known about the interrelationship of aging, RA and RA-associated cardiac diseases, we sought to investigate whether we could find possible common mechanisms driving these three different conditions.

Materials and methods

Mice

Tg197 (23), *ColVI-Cre* (24), *Tnfr1*$^{fl/fl}$ (94)**,** *Tnfr1*$^{cneo/cneo}$ (93) and TgA86 (225) mice are previously described; *Rosa26*$^{mT/mG}$ mice (96) were purchased from the Jackson Laboratory, FVB mice were purchased by Envigo, UK. *Ercc1*$^{\Delta/+}$ and *Ercc1*$^{+/-}$ (194), as well as *Ercc1*$^{fl/fl}$ (201) mice were kindly provided by Prof. J.H.J. Hoeijmakers' lab (Erasmus, Netherlands) and by Prof. G. Garinis' lab (IMBB, Heraklion, Crete). Tg197, *ColVI-Cre, Tnfr1*$^{fl/fl}$, *Tnfr1*$^{cneo/cneo}$, TgA86 and *Rosa26*$^{mT/mG}$ mice were kept either at C57BL6J or at a F1 CBA/C57BL6J hybrid background. *Ercc1*$^{\Delta/-}$ mice were obtained by crossing *Ercc1*$^{+/-}$ (in the C57BL6J background) with *Ercc1*$^{\Delta/+}$ mice (in the FVB background) to yield *Ercc1*$^{\Delta/-}$ with an F1 C57BL6J/FVB hybrid background. Mice were maintained in the animal facilities of Biomedical Sciences Research Center (BSRC) "Alexander Fleming", under SPF conditions. The animal facility was under a 12:12-h light/dark cycle at a constant temperature of 22 ± 2°C and relative humidity of ~60%. For anti-TNF treatment, Tg197 mice were treated twice weekly from 4 to 11 weeks of age with 10mg/kg Remicade (Infliximab, Janssen Biotech). All mice were handled according to the guidance of the Institutional Animal Care and Use Committee of BSRC "Alexander Fleming". All mice were observed for morbidity and euthanized when needed according to animal welfare guidelines. Experimental termination time points for Tg197 mice were set to a maximum of 12 weeks of age, except for the case of the survival curve experiment, where the mice were sacrificed when their mortality reached 50%.

Clinical and histopathological arthritic assessment

The evaluation of the severity of arthritis symptoms was performed clinically and histopathologically in a semi-quantitative manner, as previously described (226). Briefly, clinical arthritis score ranged from 0 to 3, with 0 indicating no symptoms, 1 indicating mild arthritis, 2 moderate and 3 severe arthritis. Histopathological arthritis assessment was performed in sections of the ankle joints of the mice in a similar manner. Briefly, the scoring system ranged from 0 to 4, with 0 indicating no symptoms, 1 indicating synovial hyperplasia, 2 pannus formation and bone erosion, 3 cartilage destruction and bone erosion and 4 extensive pannus, cartilage and bone erosion.

Collagen Antibody Induced Arthritis

In the Collagen Antibody Induced Arthritis (CAIA) model, arthritis was stimulated through the administration of 2-8 mg of a cocktail of monoclonal antibodies (Arthritomab Antibody Cocktail [CIA-MAB-2C], MD-Biosciences) that were directed to conserved auto-antigenic epitopes of collagen type II, followed by endotoxin challenge, according to Khachigian, 2006 (227). A LPS injection was performed 3 days after the initial disease induction step to boost the protocol. The mice started developing pathology characterized by severe inflammation of front and hind limbs after 4-5 days post antibody injection and the pathology reached its peak on days 8-10. The incidence was 90-100% and symptoms persisted up to two weeks after the induction. Clinical evaluation was performed in a modified scoring system of the one of chronic polyarthritis (0 to 4 for each limb; each mouse is scored by the sum of the four limbs, i.e. total 0 to 16). Histopathological evaluation was performed the same way to the one performed for chronic polyarthritis features.

Antibodies

Antibodies used for immunohistochemistry included: Gr-1, F4/80 (MCA2387GA; MCA497, AbD Serotec), B220 (553084, BD Pharmigen), CD3 (ab1669, Abcam). Antibodies used for FACS or immunofluorescence included: CD45 (103128), CD31 (102420), CD90.2 (105316), CD105 (120414), Podoplanin (127411), CD106/VCAM-1 (105717) and PDGFRa/CD140a (135905) from Biolegend, CD29 (47-0291-80, eBioscience) and CD54/ICAM1 (553253, BD Pharmigen). For the intracellular staining, the antibody used was Vimentin (ab92547, Abcam).

Immunohistochemistry and immunofluorescence

Paraffin-embedded transverse heart sections were stained with Hematoxylin/Eosin (H&E) staining, Masson's Trichrome staining and with specific antibodies in combination with the Vectastain Elite ABC HRP and the Vectastain DAB kits (Vector Laboratories) and images were acquired with Leica DM2500 microscope equipped with Leica SFL4000 camera (Leica Microsystems). Heart transverse OCT cryosections were imaged using a TCS SP8X White Light Laser confocal system (Leica).

Genotyping PCR

Mouse line	Primers name	DNA sequence
Tg197	HTNFglobin s	5' - TAC-CCC-CTC-CTT-CAG-ACA-CC - 3'
	HTNFglobin a	5' - GCC-CTT-CAT-AAT-ATC-CCC-CA - 3'
ColVI-Cre	ACPR s	5' - ATT ACC GGT CGA TGC AAC GAG T - 3'
	ACPR a	5' - CAG GTA TCT CTG ACC AGA GTC A - 3'
Tnfr1$^{fl/fl}$	mp55 3 lox s	5' - CAAGTGCTTGGGGTTCAGGG - 3'
	mp55 3 lox a	5' - CGTCCTGGAGAAAGGGAAAG - 3'
Tnfr1$^{cneo/cneo}$	p55neo s	5' - TGGTGGCCTTAAACCGATCC - 3'
	p55neo a	5' - AGAGAGGTTGCTCAGTGTGAGGC - 3'
	Neo s	5' - ATGATTGAACAAGATGGATTGCAC - 3'
TgA86	TgA86 s	5' - TAA TGG GCA GGG CAA GGT GG - 3'
	TgA86 a	5' - TTC ACT TCC GGT TCC TGC ACC CT - 3'
Rosa26$^{mT/mG}$	Rosa 26 mTmG (oIMR7318)	5' - CTCTGCTGCCTCCTGGCTTCT - 3'
	Rosa 26 mTmG (oIMR7319)	5' - CGAGGCGGATCACAAGCAATA - 3'
	Rosa 26 mTmG (oIMR7320)	5' - TCAATGGGCGGGGGTCGTT - 3'
Ercc1$^{\Delta/-}$	Ercc1d exon7	5' - AGC CGA CCT TAT GGA AAC - 3'
	Ercc1d intron7	5' - ACA GAT GCT GAG GGC AGA CT - 3'
	Ercc1d neo	5' - TCG CCT TCT TGA CGA GTT CT - 3'
	Ercc1d 3utr	5' - CTA GGT GGC AGC AGG TCA TC - 3'
Ercc1$^{fl/fl}$	432E	5' - TGC AGA GCC TGG GGA AGA ACT TCG C - 3'
	F25732	5' - TCA AAG TAT GGT AGC CAA GGC AGC - 3'

Table 10. **Primer sequences for genotyping of the mouse lines used**

Genomic DNA was isolated from tail segments. Genotypes were determined by PCR, using the primers outlined in Table 10.

Quantification of valvular thickness

To quantify adult valve thickness, the widest portion of the valve leaflets was measured in H&E-stained transverse heart sections using the ImageJ software (NIH). Four independent measurements were taken per leaflet in a blinded to the genotype fashion from 3 consecutive sections. The values were averaged and a minimum of three animals were used per genotype for statistical analysis.

Echocardiography and Electrocardiography

Echocardiography assessment was performed in the Department of Pharmacology, Medical School NKUA, Greece as previously described (228). Briefly, mice were sedated with intraperitoneal injection of ketamine-midazolam cocktail and, after chest hair removal, they were placed on a heated platform to maintain the body temperature at 37^{o}C. Echocardiographic images in parasternal short and long axes were acquired using a Vivid 7 version Pro ultrasound system (GE Healthcare, Wauwatosa, Wisconsin), equipped with a 14.0-MHz probe (i13L). Recordings were made when heart rate was 300-450 BPM, in a blinded to the genotype fashion. Parameters assessed include LVEDd, LVEDs, LVLd, LVPWd, IVSd, SVPW, LA and were measured using 2D images. The modified Simpson equation was used for the calculation of LVEDV, LVESV and EF. SVPW, determined from two-dimensional guided M-mode recordings obtained at the midventricular level, was used to assess the regional contractile function of the LV myocardium, while EF% was used to determine the global contractile LV function. For the analysis, all measurements (except for EF and SVPW) were normalized with the body weight of each mouse. Doppler analysis was used to determine velocities of the aortic, mitral and pulmonary valve. ECGs were performed during echocardiography. Three ECG leads (I, II, AVf) were recorded via three electrode pads attached to the 3 paws (front limbs and left hind limb) of each animal. Intervals and amplitudes were evaluated from continuous recording of at least 15 ECG signals in the beginning, the middle and the end of the whole procedure. Heart rate was calculated by the ultrasound system used.

Isolation and culturing of SFs and VICs

SFs were isolated as previously described (229) and cultured up to the 3rd-4th passage when they were used for sequencing. VICs were isolated from the valve leaflets of mice according to a modified protocol (143). Briefly, hearts were dissected to remove their myocardial area surrounding the valves and the part that contains the

valve leaflets was cut into 1-2 mm pieces and digested for 10 min at 37^{o}C in HBSS containing 500U/ml Collagenase XI (Sigma-Aldrich). The digestion process was repeated for a total of 3 times and the final collected cells were plated in cell culture flasks and cultured up to the 3rd-4th passage, when they were used for cellular assays and sequencing.

Fluorescence activated cell sorting (FACS)

For intracellular stainings, cells were fixed and then permeabilized, using Fixation and Permeabilization Buffer Set (eBioscience). For whole tissue analysis, valve leaflets from *ColVI-Cre-Rosa26*$^{mT/mG}$ mice were digested with Collagenase XI (as previously described). Cell pellets were resuspended in 1ml of Gey' s solution on ice, for the removal of erythrocytes and they were subsequently resuspended in PBS supplemented with 5% FBS. FACS experiments were performed using a FACS CantoII flow cytometer (BD) and analysis was performed using the FACS Diva (BD) or FlowJo software (FlowJo, LLC).

Proliferation assay

To determine cellular proliferation, either the Cell Proliferation ELISA, BrdU kit (Sigma-Aldrich) or alamarBlue™ Cell Viability Reagent (ThermoFischer Scientific, #DAL1025) were used according to manufacturer's guidelines.

ELISA

Detection of hTNF or mTNF was performed using the hTNF or mTNF Quantikine Elisa (R&D systems).

Wound-healing assay

To determine the migratory capacity of the cells, we used the wound-healing assay as previously described (230). Briefly, cells were seeded and cultured until they reached confluency, at which point a scratch was created using a 10μl white pipette tip. The closure of the wound was live imaged using the Zeiss Axio Observer Z1 Microscope equipped with AxioCam MRm camera (Zeiss) and the percentage of wound closure was calculated for each well at 20-24 hours using the ImageJ software (NIH).

3’ RNAseq and deep sequencing

RNA-seq was performed in three biological replicates of cultured VICs and SFs isolated from Tg197 mice and WT littermates at their 8th week of age. RNA was extracted using TRIzol reagent (Invitrogen) and further purified using the RNeasy Mini Kit (Qiagen). All samples were used to a mean concentration of approximately 100-150ng/μl, measured by ND1000 Spectrophotometer (PEQLAB). The quality of the samples was measured in a bioanalyzer using the Agilent RNA 6000 Nano Kit reagents and protocol (Agilent Technologies) and only RNA samples with RNA Integrity Number (RIN) >7 were chosen for further analysis. For the preparation of the library for each sample, the 3’ mRNA-Seq Library Prep Kit Protocol for Ion Torrent (QuantSeq-LEXOGEN™ Vienna, Austria) was used. Each library’s quality and quantity were assessed in bioanalyzer using the DNA High Sensitivity Kit reagents and protocol (Agilent Technologies). The quantified libraries were processed together at a final concentration of 50pM, templated and enriched on an Ion Proton Chef instrument. Templating was performed, using the Ion PI™ IC200™ Chef Kit (ThermoFisher Scientific) and sequencing, with the Ion PI™ Sequencing 200 V3 Kit on Ion Proton PI™ V2 chips (ThermoFisher Scientific).

RNA seq analysis

The raw bam files were summarized to read counts table using the Bioconductor package Genomic Ranges (231). The gene counts table was normalized for inherent systematic or experimental biases using the Bioconductor package DESeq (232), after removing genes that had zero counts over all the RNA-Seq samples. The resulting gene counts table was subjected to differential expression analysis using the Bioconductor package DESeq and differentially expressed genes were extracted according to an absolute fold change cutoff value of 1 in log2 scale and pvalue cutoff of 0.05. All the above were performed through the Bioconductor package metaseqr (233), Volcano plots were generated in R (234) with the use of ggplot2and an in-house developed script. Venn diagrams were created with InteractiVenn (235). Functional enrichment analysis was performed with enrichr online tool (236) extracting the enriched KEGG pathways (235) with the use of a pvalue cutoff of 0.05. Alluvial diagrams were drawn with RAWGraphs (http://rawgraphs.io). Regulatory networks were inferred with the use of RNEA tool (237) and they were visualized in Cytoscape (238).

Statistical analysis

Data are presented as mean±SEM and student's t test was used for the evaluation of statistical significance, with p values <0.05 being considered statistically significant. Analysis was performed using the GraphPad Prism 6.

Results: Part I

Systemic *Ercc1* deficiency does not spontaneously induce RA-like symptoms in *Ercc1*$^{\Delta/-}$ mice

Since there is evidence suggesting that senescence plays a role in the development of RA, we investigated whether accumulation of senescent cells due to NER deficiency would cause RA-like symptoms. For this, we used *Ercc1*$^{\Delta/-}$ mice, in which the encoded protein contains a seven amino-acid carboxy-terminal truncation, leading to reduced lifespan and aging-related multiple organ dysfunction (194). As shown in Figure 11, systemic *Ercc1* deficiency did not induce any RA-like pathology, up until the age of 18 weeks, when premature deaths start being observed, as previously reported (194). More specifically, although *Ercc1*$^{\Delta/-}$ mice show significant cachexia compared to WT (Figure 11A), there is no clinical (Figure 11B) or histopathological signs (Figure 11C, D) of arthritis *in vivo* up until the age of 18 weeks.

To evaluate whether SFs isolated from *Ercc1*$^{\Delta/-}$ mice acquire an arthritogenic phenotype, we assessed their proliferative and migratory capacity (Figure 11E, F). Interestingly, although SFs isolated from *Ercc1*$^{\Delta/-}$ mice at the age of 12 weeks did not show significant differences in their migratory capacity compared to WT (Figure 11F), they had comparable proliferative capacity to arthritogenic hyperproliferative SFs isolated from Tg197 (Figure 11E). However, this hyperproliferative feature was not sufficient to induce pannus formation and hence RA-like pathology in *Ercc1*$^{\Delta/-}$ mice (Figure 11D).

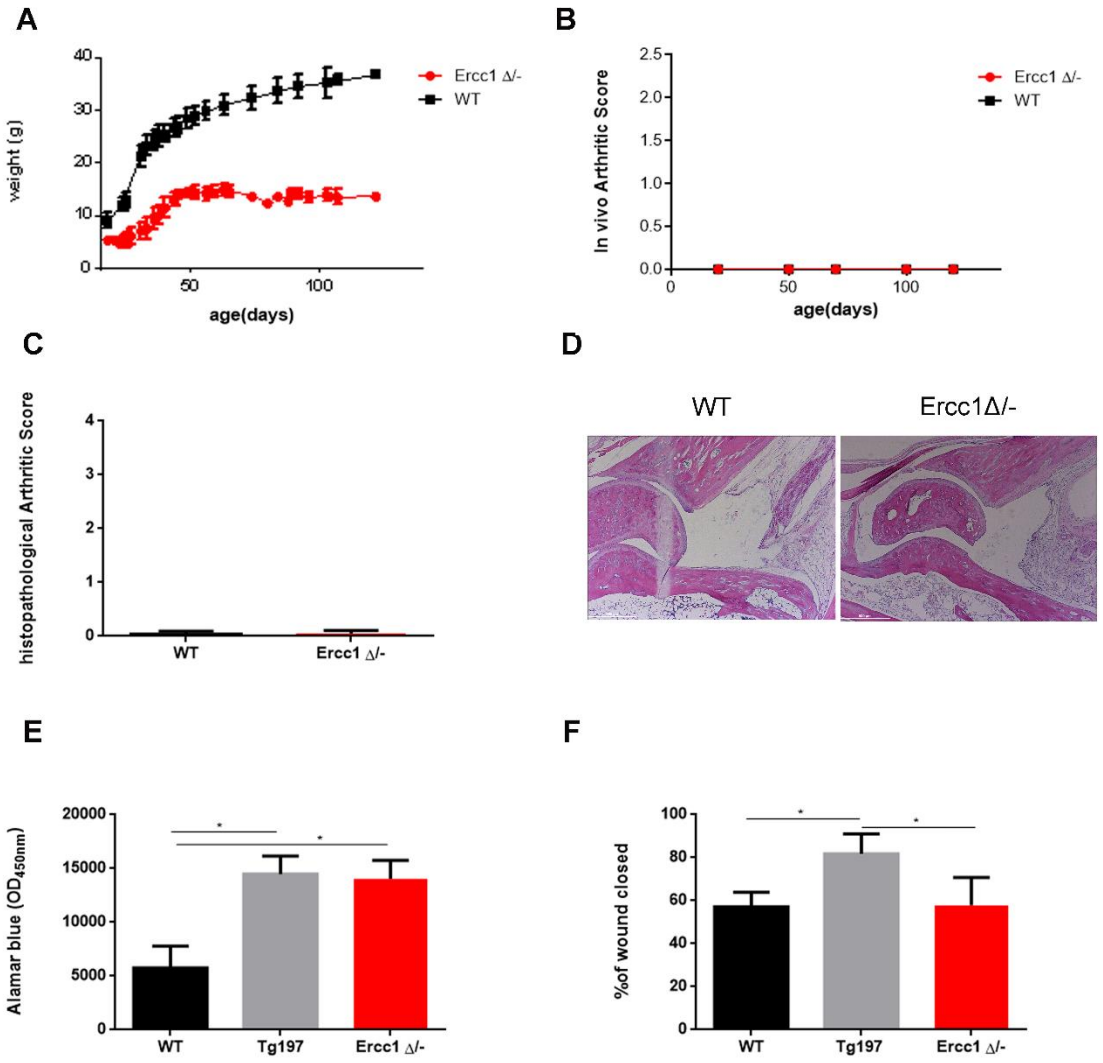

Figure 11. **Systemic *Ercc1* deficiency does not spontaneously induce RA-like symptoms. (A)** Comparison of the body weight between WT and *Ercc1*$^{\Delta/-}$ mice until the age 18 weeks (data are presented as mean± SEM). **(B, C)** Comparison of the *in vivo* **(B)** and the histopathological **(C)** arthritic score between WT and *Ercc1*$^{\Delta/-}$ mice at the age 18 weeks of age (data are presented as mean± SEM). **(D)** Representative images of H&E-stained ankle joint sections of WT and *Ercc1*$^{\Delta/-}$ mice at 18 weeks of age. **(E, F)** Levels of Alamar Blue absorbance **(E)** and wound healing ability calculated by percentage of wound closure **(F)** of SFs isolated from WT, as a negative control, Tg197, as a positive control, and *Ercc1*$^{\Delta/-}$ mice at the age of 12 weeks of age (data are presented as mean± SEM, *n*=3 from three individual experiments; *, P<0.02).

Systemic *Ercc1* deficiency does not affect RA-like symptoms in Tg197 mice

Although we detected no signs of spontaneous arthritis symptoms in *Ercc1*$^{\Delta/-}$ mice, we investigated whether accumulation of senescent cells would interfere with the arthritic phenotype of Tg197 mice. For this reason, we crossed Tg197 mice with *Ercc1*$^{\Delta/-}$ mice and we evaluated the severity of chronic polyarthritis developed in these mice. As seen in Figure 12A, Tg197 *Ercc1*$^{\Delta/-}$ mice show greater cachexia than Tg197 alone, which is probably due to the systemic accumulation of DNA damage. Although a significant difference between Tg197 and Tg197 *Ercc1*$^{\Delta/-}$ at 8th week of age is observed at the clinical evaluation of arthritis (Figure 12B), the histopathological score did not reflect any significant differences between Tg197 and Tg197 *Ercc1*$^{\Delta/-}$ mice (Figure 12C, D). Since systemic cachexia is one of the parameters evaluated in the clinical evaluation of arthritis symptoms, the discrepancy between clinical and histopathological scorings may be attributed to the worsened cachectic phenotype of Tg197 *Ercc1*$^{\Delta/-}$ mice due to *Ercc1* deficiency.

To evaluate possible differences between SFs isolated from Tg197 and Tg197 *Ercc1*$^{\Delta/-}$ mice, we isolated cells at the age of 8 weeks, where disease is already established. As expected from the *in vivo* data, there was no difference in the arthritogenic characteristics, namely hyperproliferation and high migratory capacity, of Tg197 *Ercc1*$^{\Delta/-}$ SFs compared to the ones of Tg197 SFs (Figure 12E, F). Interestingly, there was a significantly increase in secreted levels of hTNF in the supernatants of SFs isolated from Tg197 *Ercc1*$^{\Delta/-}$ compared to those of Tg197 (Figure 12G). However, this increase did not affect the severity of the disease *in vivo*. Therefore, we could conclude that systemic *Ercc1* deficiency is not able to affect the development of chronic polyarthritis symptoms in Tg197 mice.

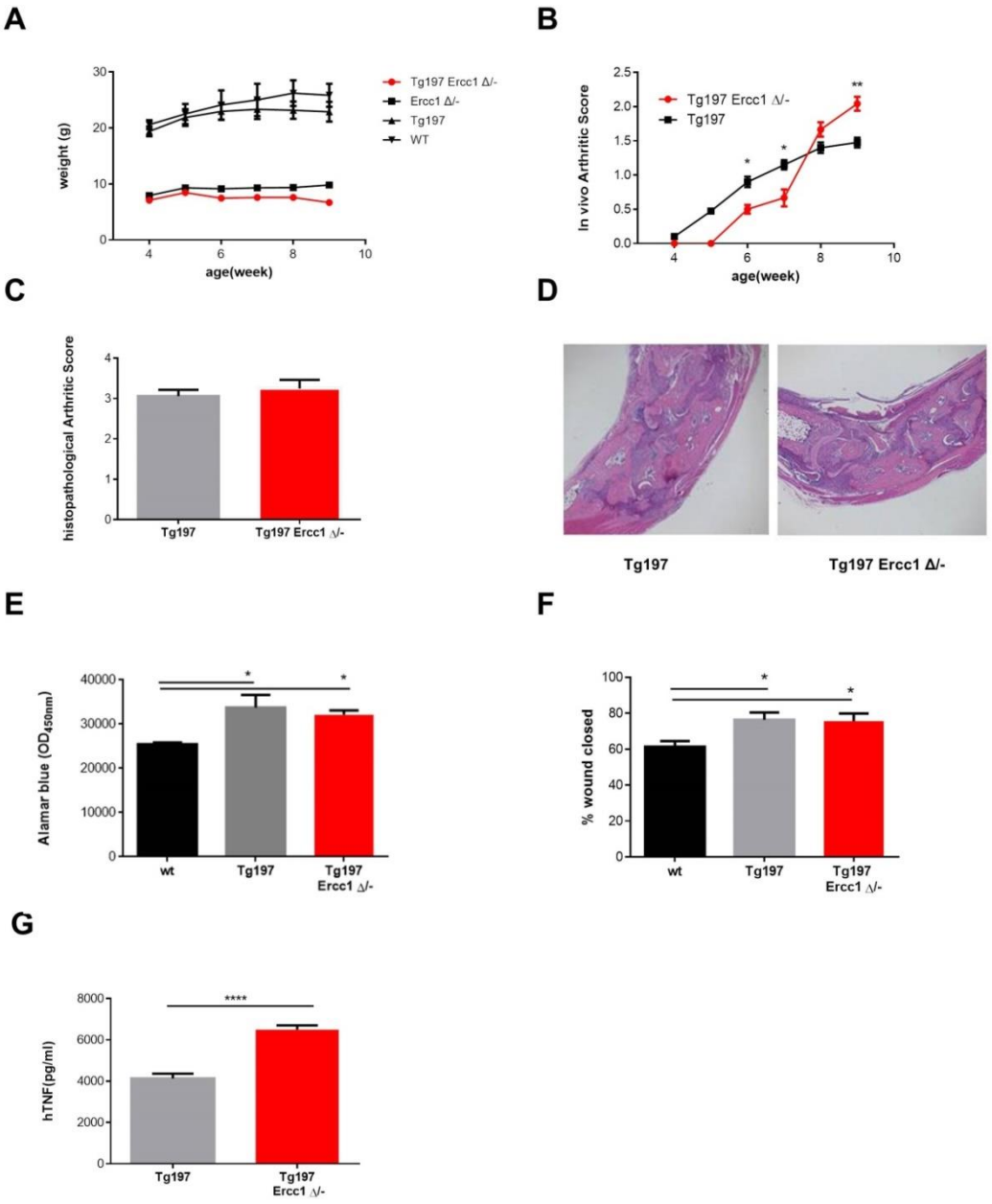

Figure 12. **Systemic *Ercc1* deficiency does not affect RA-like symptoms in Tg197 mice. (A)** Comparison of the body weight between WT, Tg197, *Ercc1*$^{\Delta/-}$ and Tg197 *Ercc1*$^{\Delta/-}$ mice until the age 9 weeks (data are presented as mean± SEM). **(B, C)** Comparison of the *in vivo* **(B)** and the histopathological **(C)** arthritic score between Tg197 and Tg197 *Ercc1*$^{\Delta/-}$ mice at the age 9 weeks of age (data are presented as mean± SEM; *, P<0.02; **, P<0.005). **(D)** Representative images of H&E-stained ankle joint sections of Tg197 and Tg197 *Ercc1*$^{\Delta/-}$ mice at 9 weeks of age. **(E, F, G)** Levels of Alamar Blue absorbance **(E)**, wound healing ability calculated by percentage of wound closure **(F)** and secreted hTNF in the supernatants **(G)** of SFs isolated from Tg197 and Tg197 *Ercc1*$^{\Delta/-}$ mice at the age of 8 weeks of age (data are presented as mean± SEM, *n*=3 from three individual experiments; *, P<0.02; ****, P<0.0001).

Mesenchymal-specific *Ercc1* deficiency causes slight cachexia, without inducing RA-like symptoms

As DNA damage causes dysfunction to the mesenchymal-origin adipocytes, leading to chronic inflammation and lipodystrophy (207), we sought to address whether mesenchymal-specific *Ercc1* deficiency could cause joint inflammation and hence RA-like symptoms. To do this, we intercrossed animals homozygous for the floxed *Ercc1* allele with those carrying the *ColVI-Cre* transgene, which has been previously used to target mesenchymal cells in the joints, small intestine (24), colon (239) and other organs (92).

Firstly, *ColVI-Cre Ercc1*$^{f/-}$ mice showed reduced body weight compared to their controls (Figure 13A). The inability of these mice to gain weight in the same way as their littermates was further explored. We examined histopathologically all the tissues where *Cre* recombination has been previously reported, such as skin, intestine, muscles, adipose tissue and joints, as well as the tissues where *Cre* recombination does not occur, such as liver, lungs, heart, stomach, pancreas and kidney. The only abnormality was found in the extensor digitorum longus and tibialis anterior muscles, where we detected higher nuclear density, which is an indication of atrophic muscular microfibers (240) (Figure 13B). Therefore, there are indications that *ColVI-Cre Ercc1*$^{f/-}$ mice show some level of cachexia due to their atrophic muscles, resembling a reported phenotype caused by systemic *Ercc1* ablation (191).

We further investigated whether *ColVI-Cre Ercc1*$^{f/-}$ mice had any sings of spontaneous joint inflammation. As shown in Figure 13C, *ColVI-Cre Ercc1*$^{f/-}$ mice did not develop any inflammatory phenotype in their joints up to their 6th month of age. In agreement to this finding, SFs isolated from *ColVI-Cre Ercc1*$^{f/-}$ mice at their 6th month of age showed no difference compared to their control littermates regarding their proliferative and migratory capacities (Figure 13D, E). Therefore, DNA damage accumulation specifically in the SFs was not sufficient to induce any inflammatory phenotype that could potentially lead to the development of chronic polyarthritis.

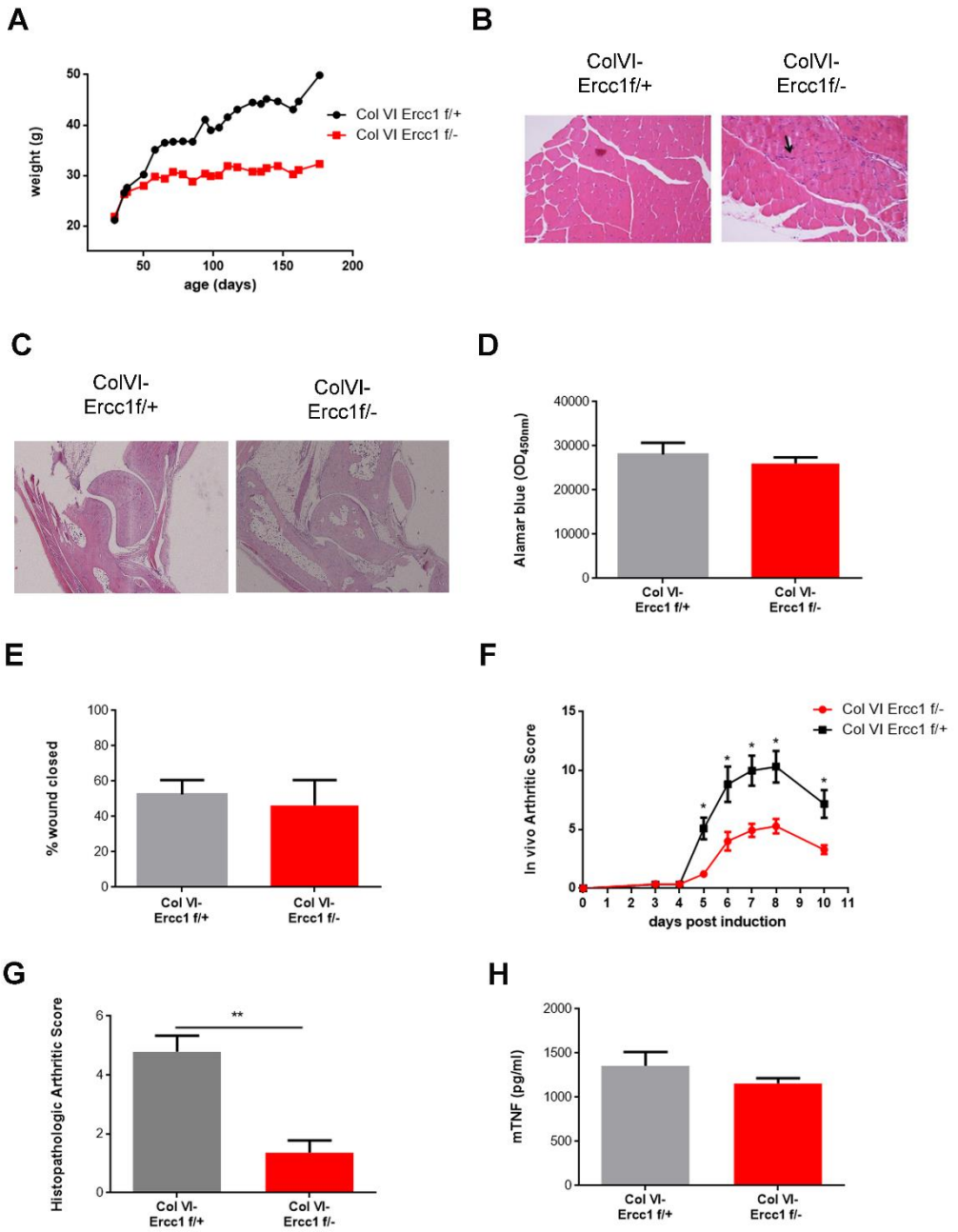

Figure 13. **Mesenchymal-specific *Ercc1* deficiency causes cachexia and amelioration of CAIA arthritis. (A)** Comparison of the body weight between *ColVI-Cre Ercc1$^{f/-}$* and *ColVI-Cre Ercc1$^{f/+}$* mice until the age of 26 weeks (data are presented as mean± SEM). **(B)** Representative images of H&E-stained tibialis anterior muscle sections of *ColVI-Cre Ercc1$^{f/-}$* and *ColVI-Cre Ercc1$^{f/+}$* mice at 26 weeks of age (black arrow indicate the higher nuclear density). **(C)** Representative images of H&E-stained of ankle joints sections of *ColVI-Cre Ercc1$^{f/-}$* and *ColVI-Cre Ercc1$^{f/+}$* mice at 26 weeks of age. **(D, E)** Levels of Alamar Blue absorbance **(D)** and wound healing ability calculated by percentage of wound closure **(E)** of SFs isolated from *ColVI-Cre Ercc1$^{f/-}$* and *ColVI-Cre Ercc1$^{f/+}$* mice at the age of 28 weeks of age (data are presented as mean± SEM, *n*=3 from three individual experiments). **(F, G)** Comparison of CAIA *in vivo* **(F)** and histopathological **(G)** arthritic score between

ColVI-Cre Ercc1$^{f/-}$ and *ColVI-Cre Ercc1$^{f/+}$* mice (data are presented as mean± SEM; *, P<0.02; **, P<0.005). **(H)** Levels of circulated mTNF in serum isolated by *ColVI-Cre Ercc1$^{f/-}$* and *ColVI-Cre Ercc1$^{f/+}$* mice 1.5hours post induction with 100μg LPS.

Mesenchymal-specific *Ercc1* deficiency ameliorates arthritis symptoms in CAIA-induced arthritis

Although our results showed that mesenchymal-specific *Ercc1* deficiency could not cause spontaneous inflammation, we investigated how *ColVI-Cre Ercc1$^{f/-}$* mice would react to the inflammatory stimulus of CAIA-induced arthritis. Unexpectedly, *ColVI-Cre Ercc1$^{f/-}$* mice showed amelioration of joint inflammation compared to their control littermates, which was evident both clinically (Figure 13F) and histopathologically (Figure 13G). To investigate whether this amelioration could be attributed to a different response of *ColVI-Cre Ercc1$^{f/+}$* and *ColVI-Cre Ercc1$^{f/-}$* mice towards LPS stimulation, we measured mTNF levels 1.5 hours post LPS induction in these mice. As seen in Figure 13H, mTNF levels are comparable between *ColVI-Cre Ercc1$^{f/-}$* mice and their control littermates. Therefore, the mechanism behind the amelioration of CAIA arthritis due to mesenchymal-specific *Ercc1* ablation remains still unclear.

Mesenchymal-specific *Ercc1* deficiency does not affect RA-like symptoms in Tg197 mice

We further investigated whether mesenchymal-specific accumulation of senescent cells would interfere with the arthritic phenotype of Tg197 mice. For this reason, we crossed Tg197 mice with *ColVI-Cre Ercc1$^{f/-}$* mice and we evaluated the severity of chronic polyarthritis developed in these mice. As shown in Figure 14, there was no significant difference between Tg197 *ColVI-Cre Ercc1$^{f/-}$* and their controls, Tg197 *ColVI-Cre Ercc1$^{f/+}$,* neither in the body weight (Figure 14A), nor in the clinical (Figure 14B) and histopathological (Figure 14C, D) features of arthritis.

To evaluate possible differences between SFs isolated from Tg197 *ColVI-Cre Ercc1$^{f/-}$* and their controls, Tg197 *ColVI-Cre Ercc1$^{f/+}$*, we isolated cells at 8 weeks of age and we observed no difference regarding the arthritogenic characteristics of Tg197 SFs (data not shown). Interestingly, there was a significantly increase in secreted levels of hTNF in the supernatants of SFs isolated from Tg197 *ColVI-Cre Ercc1$^{f/-}$* compared to those of Tg197 *ColVI-Cre Ercc1$^{f/+}$,* resembling the higher levels of Tg197 *Ercc1$^{\Delta/-}$* SFs than those of Tg197 (Figure 12G). However, as in Tg197 *Ercc1$^{\Delta/-}$* mice, this increase did not affect the severity of the disease *in vivo*. Therefore, we could

conclude that mesenchymal-specific *Ercc1* deficiency is not able to affect the development of chronic polyarthritis symptoms in Tg197 mice.

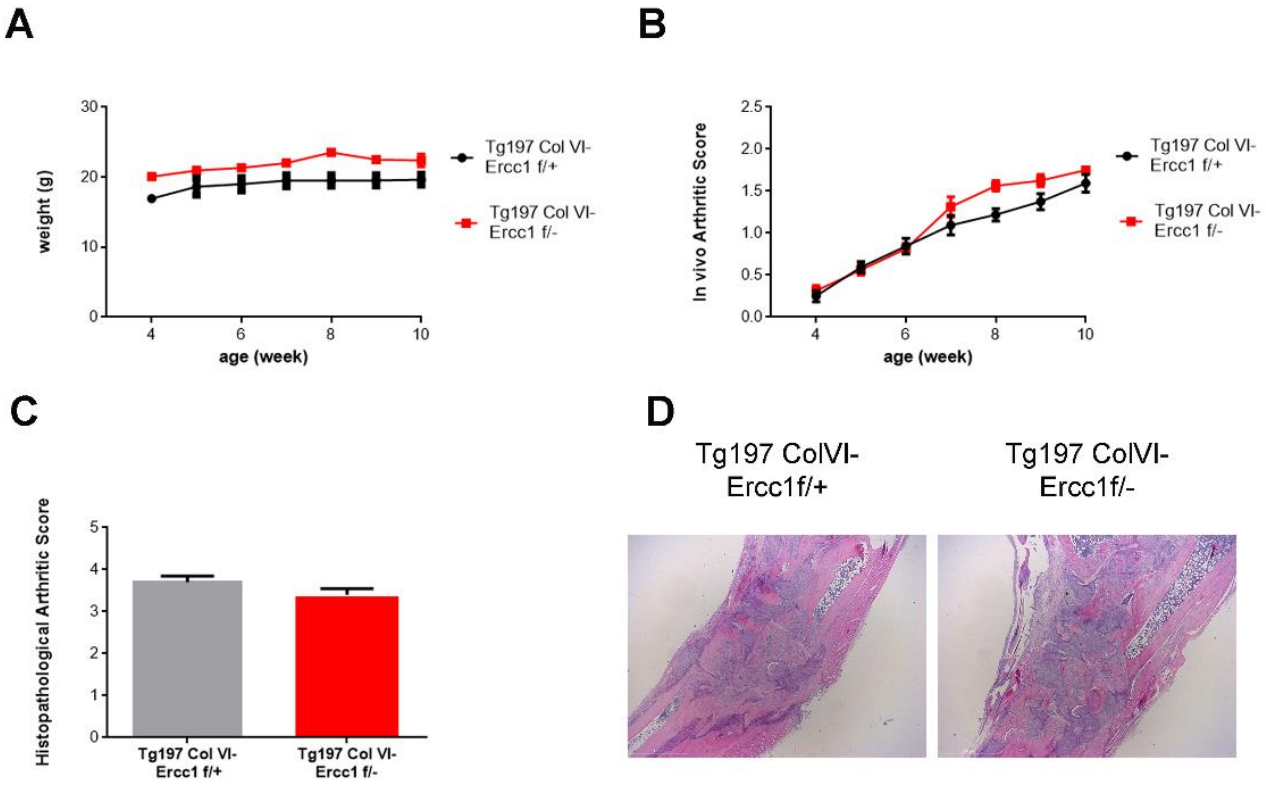

***Figure 14*. Mesenchymal-specific *Ercc1* deficiency does not affect RA-like symptoms in Tg197 mice. (A)** Comparison of the body weight between Tg197 *ColVI-Cre Ercc1*$^{f/+}$ and Tg197 *ColVI-Cre Ercc1*$^{f/-}$ mice until the age 10 weeks (data are presented as mean± SEM). **(B, C)** Comparison of the in vivo **(B)** and the histopathological **(C)** arthritic score between Tg197 *ColVI-Cre Ercc1*$^{f/+}$ and Tg197 *ColVI-Cre Ercc1*$^{f/-}$ mice until the age 10 weeks (data are presented as mean± SEM). **(D)** Representative images of H&E-stained ankle joint sections of Tg197 *ColVI-Cre Ercc1*$^{f/+}$ and Tg197 *ColVI-Cre Ercc1*$^{f/-}$ mice at the age of 10 weeks.

Discussion: Part I

Aged people show a low-grade inflammation, including higher levels of TNF compared to their younger counterparts, which could explain the higher incidence of Rheumatoid Arthritis in older people. The involvement of TNF in the pathogenesis of RA is well established; however, its role in the development of aging remains unknown. RA patients show increased mortality, as well as aged immune system, a term called immunosenescence; however, the role of aging in the pathology of RA would need further exploration.

We demonstrate here that systemic accumulation of DNA damage due to *Ercc1* deletion, which leads to a systemic premature aging phenotype, does not lead to the development of RA-like pathology in *Ercc1*$^{\Delta/-}$ mice. Although SFs isolated from joints of *Ercc1*$^{\Delta/-}$ mice showed a slight increase in their proliferative capacity, a hallmark of arthritogenic SFs, this was not sufficient to alter the homeostasis of the joint of these mice. This could be attributed to the fact that SFs from *Ercc1*$^{\Delta/-}$ mice did not show features of aging, such as non-spindle morphology and decreased proliferative capacity, therefore our initial hypothesis that aged SFs could secrete as much TNF as needed for the initiation of RA-like disease, similar to TNF-driven pathology of the TghuTNF (Tg197) arthritis model, was not confirmed. We further investigated if the progeroid syndrome of *Ercc1*$^{\Delta/-}$ mice could affect the RA-like pathology of the Tg197 model. Systemic *Ercc1* ablation did not affect the clinical or the histopathological symptoms of the disease, which was also reflected in the arthritogenic phenotype of SFs derived from Tg197 *Ercc1*$^{\Delta/-}$ mice that was not affected. Although SFs derived from Tg197 *Ercc1*$^{\Delta/-}$ secreted higher levels of hTNF compared to Tg197 SFs, this did not seem to affect the clinical features of arthritis in Tg197 *Ercc1*$^{\Delta/-}$ mice.

According to recent findings by Karakasilioti *et al.,* 2013 (207), persistent adipocyte-specific DNA damage triggers the expression of pro-inflammatory cytokines, leading to chronic inflammation and eventually to tissue degeneration. As adipose tissue and synovial membrane are of shared mesenchymal origin (241)- and likely to coexist (242)- we hypothesized that mesenchymal-specific *Ercc1* deficiency would similarly cause chronic joint inflammation, hence RA-like symptoms. For this reason, we observed *ColVI-Cre Ercc1*$^{f/-}$ mice for any clinical signs of joint inflammation and distortion. Up until their 26th week of age, *ColVI-Cre Ercc1*$^{f/-}$ animals did not show any clinical or histopathological features of RA-like pathology, such as inflammation,

pannus formation, cartilage and bone destruction. This finding was also confirmed by the *in vitro* analysis of SFs derived from the *ColVI-Cre Ercc1*$^{f/-}$ animals that did not show any signs of arthritogenicity, that is higher proliferation or migratory capacity compared to their control cells. Accordingly, the development of arthritis in Tg197 mice, when combined with *ColVI-Cre Ercc1*$^{f/-}$ animals, was not affected. On the contrary, when *ColVI-Cre Ercc1*$^{f/-}$ mice were induced with CAIA-induced arthritis, they showed an ameliorated phenotype compared to their control littermates. This amelioration due to accumulation of DNA damage could be attributed to possible senescent phenotype of SFs or/and other mesenchymal cells taking part in this induced model and it could be further studied in the future.

Interestingly, *ColVI-Cre Ercc1*$^{f/-}$ mice showed inability to gain weight as their littermates, which is probably due to the muscle atrophy that was observed. This phenotype could be further analysed, beyond this study, as it would be interesting for this mouse to be used as a model of premature muscular aging.

Results: Part II

TNF-dependent left-sided heart valve pathology develops as a comorbid condition in the Tg197 arthritis model

Histopathological evaluation of heart tissue from Tg197 animals revealed pathological alterations localised in the left side of the heart, affecting specifically the aortic (Figure 15A) and mitral valvular area (Figure 15B), while the pulmonary valve as well as the blood arteries and vessels appeared unaffected (Figure 16,17). Pathology was associated with aortic and mitral valve thickening (Figure 15C) mainly due to fibrosis, which extended to the root of the valve, as shown by the intense Masson's staining (Figure 15A, B). Inflammation appeared to have only a minimal contribution, as indicated by the limited number of infiltrating inflammatory cells in the valves at 12 weeks of age (Figure 18).

Signs of heart valve pathology were detected in the Tg197 mice already from 4 weeks of age and became progressively worse as animals aged (Figure 17) in parallel to their arthritis pathology. By 8 weeks of age, when Tg197 mice had established arthritis, pathology in both valves was manifested with 100% penetrance and without a gender bias. Treatment of Tg197 animals with the anti-TNF Infliximab (Remicade), from 4 to 11 weeks, of age resulted in the amelioration of the heart valve disease, demonstrated by the decrease in valvular thickening and fibrosis (Figure 15C, 19).

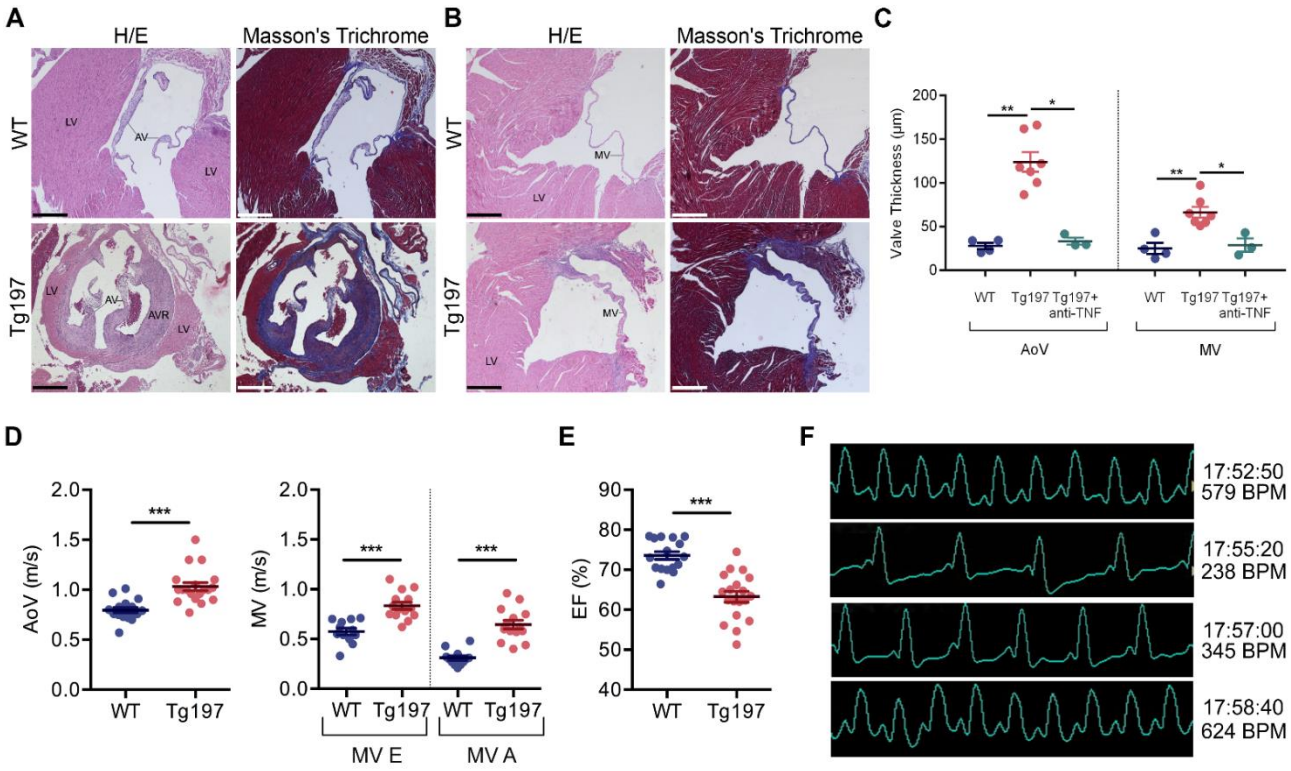

***Figure 15*. Tg197 arthritis model develops TNF-dependent left-sided heart valve disease which leads to LV dysfunction**. **(A, B)** Representative images of hematoxylin/eosin (H&E)- and Masson's Trichrome-stained transverse heart sections showing the aortic **(A)** and the mitral **(B)** valve leaflets of Tg197 and WT littermate animals at 12 weeks old of age [AV: aortic valve leaflets, LV: left ventricle, AVR: aortic valve root, MV: mitral valve leaflet] (Scale bar, 400µm). **(C)** Comparison of the aortic (AoV) and mitral valve (MV) thickness between WT, Tg197 and Tg197 treated with anti-TNF Infliximab (Remicade) animals at 11-12 weeks of age (data are presented as individual values, with mean± SEM; *, P<0.02; **, P<0.01). **(D)** Blood aortic (AoV) and mitral velocities (MV E and A) acquired by Doppler analysis of Tg197 mice and WT littermates at their 12 weeks of age (left and right panel respectively; data are presented as individual values, with mean± SEM; ***, P<0.0001). **(E)** Ejection fraction (EF%) of Tg197 mice and WT littermates at their 12 weeks of age, calculated by the modified Simpson equation, using 2D images in echocardiography analysis (data are presented as individual values, with mean± SEM; ***, P<0.0001). **(F)** Representative ECGs of Tg197 animals with few minutes interval (4 consecutive time points with ~1-minute interval, starting from the upper panel), at their 12 weeks of age.

Heart valve pathology leads to left ventricular dysfunction in the Tg197 animals

To assess whether the valvular thickening and fibrosis observed in Tg197 animals also affect their cardiac function, we performed echocardiography and electrocardiography (ECG) analysis in 12-week-old mice. Tg197 mice displayed increased aortic and mitral valve velocities (Figure 15D), indicative of valvular stenosis. Moreover, in approximately 15% of the transgenic mice examined, aortic and/or mitral regurgitation was detected (Figure 20), suggesting valvular insufficiency. An additional consequence of the mitral valve dysfunction was the observed increased atrial pressure leading to dilation of the left atrium (Table 11). Echocardiography data analysis consistently showed that Tg197 animals displayed left ventricular (LV) dilation with some degree of hypertrophy, indicated by the increased left ventricular dimensions (LVEDd, LVEDs, LVLd, LVPWd, IVSd) and the significant increase of heart-to-body weight ratio in comparison to WT mice (Table 11). Tg197 mice also exhibited significant reduction of the global cardiac function, as indicated by their reduced ejection fraction (EF%) (Figure 15E) and, more importantly, by their reduced regional contractile function reflected in the lower SVPW (Table 11).

Interestingly, we have observed that Tg197 animals exhibit increased premature mortality of unknown aetiology starting at 10 weeks of age, reaching a ~50% incidence at 13 weeks of age (Figure 21). Notably, assessment of cardiac function of Tg197 animals showed that they were prone to exhibit fatal episodes of arrhythmias in advanced disease stages (12 weeks), mainly switching from bradycardia (~200 bpm) to tachycardia (~500-650 bpm) in a few-minutes interval during ECG (Figure 15F). Therefore, arrhythmic episodes could be associated with the premature deaths observed in Tg197 animals.

Collectively, our data show that the histopathological findings in Tg197 heart valves are associated with left-sided valvular degeneration and dysfunction and are accompanied by echocardiographic findings of left ventricular cardiomyopathy.

Table 11. **Echocardiographic parameters in Tg197 and WT mice at 12 weeks of age.**

	WT (n=16)	**Tg197 (n=19)**	**P-value**
Body weight, *g*	26.25 ±1.06	16.73±0.091	<0.0001
Heart weight, *mg*	107.10±3.39	83.00±5.31	<0.0001
HW/BW, *mg/g*	4.11±0.08	5.05±0.27	0.0054
LVEDd, *mm/BW*	0.14±0.01	0.22±0.01	<0.0001
LVEDs, *mm/BW*	0.08±0.01	0.14±0.01	<0.0001
LVLd, *mm/BW*	0.28±0.01	0.38±0.01	<0.0001
LVPWd, *mm/BW*	0.026±0.001	0.038±0.002	<0.0001
IVSd, *mm/BW*	0.026±0.001	0.038±0.002	<0.0001
LA, *mm/BW*	0.083±0.003	0.132±0.006	<0.0001
SVPW, *cm/s*	3.02±0.08	2.14±0.07	<0.0001
E/A ratio	1.87±0.13	1.33±0.09	0.0009

HW/BW: Heart weight-to-body weight ratio; LVEDd: left ventricular end-diastolic diameter; LVEDs: left ventricular end-systolic diameter; LVLd: left ventricular length in diastole; LVPWd: left ventricular end-diastolic posterior wall thickness; IVSd: end-diastolic interventricular septal thickness; LA: left atrium; SVPW: systolic velocity of the posterior wall; E/A ratio: ratio between E (peak early diastolic flow) and A (peak late diastolic flow). Values were normalized with the body weight (except for SVPW), as indicated in the Table. Data are expressed as mean± SEM.

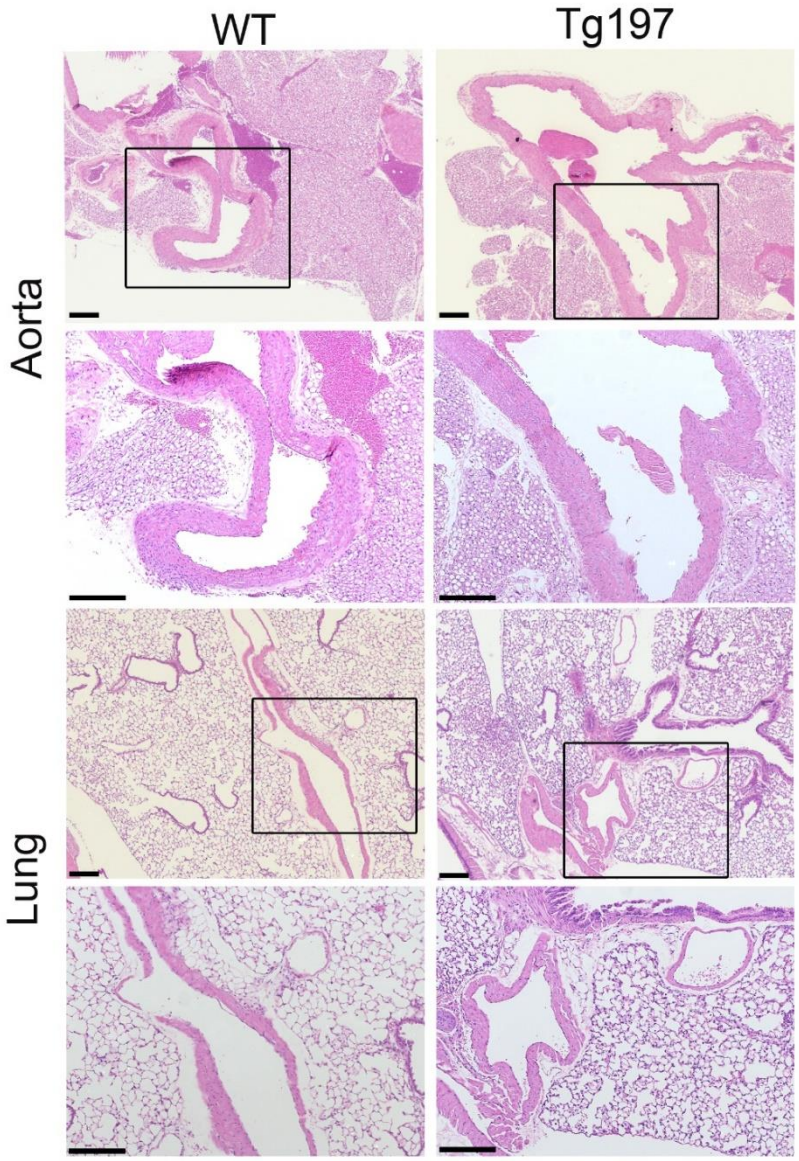

Figure 16. **Peripheral vessel wall of the arteries appears unaffected in Tg197 animals.** Representative images of hematoxylin/eosin (H&E)- stained aortic and lung sections of Tg197 and WT littermate animals at 12 weeks old of age, where vessels and arteries can be seen [lower panel: higher magnification of the upper panel part specified by the box] (Scale bar, 200μm).

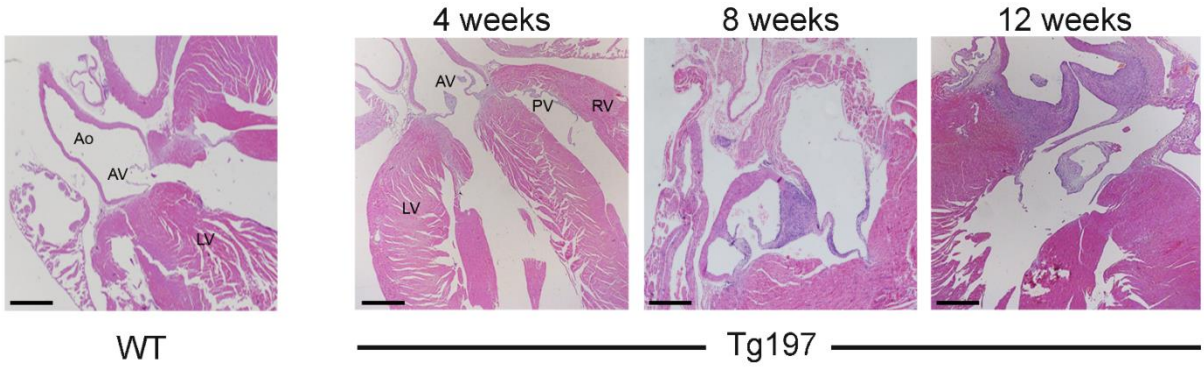

Figure 17. **Tg197 heart valve pathology progresses with time**. Representative H&E-stained longitudinal heart sections of WT animals at 8 weeks of age and Tg197 animals at 4**,** 8 and 12 weeks of age, showing the progression of the heart valve pathology. [AV: aortic valve leaflets, LV: left ventricle, MV: mitral valve leaflet, PV: pulmonary valve, RV: right ventricle; Ao: aorta] (Scale bar, 200μm).

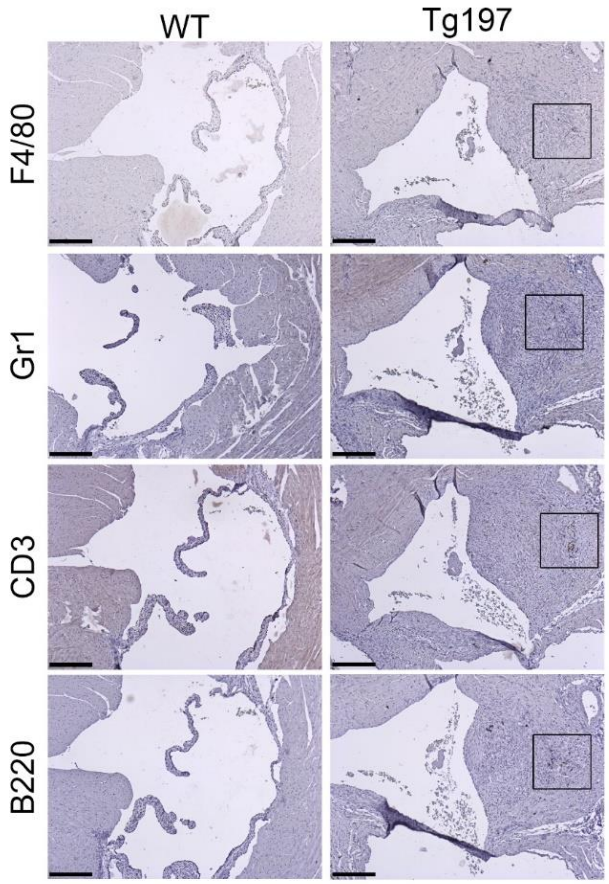

Figure 18. **Inflammation has a minimal contribution to the heart valve disease phenotype of Tg197 mice.** Representative immunohistochemical stainings for the detection of macrophages (F4/80), neutrophils (Gr1), B cells (B220) and T cells

(CD3) on transverse heart sections from WT and Tg197 hearts at 12 weeks of age (positive staining marked in boxed areas) (Scale bar, 200μm).

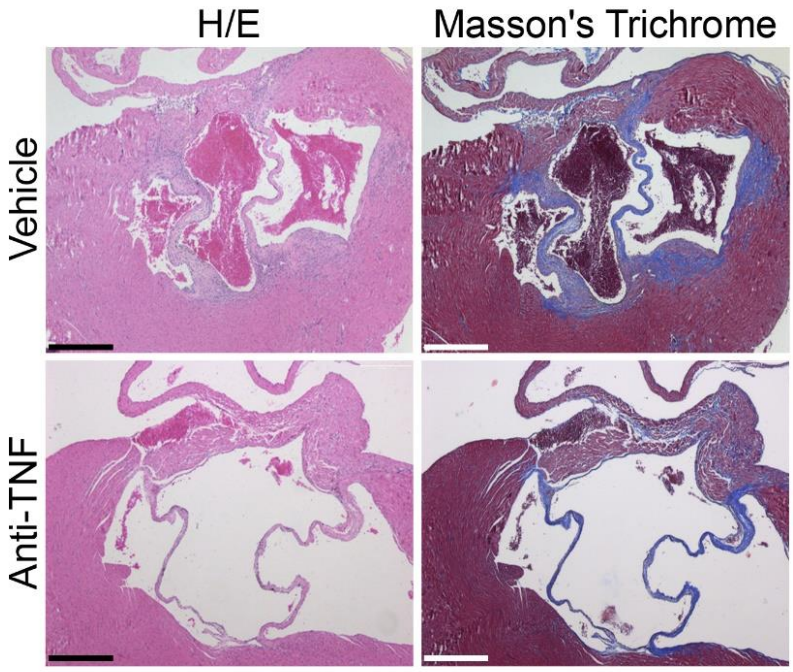

Figure 19. **Treatment of Tg197 animals with the anti-TNF Infliximab (Remicade) results in the amelioration of the heart valve pathology.** Representative images of H&E- and Masson's Trichrome-stained transverse heart sections of Tg197 animals at 11 weeks of age, treated with vehicle or prophylactic anti-TNF treatment (from 4th-11th week of age) (Scale bar, 400μm).

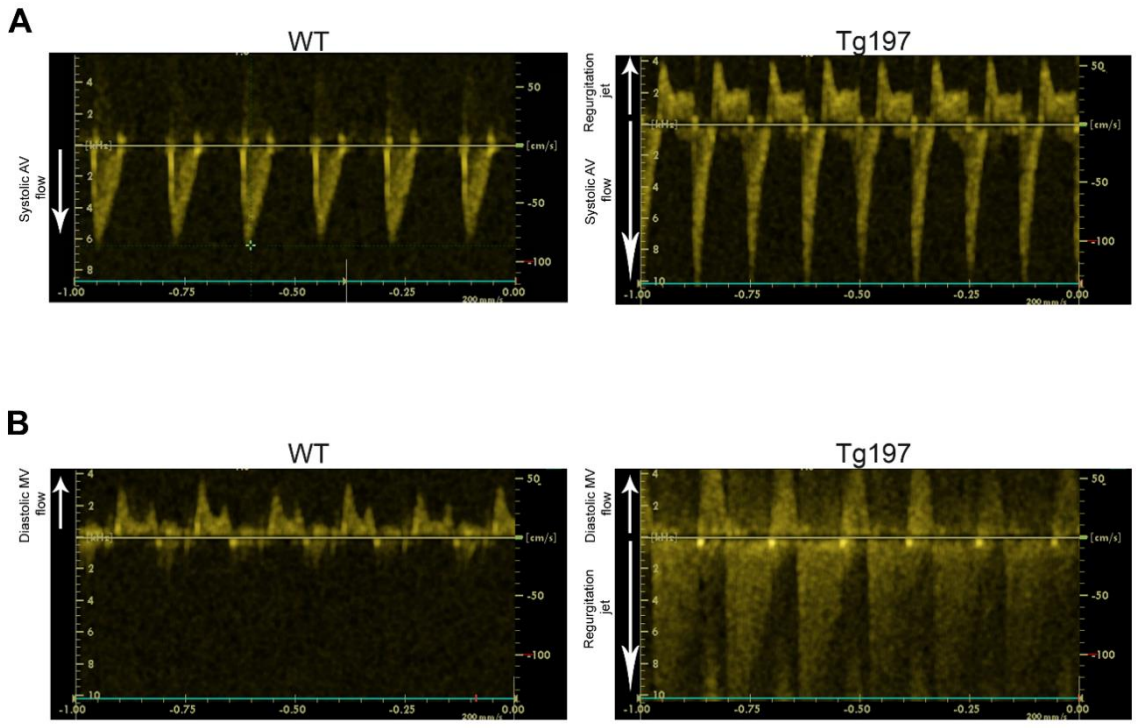

Figure 20. **Valvular regurgitation detected in Tg197 animals by echocardiographic screening.** Representative examples of aortic valve **(A)** and mitral valve **(B)** regurgitation observed in Tg197 animals at 12 weeks of age (arrows indicate the normal and the backward blood flow in healthy WT and Tg197 animals).

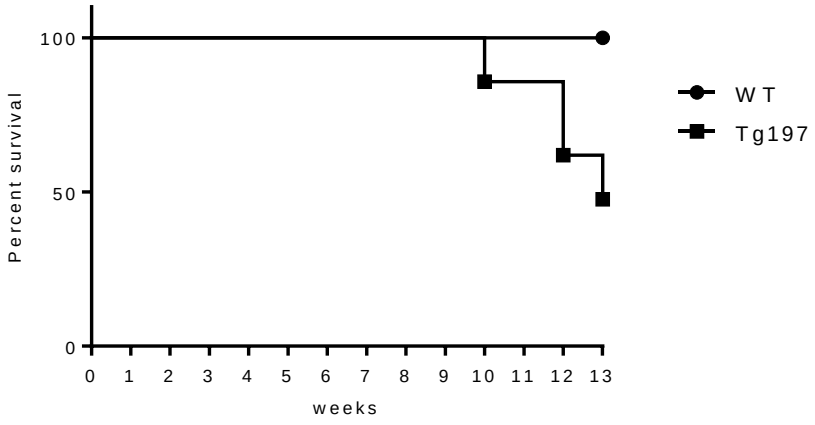

Figure 21. **Kaplan Meier survival curve of WT and Tg197 mice.** Representative survival curve (n=20) showing the premature mortality observed in Tg197 animals. (The experiment was terminated when mortality was over 50% due to ethical concerns).

Hypertrophic valves of Tg197 mice consist mainly of activated Valve Interstitial Cells (VICs)

Since SFs have been previously established as drivers of arthritogenesis in the Tg197 model (24), we investigated whether VICs play also a pathogenic role in the observed Tg197 heart valve pathology. To this end, we first crossed the reporter mouse *Rosa26*$^{mT/mG}$ which expresses GFP upon recombination, with the *ColVI-Cre* mouse, which has been previously used to target mesenchymal cells in the joints, small intestine (24), colon (239) and other organs (92). Examination of the heart valves of *ColVI-Cre-Rosa26*$^{mT/mG}$ mice revealed co-localisation of GFP expression with Vimentin (Figure 22A), a known marker of fibroblasts and VICs (142,243), indicating efficient targeting of VICs by *ColVI-Cre*, and confirming their mesenchymal origin (139). Efficient recombination was confirmed by further characterization of GFP$^+$ cells derived from dissociated heart valve tissue from *ColVI-Cre-Rosa26*$^{mT/mG}$ mice using FACS analysis. GFP$^+$ cells strongly expressed VIC and mesenchymal cell markers (Vimentin, CD29 and Podoplanin), while displaying no expression of hematopoietic (CD45) and endothelial (CD31) markers (Figure 22B). These results suggest that the *ColVI-Cre* mouse effectively targets mainly Vimentin$^+$, CD29$^+$ and Podoplanin$^+$ mesenchymal-like VICs in the heart valve.

To explore the role of VICs in the Tg197 heart valve pathology, we crossed the *ColVI-Cre-Rosa26*$^{mT/mG}$ mice with Tg197 mice. The thickened fibrotic heart valves of these mice were mainly populated by GFP$^+$ VICs (Figure 22C), supporting their central role in the heart valve phenotype. The pathogenic potential of VICs in Tg197 animals was further assessed by the expression of α-SMA, a well-established marker of activated myofibroblastic VICs (145). Interestingly, α-SMA-expressing VICs were detected in the thickened valvular area and root of Tg197 mice (Figure 22D), indicating that the pathology observed is mainly characterized by accumulation of activated VICs.

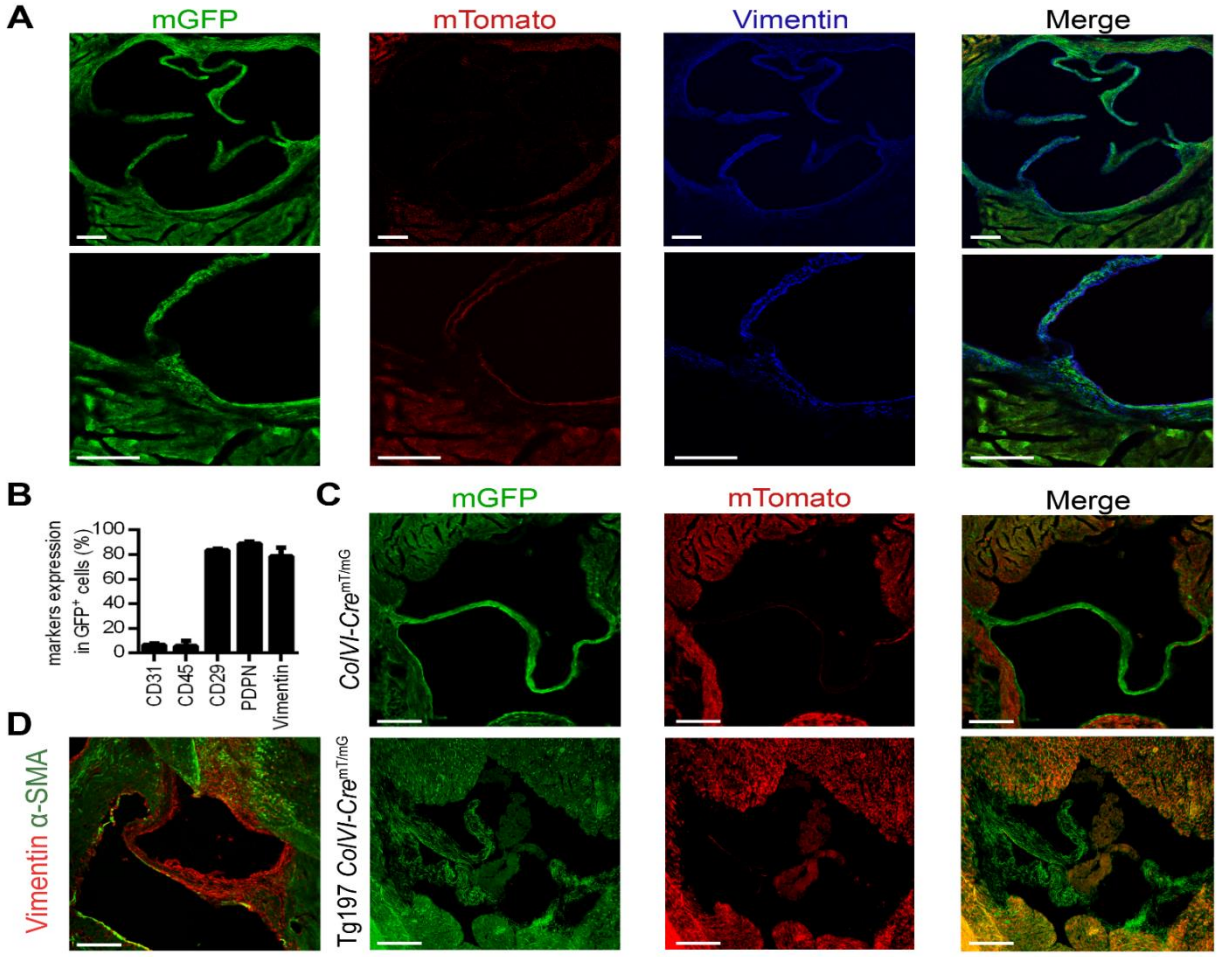

Figure 22. **Heart valve disease of Tg197 mice is caused by accumulation of activated mesenchymal Valve Interstitial Cells (VICs). (A)** Representative images of transverse heart cryosections of *ColVI-Cre-Rosa26*$^{mT/mG}$ mice, at their 8 weeks of age, and colocalization of GFP expression with Vimentin expression in the heart valve (lower panel: higher magnification of the upper panel) (Scale bar:100μm). **(B)** FACS analysis of *ColVI*-expressing cells (GFP^{+}) with markers for endothelial (CD31), hematopoietic (CD45) and fibroblast/ mesenchymal cells (CD29, Podoplanin[PDPN], Vimentin) from dissociated heart valves of *ColVI-Cre-Rosa26*$^{mT/mG}$ mice, at their 8 weeks of age (data are presented as mean± SEM, *n*=3 from three individual experiments). **(C)** Representative images of transverse heart cryosections of *ColVI-Cre*$^{mT/mG}$ and Tg197 *ColVI-Cre*$^{mT/mG}$ mice at their 12 weeks of age (Scale bar: 100μm). **(D)** Representative image of transverse heart cryosections of Tg197 mice at their 12 weeks of age and colocalization of a-SMA expression with Vimentin expression in the heart valve and root (Scale bar:100μm).

TNFR1 signaling in mesenchymal cells is necessary and sufficient for the development of Tg197 heart valve pathology

Having established the contribution of activated mesenchymal VICs and TNF-dependency of the valvular hyperplasia in Tg197 mice, we further explored the role of mesenchyme-specific TNF signaling in the development of this pathology. To address whether TNF signaling in mesenchymal VICs is required for the development of heart valve pathology, Tg197 animals were crossed with *ColVI-Cre Tnfr1*$^{fl/fl}$ animals (94). Tg197 *ColVI-Cre Tnfr1*$^{fl/fl}$ mice exhibited ameliorated heart valve pathology, as indicated by the lack of heart valve thickening and fibrosis (Figure 23A, C). This finding suggests that TNF signaling, through TNFR1 in mesenchymal cells, is essential for the pathogenesis of heart valve disease in the Tg197 model.

Next, we examined whether TNF signaling in mesenchymal cells was also sufficient to induce heart valve pathology in Tg197 mice. To this end, we crossed Tg197 with *ColVI-Cre Tnfr1*$^{cneo/cneo}$ mice to achieve specific reactivation of TNFR1 signaling only in mesenchymal cells (93). Tg197 *ColVI-Cre Tnfr1*$^{cneo/cneo}$ mice developed valvular thickening and extensive fibrosis, while control Tg197 *Tnfr1*$^{cneo/cneo}$ did not show any signs heart valve thickening and fibrosis (Figure 23B, D), demonstrating that TNF signaling through TNFR1 in mesenchymal cells is sufficient to trigger heart valve pathology in Tg197 mice. Consequently, TNF signaling in the mesenchyme is both necessary and sufficient for the development of heart valve pathology in Tg197 animals.

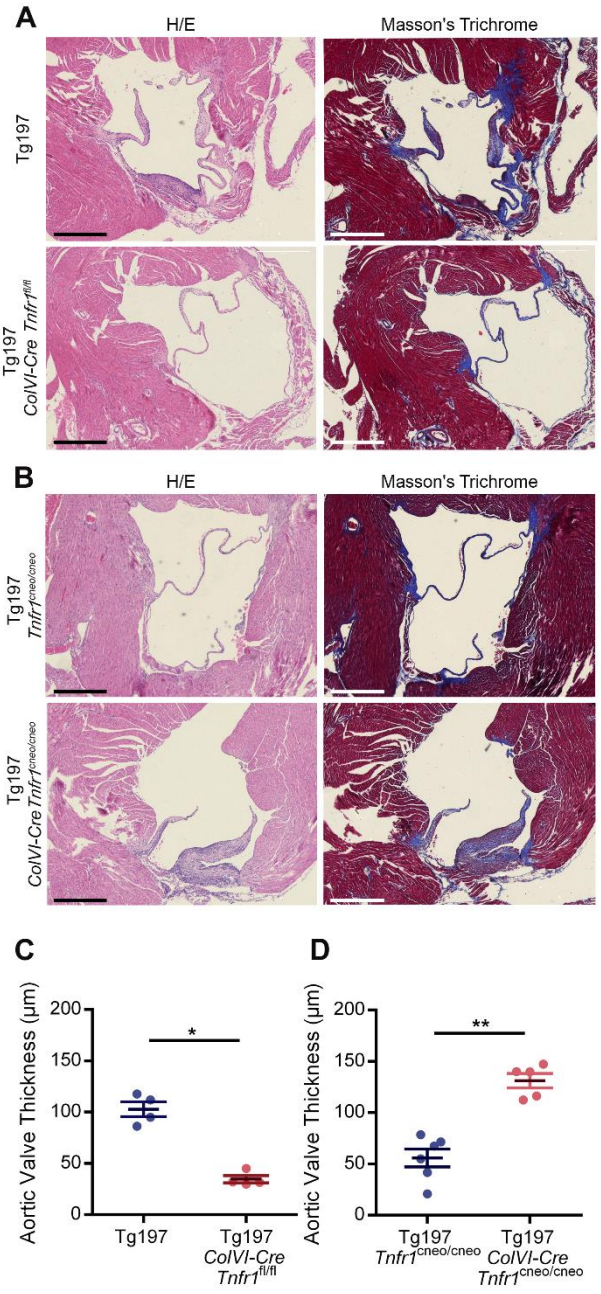

Figure 23. **TNF signaling on VICs is required and sufficient for the development of heart valve disease of Tg197 animals. (A)** Representative images of H&E- and Masson's Trichrome-stained transverse heart sections of Tg197 and Tg197 *ColVI-Cre Tnfr1*$^{fl/fl}$ and animals at 12 weeks of age (Scale bar, 500µm). **(B)** Representative images of H&E- and Masson's Trichrome-stained transverse heart sections of Tg197 *Tnfr1*$^{cneo/cneo}$ and Tg197 *ColVI-Cre Tnfr1*$^{cneo/cneo}$ and at 12 weeks of age (Scale bar, 500µm). **(C)** Comparison of the aortic valve thickness between Tg197 and Tg197 *ColVI-Cre Tnfr1*$^{fl/fl}$ animals at 12 weeks of age (data are presented as individual values, with mean± SEM; *, P<0.03). **(D)** Comparison of the aortic valve thickness between Tg197 *Tnfr1*$^{cneo/cneo}$ and Tg197 *ColVI-Cre Tnfr1*$^{cneo/cneo}$ at 12 weeks of age (data are presented as individual values, with mean± SEM; **, P<0.005).

Ex vivo-derived Tg197 VICs exhibit an activated phenotype

It is known that ex vivo human RA and mouse arthritogenic SFs exhibit increased proliferative and migratory capacities (86,87,244). To investigate whether pathogenic VICs display a similar phenotype, we isolated VICs from Tg197 and WT animals at 8 weeks of age, when heart valve disease is well established.

We first confirmed the homogeneity of VICs cultures, by characterizing cultured VICs isolated from *ColVI-Cre-Rosa26*$^{mT/mG}$ animals. FACS analysis confirmed that approximately 80% of the isolated VICs were GFP^{+} and displayed high expression of known fibroblast and mesenchymal cell markers including CD29, Vimentin, Podoplanin, CD140a, CD90.2, CD105, VCAM-1 and ICAM-1 (Figure 24A), while they lacked expression of hematopoietic (CD45) and endothelial (CD31) markers, thus preserving the observed in vivo expression marker profile (Figure 22B).

We further assessed the activation status of Tg197-derived VICs. These cells were found to overexpress hTNF (Figure 24B) and displayed increased proliferative and migratory capacities (Figure 24C, D), similarly to Tg197-derived SFs (87). Therefore, VICs are shown to exhibit an activated phenotype with similar characteristics to the one exhibited by the arthritogenic Tg197 SFs ex vivo (86,87).

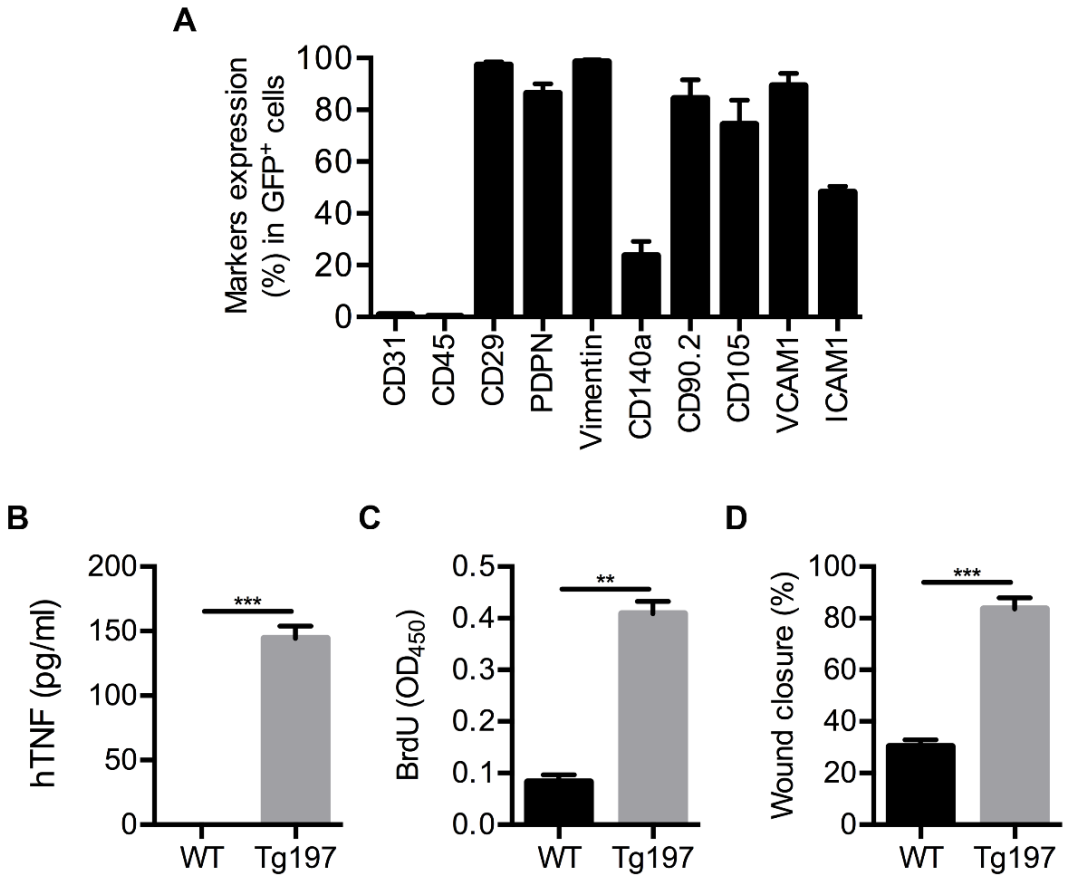

Figure 24. **Activated phenotype of Tg197-derived VICs *ex vivo*. (A)** FACS analysis of *ColVI*-expressing cells (GFP^+) with markers for endothelial (CD31), hematopoietic (CD45) and fibroblast/ mesenchymal cells (CD29, Podoplanin [PDPN], Vimentin, CD140a, CD90.2, CD105, VCAM1, ICAM1) in isolated VICs from *ColVI-Cre-Rosa26*$^{mT/mG}$ mice at 8 weeks of age. **(B, C, D)** Levels of secreted hTNF in the supernatants **(B)**, BrdU incorporation **(C)** and wound healing ability calculated by percentage of wound closure **(D)** of VICs isolated from WT and Tg197 mice at 8 weeks of age (data are presented as mean± SEM, *n*=3 from three individual experiments; **, P<0.001; ***, P<0.0005).

Tg197 VICs express common pathogenic signatures with Tg197 SFs

Arthritogenic SFs have been recently found to exhibit a distinct expression profile, characterized by pathogenic deregulation of genes affecting key pathways for the development of polyarthritis symptoms (90). We, therefore, explored the commonalities of pathogenic Tg197 VICs and SFs at the gene expression, pathway and transcriptional regulation level. For this purpose, we isolated SFs and VICs from 8-week-old Tg197 animals, with established arthritis and heart valve disease, and compared their expression profiles to those of SFs and VICs isolated from WT littermates by using RNA-sequencing.

Both Tg197 SFs and VICs displayed more than 500 significant differentially expressed genes (DEGs) compared to their WT controls (Figure 25A). More specifically, a total of 408 and 381 genes were upregulated in Tg197 VICs and SFs respectively, with almost 30% of them commonly upregulated in both cell types (Figure 25B), while a total of 327 and 160 genes were downregulated in Tg197 VICs and SFs respectively with approximately 10% of them commonly downregulated in both cell types (Figure 25B). Further functional enrichment analysis of the common upregulated genes placed immune and inflammatory responses, as well as NF-κB signaling at the top enriched pathways. Pathways enriched in the overlapping downregulated genes included extracellular matrix organization and regulation of growth, indicating ECM remodeling and deregulated cell growth (Figure 26).

To further explore the similarities of these two pathogenic cell types at the pathway level, functional enrichment analysis was performed for all DEGs in SFs and VICs. Interestingly, KEGG pathways enriched in SFs' and VICs' upregulated genes show a great overlap (60%) (Figure 25C). These pathways were subsequently clustered into broader KEGG pathway categories. The most pronounced category was immune response, which included pathways such as chemokine and TLR signaling, while the most prominent correlation was to human "rheumatoid arthritis" term, with known RA- and cardiovascular disease-related genes [*Tnf, Il1b* (245) and *Acp5* (246)] being upregulated in both cell types. Other categories include cancer and infectious diseases, such as Tuberculosis and Pertussis which have also been associated with inflammation and TNF signaling. TNF and NF-κB signaling were also enriched in both cell types, with a distinct set of genes such as Mmp9, *Tnf, Il1b, Cxcl2;3;12, Ccl4* and *Cd14* being upregulated in both Tg197 SFs and VICs (Figure 25D). Interestingly, some of the functions enriched only in VICs' DEGs involve cardiovascular diseases,

indicating the differences between VICs and SFs due to their different tissue of origin (Figure 26C).

Furthermore, the RNEA tool (237), which infers regulatory networks by predicting interactions between transcription factors and their target genes, was used to explore the similarities between VICs and SFs at the transcriptional regulation level. Regulatory networks were extracted from both cells' gene expression profile and their intersection is reported in Figure 25E. Interestingly, *Sfpi1* and *Pparg*, which are known to regulate mesenchymal activation (90), were revealed by this analysis as the two main common regulators of the two networks; *Tnf* was also found to be a central regulator. These findings strongly suggest that Tg197 VICs share a commonly altered expression profile with Tg197 SFs at the gene expression, functional pathways and transcriptional regulation circuit levels.

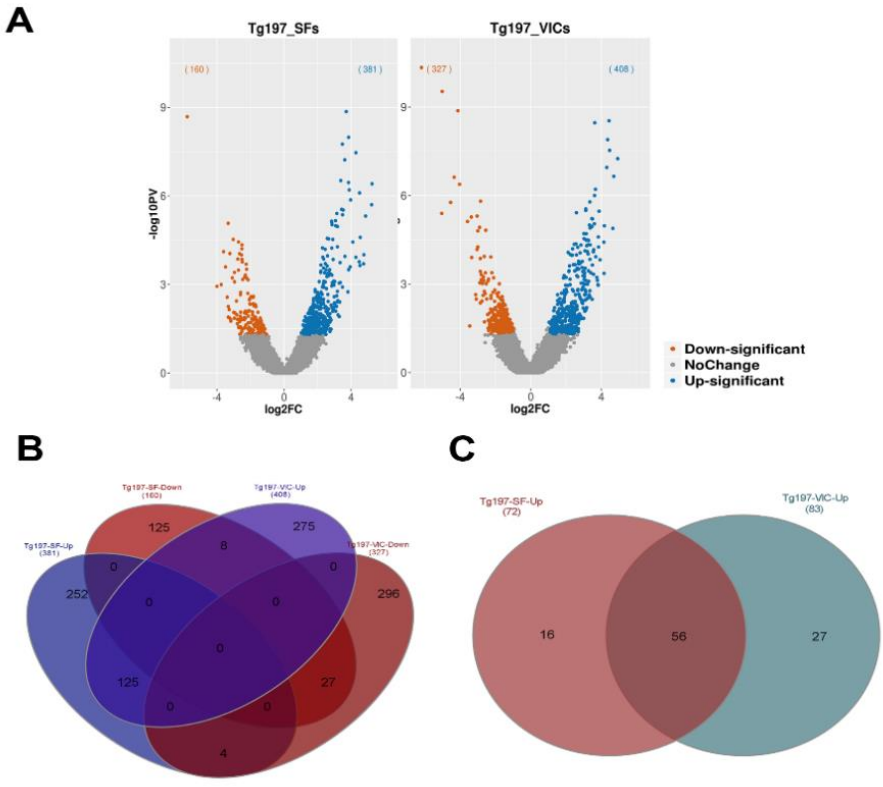

Figure 25. **Tg197 VICs exhibit common pathogenic molecular signatures with Tg197 SFs at 8 weeks of age. (A)** Volcano plots with the number of differentially expressed genes (DEGs) of Tg197 VICs and SFs compared to WT. **(B)** Venn diagram showing the overlap of DEGs in Tg197 VICs and SFs. **(C)** Venn diagram showing overlap of enriched KEGG pathways derived from functional enrichment analysis of upregulated DEGs in Tg1917 VICs and SFs. **(D)** Alluvial diagram illustrating overlapping KEGG pathways in Tg197 VICs and SFs, grouped according to their KEGG broader categories. **(E)** Intersection of regulatory networks of Tg197 VICs and SFs. (**Figure continued on next page)**

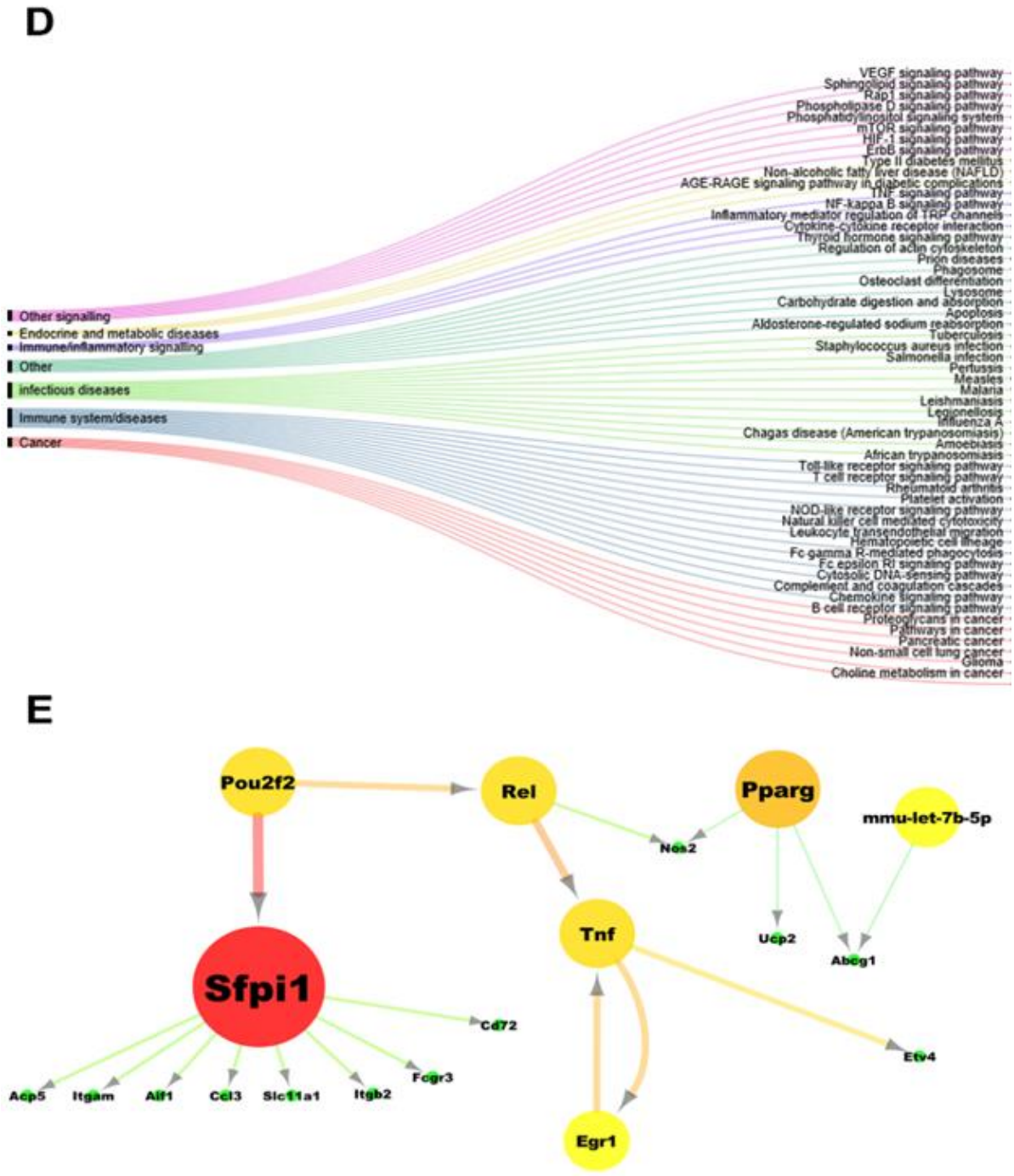

(Figure 25 continued)

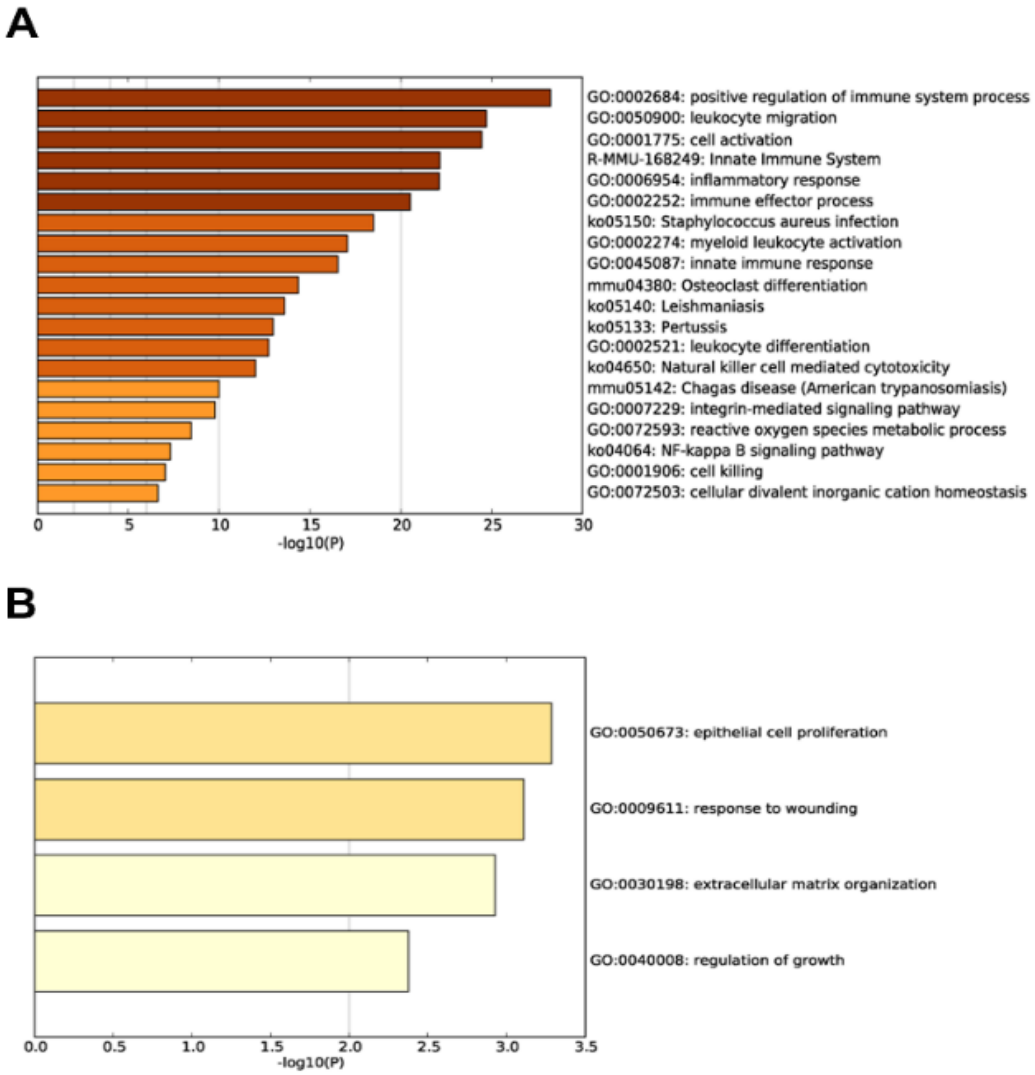

Figure 26. **Further functional enrichment analysis of the overlapping upregulated/downregulated genes in Tg197 VICs and SFs isolated at 8 weeks of age. (A, B)** Pathways enriched in the overlapping significantly upregulated **(A)** and downregulated **(B)** DEGs in Tg197 VICs and SFs. **(C)** Extended alluvial diagram which illustrates KEGG pathways in VICs and SFs alone as well as the overlapping KEGG pathways in Tg197 VICs and SFs, grouped according to their KEGG broader categories. (**Figure continued on next page)**

C

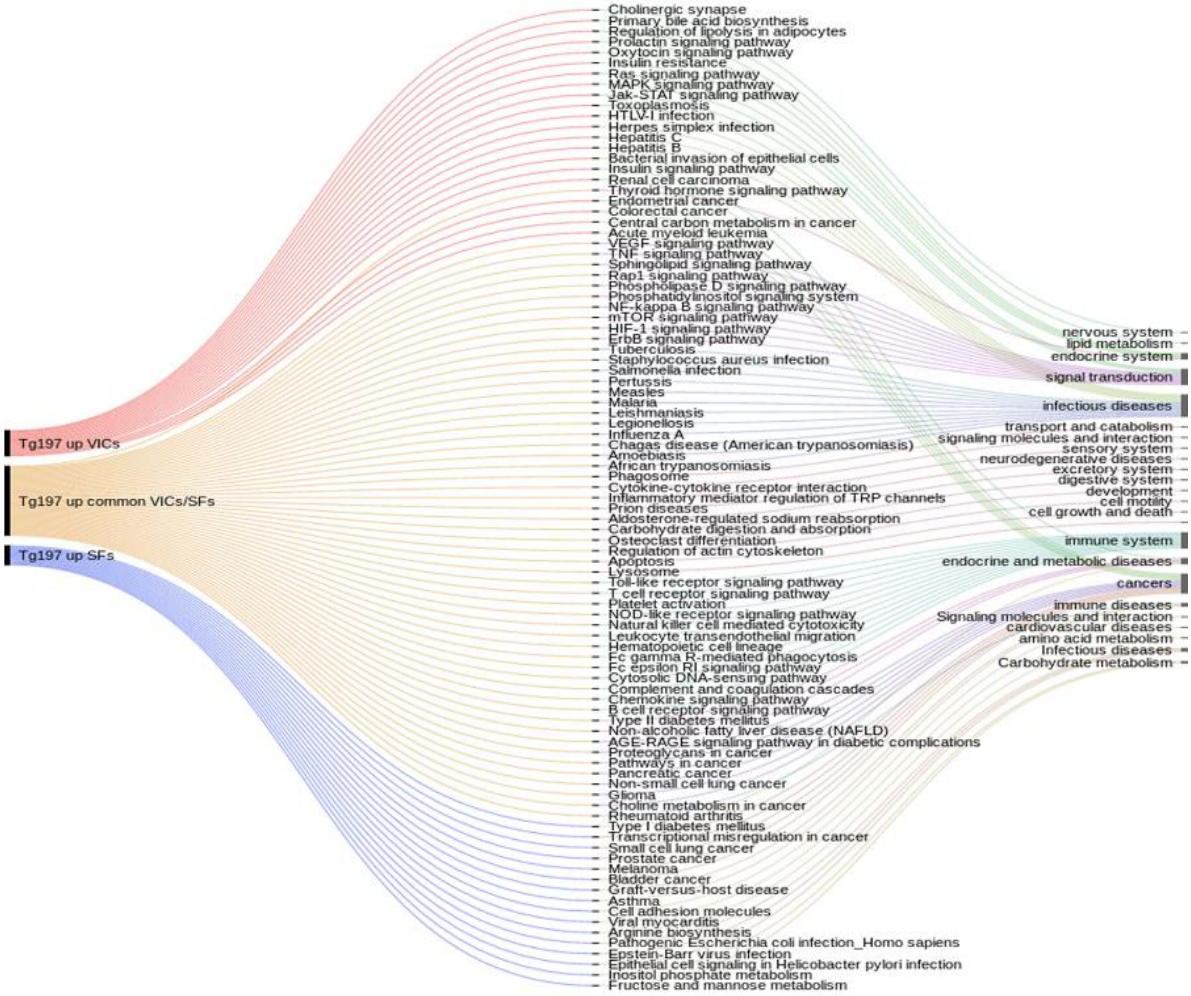

(Figure 26 continued)

Discussion: Part II

RA and SpA patients show a higher risk of developing associated cardiac diseases, which highly contribute to their increased mortality rates (101). More specifically, they exhibit a 30% increased incidence of valvular pathologies, including nonspecific valvular thickening and mild valve regurgitation (103,247). Recent studies using sensitive imaging methods, such as transesophageal echocardiography, report an even greater prevalence of left-sided Heart Valve Disease (HVD) in RA patients with valve thickening in half of the cases involving both mitral (47%) and aortic (32%) valves and valve regurgitation (21%) (248). The involvement of TNF in the pathogenesis of RA and SpA is well established; however, its role in the development of arthritis-related cardiac comorbidities remains unknown.

We demonstrate here that overexpression of TNF, in the TghuTNF (Tg197) arthritis model, in addition to the chronic polyarthritis (23) drives also the development of spontaneous left-sided heart valve disease, which mainly leads to valvular thickening with some degree of stenosis and occasionally to valve insufficiency, comorbid pathologies often observed in RA/SpA patients (103,112). Interestingly, a similar left-sided heart valve pathology, exhibiting valvular thickening and fibrosis was also observed in the TgA86, transmembrane TNF overexpressing, mouse model of SpA (225,249) (Figure 27), further strengthening the pathogenic role of TNF in the development of arthritis-related cardiac comorbidities. The greater mechanical stress and hemodynamic pressures imposed on the left side of the heart is a likely explanation for the discrepancy between the diseased left- and unaffected right-sided valves, also observed in RA/SpA patients.

AV stenosis and MV and/or AV regurgitation have been shown to result in LV hypertrophy with preserved ejection fraction and occasionally in LV dilation with some degree of contractile dysfunction (250). Similarly, in the Tg197 model, valvular pathology contributes to the observed extensive LV dilation with some degree of LV hypertrophy as well as to the concomitant contractile dysfunction. However, additional mechanisms that have been proposed as contributing factors in the increased prevalence of global heart failure in RA/SpA patients, such as myocardial fibrosis and edema as well as arterial blood pressure, coronary heart disease and myocardial remodeling (251) remain to be studied for their contribution in the global heart impairment observed in Tg197 animals. We have also detected repeated arrhythmic episodes in Tg197 mice which could explain the premature sudden

deaths observed in this model recapitulating the increased risk of sudden cardiac death experienced by RA/SpA patients, due to atrial fibrillation and other types of tachyarrhythmias which suggest diffuse myocardial electrical instability (252,253). Overall, our data demonstrate that the Tg197 arthritis model develops heart valve disease and cardiac arrhythmias that closely mimic the cardiac clinical findings and premature mortality observed in arthritis patients, supporting the value of this model in providing mechanistic insights into the pathogenesis of these comorbidities. The reversal of the cardiac phenotype by pharmacological inhibition of TNF in this model supports the vital role of TNF in the development of RA/SpA-related cardiac valvular comorbidities and suggests that anti-TNF therapy could also prevent cardiac comorbidities and avoid adverse cardiovascular side effects caused by other drugs, such as DMARDs (101). Our findings also highlight the importance of regular echocardiographic screening on RA and SpA patients.

The association between elevated TNF levels and valvular pathology has been previously suggested in other mutant mice (134,135). Notably, these mice exhibit an inflammatory valvulitis, in contrast to the hypertrophic valves of Tg197 mice, which consist mainly of activated mesenchymal VICs. This discrepancy could be attributed to various factors, such as differences in the genetic background or in the cytokine imbalances driving the pathology. More specifically, the inflammatory phenotype of IL1Ra-deficient mice (134) has been observed in the inflammation-susceptible BALB/c genetic background (254) whereas in the C57 background they show milder pathology (134). Additionally, pathology in the IL1Ra- (134) as well as in the TTP-deficient (135) and K/BxN transgenic (255) mice could be driven by diverse upstream mechanisms providing additional pathogenic cytokine misbalances apart from TNF.

Extensive characterization and comparison of the transcriptional profiles of pathogenic Tg197 VICs and SFs, compared to their healthy counterparts, revealed a shared altered and pathogenic profile of these two cell types. Inflammatory and immune responses were among the commonly enriched KEGG pathways in both Tg197 SFs and VICs, supporting their activated and pathogenic status. Our analysis further supports the central role of *Tnf* in both cell types and pathologies. Interestingly, *Sfpi1,* a NF-κB-modulator (256), emerged as a common transcriptional regulator of both activated VICs and SFs highlighting the importance of NF-κB signaling in this process, as was also confirmed by the enrichment of the NF-κB signaling pathway in both cell types. Moreover, *Sfpi1*, encoding the myeloid-specific

transcription factor PU.1 (257), has been found upregulated in RA-FLS (258), while being also implicated in the pathogenesis of heart hypertrophy(259). Collectively, the centrality of *Sfpi1*, in combination with the enriched immune and TLR signaling, as well as NF-κB signaling pathways, in both Tg197 VICs and SFs could support their conversion to activated mesenchymal cells possessing pathogenic innate immune properties. This hypothesis is further supported by recent findings suggesting that Tg197 SFs undergo a metabolic reprogramming (260), similar to the metabolic alterations reported in both inflammatory heart diseases and RA (261,262). Therefore, we hypothesize that VICs and SFs become pathogenic upon common TNF-induced metabolic reprogramming acquiring a detrimental innate phenotype, which should be further explored.

We finally show here that mesenchymal-specific TNF signaling, through TNFR1, is both required and sufficient for the development of heart valve pathology. Notably, SF- and IMC-specific TNFR1 signaling has been previously demonstrated to be causal in orchestrating comorbid polyarthritis and Crohn's-like IBD in a TNF overexpressing mouse model (24). It may, therefore, be strongly postulated that mesenchymal cell responses to TNF, explain complex chronic inflammatory disease comorbidities involving joint, intestinal and, as shown in the present study, also cardiac pathologies. Future detailed insights into the molecular and cellular mechanisms commonly underlying aetiopathogenesis of mesenchymal cell-driven comorbidities, such as those expressed under the RA/SpA paradigm, may also offer novel approaches to therapeutically target common pathogenic processes.

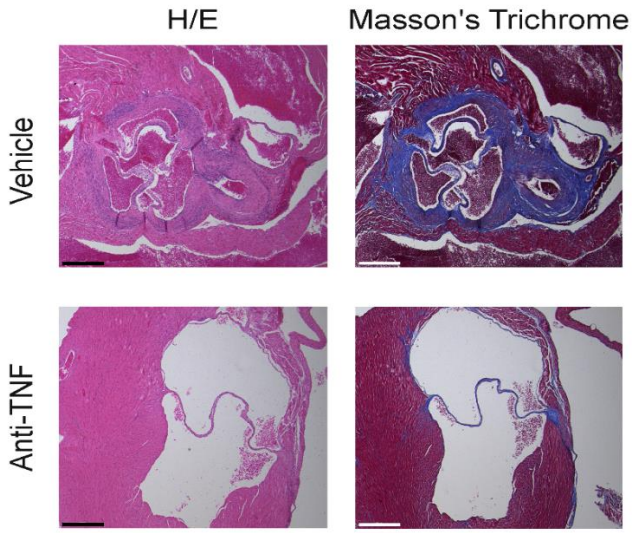

Figure 27. **TgA86 SpA model develops TNF-dependent left-sided heart valve pathology.** Representative images of H&E- and Masson's Trichrome-stained transverse heart sections showing the aortic valve of TgA86 animals at 15 weeks, treated with vehicle or prophylactic anti-TNF treatment (from 4th-15th week of age) (Scale bar, 400μm).

Results: Part III

Systemic, but not mesenchymal-specific, *Ercc1* deficiency ameliorates heart valve pathology of Tg197

As shown earlier, neither systemic nor mesenchymal-specific *Ercc1* deficiency in Tg197 animals had any effect in its arthritis pathology. Since we have thoroughly investigated the comorbid heart valve disease of this model (Tg197), we sought to study whether systemic or mesenchymal-specific *Ercc1* deficiency affects it. Unexpectedly, heart valve disease of Tg197 *Ercc1*$^{\Delta/-}$ animals was completely abolished compared to Tg197 mice (Figure 28), while it was not altered in the Tg197 ColVI-*Ercc1*$^{f/-}$ animals compared to Tg197 ColVI-*Ercc1*$^{f/+}$ control mice, at 12 weeks of age. To explain this phenotype, we tried to isolate VICs from Tg197 *Ercc1*$^{\Delta/-}$ mice and further examine how they differ from WT or from Tg197 VICs. Unfortunately, we never managed to isolate successfully VICs from these mice as the size of the progeroid Tg197 *Ercc1*$^{\Delta/-}$ heart was too small to isolate as many cells as needed for functional assays.

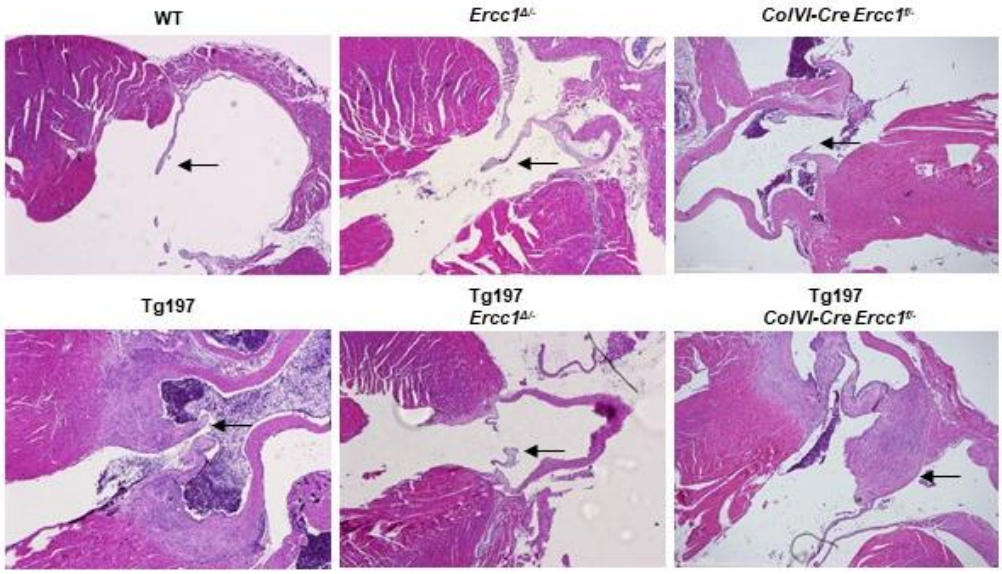

Figure 28. **Systemic, but not mesenchymal-specific, *Ercc1* deficiency ameliorates heart valve pathology of Tg197.** Representative images of H&E-stained longitudinal heart sections showing the aortic valve leaflets of WT, *Ercc1*$^{\Delta/-}$, *ColVI-Cre Ercc1*$^{f/-}$, Tg197 and Tg197 *Ercc1*$^{\Delta/-}$ and Tg197 *ColVI-Cre Ercc1*$^{f/-}$ animals at 12 weeks of age (aortic valve is indicated with the black arrow).

Discussion: Part III

Aging has been associated with higher incidence of cardiac dysfunction; however, there are still unanswered questions about the exact molecular mechanisms driving this predisposition. In the past, *Ercc1* deletion has been implicated with atherosclerotic cardiovascular disease both in mice (263) and in human patients (264). For this reason, we investigated whether systemic or mesenchymal-specific *Ercc1* deletion causes any phenotype in the heart valves of *Ercc1*$^{\Delta/-}$ or *ColVI-Cre Ercc1*$^{f/-}$ respectively and whether this deletion affects the heart valve disease developed in Tg197 mice.

We demonstrate here that systemic accumulation of DNA damage due to *Ercc1* deletion does not lead to the development of spontaneous heart valve pathology in *Ercc1*$^{\Delta/-}$ mice. Although previous studies have shown that *Ercc1*$^{\Delta/-}$ mice suffer from vasodilator impairment, hence dysfunction of endothelial cells (263), the heart valve of these mice was histopathologically normal. This could be attributed to the fact that valve endothelial cells may not be affected by the general endothelial dysfunction of this mouse.

According to recent findings by Karakasilioti *et al.,* 2013 (207), persistent adipocyte-specific DNA damage triggers the expression of pro-inflammatory cytokines, leading to chronic inflammation and eventually to tissue degeneration. As adipose tissue and Valve Interstitial Cells (VICs) are of shared mesenchymal origin, we hypothesized that mesenchymal-specific *Ercc1* deficiency would similarly cause higher levels of TNF, hence heart valve disease, similar to the one of Tg197 animals. For this reason, we observed *ColVI-Cre Ercc1*$^{f/-}$ animals for any histopathological symptoms of heart valve thickening and fibrosis. Up until their 26th week of age, *ColVI-Cre Ercc1*$^{f/-}$ animals did not show any of these disease features. Additionally, mesenchymal-specific *Ercc1* deletion did not affect the heart valve disease of Tg197 mice.

Interestingly, heart valve disease of Tg197 animals was ameliorated due to the systemic *Ercc1* deletion of Tg197 *Ercc1*$^{\Delta/-}$ animals. To explain this phenotype, we tried to isolate VICs from Tg197 *Ercc1*$^{\Delta/-}$ mice and further examine how they differ from WT and Tg197 VICs. Unfortunately, we never managed to isolate successfully VICs from these mice, as the size of the progeroid Tg197 *Ercc1*$^{\Delta/-}$ heart was too small to isolate as many cells as needed for functional assays. However, in the future, pooled samples could be used to identify major differences on VIC

characteristics of these animals. It would also be interesting if transcription profile of Valve Endothelial Cells (VECs) and VICs derived from Tg197, *Ercc1*$^{\Delta/-}$, Tg197 *Ercc1*$^{\Delta/-}$ and Tg197 *ColVI-Cre Ercc1*$^{f/-}$ animals were compared, in order to investigate the differences between endothelial and mesenchymal aging and how these affect the development of heart valve disease observed in Tg197 animals. Additionally, echocardiographic evaluation of the hearts of Tg197 *Ercc1*$^{\Delta/-}$ animals could provide with possible explanations of the above findings.

Conclusion and future perspectives

In this research, we investigated whether the established model of arthritis (TghuTNF) develops, similarly to RA patients, comorbid heart pathology and we further explored the cellular and molecular mechanisms linking arthritis to cardiac comorbidities. We also investigated whether these pathologies are affected by premature aging, which is caused by accumulation of DNA damage in the synovium and in the heart valve.

Tg197 mice were found to develop TNF-dependent left-sided heart valve disease, characterised by valvular fibrosis, which consists almost entirely of hyperproliferative mesenchymal Valve Interstitial Cells (VICs). Clinically, the development of pathology results in valve stenosis and left ventricular dysfunction, accompanied by arrhythmic episodes and, occasionally, valvular insufficiency. Therefore, we have provided novel evidence that comorbid heart valve disease and chronic polyarthritis are efficiently modeled in the Tg197 arthritis model. This model could be proven very useful for future investigation on molecular pathways implicated in both TNF-dependent heart valve diseases, as well as RA-associated heart valve diseases and several genes could be knocked in or out.

We also showed here that mesenchymal-specific TNF signaling, through TNFR1, is both required and sufficient for the development of heart valve pathology in Tg197 animals. Notably, SF- and Intestinal mesenchymal cells (IMC)-specific TNFR1 signaling has been previously demonstrated to be causal in orchestrating comorbid polyarthritis and Crohn's-like IBD in a TNF overexpressing mouse model (24). It may, therefore, be strongly postulated that mesenchymal cell responses to TNF, explain complex chronic inflammatory disease comorbidities involving joint, intestinal and, as shown in the present study, also cardiac pathologies. Future detailed insights into the molecular and cellular mechanisms commonly underlying aetiopathogenesis of mesenchymal cell-driven comorbidities, such as those expressed under the RA/SpA paradigm, may also offer novel approaches to therapeutically target common pathogenic processes.

To investigate the role of aging in the pathologies of Tg197 mice, these mice were crossed with animals characterized by systemic or mesenchymal-specific deficient DNA Damage Response. The pathology of chronic polyarthritis of Tg197 mice was not affected by either systemic or SF-specific *Ercc1* deletion. However,

mesenchymal-specific *Ercc1* deletion caused amelioration of CAIA-induced arthritis. This amelioration could be further studied, as it would provide with new evidence on the interaction between aged mesenchymal cells and inflammatory cells in the joint. In addition, mesenchymal-specific *Ercc1* KO mice showed a phenotype of premature aged muscular atrophy. This could be also further studied as a model of premature muscular aging.

Interestingly, the pathology of the heart valve of Tg197 animals was completely abolished by systemic, but not mesenchymal, *Ercc1* deletion. As we have proven that the heart valve disease is driven by mesenchymal VICs, this discrepancy was unexpected and could be studied further in the future. This could be achieved by RNA-sequencing analysis of VICs derived from mice with systemic and mesenchymal-specific deletion in WT or Tg197 mice. Additionally, echocardiographic evaluation of the hearts of Tg197 *Ercc1*$^{\Delta/-}$ animals could provide with possible explanations of the above findings.

Collectively, the findings of this research shed light on the interplay between the three inter-related diseases of Rheumatoid Arthritis, aging and heart valve disease and could be used in the future for further analysis under the scope of common pathways linking comorbid conditions.

References

1. Favalli EG, Biggioggero M, Crotti C, Becciolini A, Raimondo MG, Meroni PL. Sex and Management of Rheumatoid Arthritis. *Clin Rev Allergy Immunol*. 2019 Jun 26;56(3):333–45.
2. Smolen JS, Aletaha D, Barton A, Burmester GR, Emery P, Firestein GS, Kavanaugh A, McInnes IB, Solomon DH, Strand V, Yamamoto K. Rheumatoid arthritis. *Nat Rev Dis Prim*. 2018 Feb 8;4:18001.
3. Okada Y, Wu D, Trynka G, Raj T, Terao C, Ikari K, … Plenge RM. Genetics of rheumatoid arthritis contributes to biology and drug discovery. *Nature*. 2014 Feb 25;506(7488):376–81.
4. Holoshitz J. The rheumatoid arthritis HLA-DRB1 shared epitope. *Curr Opin Rheumatol*. 2010 May;22(3):293–8.
5. McInnes IB, Schett G. The Pathogenesis of Rheumatoid Arthritis. *N Engl J Med*. 2011 Dec 8;365(23):2205–19.
6. Liu Y, Aryee MJ, Padyukov L, Fallin MD, Hesselberg E, Runarsson A, Reinius L, Acevedo N, Taub M, Ronninger M, Shchetynsky K, Scheynius A, Kere J, Alfredsson L, Klareskog L, Ekström TJ, Feinberg AP. Epigenome-wide association data implicate DNA methylation as an intermediary of genetic risk in rheumatoid arthritis. *Nat Biotechnol*. 2013 Feb 20;31(2):142–7.
7. Chang K, Yang S, Kim S, Han K, Park S, Shin J. Smoking and Rheumatoid Arthritis. *Int J Mol Sci*. 2014 Dec 3;15(12):22279–95.
8. Zhang X, Zhang D, Jia H, Feng Q, Wang D, Liang D, … Wang J. The oral and gut microbiomes are perturbed in rheumatoid arthritis and partly normalized after treatment. *Nat Med*. 2015 Aug 27;21(8):895–905.
9. Li S, Yu Y, Yue Y, Liao H, Xie W, Thai J, Mikuls TR, Thiele GM, Duryee MJ, Sayles H, Payne JB, Klassen LW, O'Dell JR, Zhang Z, Su K. Autoantibodies From Single Circulating Plasmablasts React With Citrullinated Antigens and Porphyromonas gingivalis in Rheumatoid Arthritis. *Arthritis Rheumatol (Hoboken, NJ)*. 2016 Mar;68(3):614–26.
10. Konig MF, Abusleme L, Reinholdt J, Palmer RJ, Teles RP, Sampson K, Rosen A, Nigrovic PA, Sokolove J, Giles JT, Moutsopoulos NM, Andrade F. Aggregatibacter actinomycetemcomitans-induced hypercitrullination links periodontal infection to autoimmunity in rheumatoid arthritis. *Sci Transl Med*. 2016;8(369):369ra176.
11. Horta-Baas G, Romero-Figueroa MDS, Montiel-Jarquín AJ, Pizano-Zárate ML, García-Mena J, Ramírez-Durán N. Intestinal Dysbiosis and Rheumatoid Arthritis: A Link between Gut Microbiota and the Pathogenesis of Rheumatoid Arthritis. *J Immunol Res*. 2017;2017:4835189.
12. Firestein GS, McInnes IB. Immunopathogenesis of Rheumatoid Arthritis. *Immunity*. 2017;46(2):183–96.
13. Orr C, Vieira-Sousa E, Boyle DL, Buch MH, Buckley CD, Cañete JD, … Veale DJ. Synovial tissue research: a state-of-the-art review. *Nat Rev Rheumatol*. 2017 Sep 22;13(10):630–630.
14. Vossenaar ER, Després N, Lapointe E, van der Heijden A, Lora M, Senshu T, van Venrooij WJ, Ménard HA. Rheumatoid arthritis specific anti-Sa antibodies target citrullinated vimentin. *Arthritis Res Ther*. 2004;6(2):R142-50.
15. Castro-Sánchez P, Roda-Navarro P. Physiology and Pathology of Autoimmune Diseases: Role of CD4+ T cells in Rheumatoid Arthritis. In: Physiology and Pathology of Immunology. 2017.
16. Chen Z, Bozec A, Ramming A, Schett G. Anti-inflammatory and immune-regulatory cytokines in rheumatoid arthritis. *Nat Rev Rheumatol*. 2019 Jan 19;15(1):9–17.
17. McInnes IB, Buckley CD, Isaacs JD. Cytokines in rheumatoid arthritis — shaping the immunological landscape. *Nat Rev Rheumatol*. 2016 Jan 10;12(1):63–8.
18. Szekanecz Z, Vegvari A, Szabo Z, Koch AE. Chemokines and chemokine receptors in arthritis. *Front Biosci (Schol Ed)*. 2010 Jan 1;2:153–67.
19. Sharkey M, Lipowitz AJ, Newton CD, Environment G, Areas O, Laminitis NI, … Choy

E. The pathogenesis of rheumatoid arthritis. *Anaesthesia*. 2011;66(9746):1146–59.
20. Bottini N, Firestein GS. Duality of fibroblast-like synoviocytes in RA: passive responders and imprinted aggressors. *Nat Rev Rheumatol*. 2013 Jan 13;9(1):24–33.
21. Schett G, Gravallese E. Bone erosion in rheumatoid arthritis: mechanisms, diagnosis and treatment. *Nat Rev Rheumatol*. 2012 Nov;8(11):656–64.
22. Singh JA, Saag KG, Bridges SL, Akl EA, Bannuru RR, Sullivan MC, … American College of Rheumatology. 2015 American College of Rheumatology Guideline for the Treatment of Rheumatoid Arthritis. *Arthritis Care Res (Hoboken)*. 2016 Jan;68(1):1–25.
23. Keffer J, Probert L, Cazlaris H, Georgopoulos S, Kaslaris E, Kioussis D, Kollias G. Transgenic mice expressing human tumour necrosis factor: a predictive genetic model of arthritis. *EMBO J*. 1991 Dec;10(13):4025–31.
24. Armaka M, Apostolaki M, Jacques P, Kontoyiannis DL, Elewaut D, Kollias G. Mesenchymal cell targeting by TNF as a common pathogenic principle in chronic inflammatory joint and intestinal diseases. *J Exp Med*. 2008 Feb 18;205(2):331–7.
25. Carswell EA, Old LJ, Kassel RL, Green S, Fiore N, Williamson B. An endotoxin-induced serum factor that causes necrosis of tumors. *Proc Natl Acad Sci*. 1975 Sep 1;72(9):3666–70.
26. Beutler B, Milsark I, Cerami A. Passive immunization against cachectin/tumor necrosis factor protects mice from lethal effect of endotoxin. *Science (80-)*. 1985 Aug 30;229(4716):869–71.
27. Arch RH, Gedrich RW, Thompson CB. Tumor necrosis factor receptor-associated factors (TRAFs)---a family of adapter proteins that regulates life and death. *Genes Dev*. 1998 Sep 15;12(18):2821–30.
28. Varfolomeev E, Vucic D. Intracellular regulation of TNF activity in health and disease. *Cytokine*. 2018 Jan;101:26–32.
29. Kriegler M, Perez C, DeFay K, Albert I, Lu SD. A novel form of TNF/cachectin is a cell surface cytotoxic transmembrane protein: ramifications for the complex physiology of TNF. *Cell*. 1988 Apr 8;53(1):45–53.
30. Josephs SF, Ichim TE, Prince SM, Kesari S, Marincola FM, Escobedo AR, Jafri A. Unleashing endogenous TNF-alpha as a cancer immunotherapeutic. *J Transl Med*. 2018 Dec 31;16(1):242.
31. Bradham WS, Bozkurt B, Gunasinghe H, Mann D, Spinale FG. Tumor necrosis factor-alpha and myocardial remodeling in progression of heart failure: a current perspective. *Cardiovasc Res*. 2002 Mar;53(4):822–30.
32. Wajant H, Pfizenmaier K, Scheurich P. Tumor necrosis factor signaling. *Cell Death Differ*. 2003 Jan 25;10(1):45–65.
33. Grell M, Douni E, Wajant H, Löhden M, Clauss M, Maxeiner B, Georgopoulos S, Lesslauer W, Kollias G, Pfizenmaier K, Scheurich P. The transmembrane form of tumor necrosis factor is the prime activating ligand of the 80 kDa tumor necrosis factor receptor. *Cell*. 1995 Dec 1;83(5):793–802.
34. Kalliolias GD, Ivashkiv LB. TNF biology, pathogenic mechanisms and emerging therapeutic strategies. *Nat Rev Rheumatol*. 2016 Jan 10;12(1):49–62.
35. Tartaglia LA, Ayres TM, Wong GH, Goeddel D V. A novel domain within the 55 kd TNF receptor signals cell death. *Cell*. 1993 Sep 10;74(5):845–53.
36. Schulze-Osthoff K, Ferrari D, Los M, Wesselborg S, Peter ME. Apoptosis signaling by death receptors. *Eur J Biochem*. 1998 Jun 15;254(3):439–59.
37. Baud V, Karin M. Signal transduction by tumor necrosis factor and its relatives. *Trends Cell Biol*. 2001 Sep;11(9):372–7.
38. Rothe M, Sarma V, Dixit V, Goeddel D. TRAF2-mediated activation of NF-kappa B by TNF receptor 2 and CD40. *Science (80-)*. 1995 Sep 8;269(5229):1424–7.
39. Feldmann M, Brennan FM, Maini RN. Rheumatoid arthritis. *Cell*. 1996 May 3;85(3):307–10.
40. Kavanaugh AF, Schulze-Koops H, Davis LS, Lipsky PE. Repeat treatment of rheumatoid arthritis patients with a murine anti-intercellular adhesion molecule 1 monoclonal antibody. *Arthritis Rheum*. 1997 May;40(5):849–53.
41. Vasanthi P, Nalini G, Rajasekhar G. Role of tumor necrosis factor-alpha in rheumatoid arthritis: a review. *APLAR J Rheumatol*. 2007 Dec 5;10(4):270–4.
42. Wehmeyer C, Pap T, Buckley CD, Naylor AJ. The role of stromal cells in inflammatory

bone loss. *Clin Exp Immunol*. 2017 Jul 1;189(1):1–11.
43. Smolen JS, Landewé R, Bijlsma J, Burmester G, Chatzidionysiou K, Dougados M, … van der Heijde D. EULAR recommendations for the management of rheumatoid arthritis with synthetic and biological disease-modifying antirheumatic drugs: 2016 update. *Ann Rheum Dis*. 2017 Jun;76(6):960–77.
44. Alvaro-Gracia JM, Zvaifler NJ, Brown CB, Kaushansky K, Firestein GS. Cytokines in chronic inflammatory arthritis. VI. Analysis of the synovial cells involved in granulocyte-macrophage colony-stimulating factor production and gene expression in rheumatoid arthritis and its regulation by IL-1 and tumor necrosis factor-alpha. *J Immunol*. 1991 May 15;146(10):3365–71.
45. Matsuno H, Yudoh K, Katayama R, Nakazawa F, Uzuki M, Sawai T, Yonezawa T, Saeki Y, Panayi GS, Pitzalis C, Kimura T. The role of TNF- α in the pathogenesis of inflammation and joint destruction in rheumatoid arthritis (RA): a study using a human RA/SCID mouse chimera. *Rheumatology*. 2002 Mar;41(3):329–37.
46. Radner H, Aletaha D. Anti-TNF in rheumatoid arthritis: an overview. *Wiener Medizinische Wochenschrift*. 2015 Jan 5;165(1–2):3–9.
47. Lazzerini PE, Capecchi PL, Guidelli GM, Selvi E, Acampa M, Laghi-Pasini F. Spotlight on sirukumab for the treatment of rheumatoid arthritis: the evidence to date. *Drug Des Devel Ther*. 2016 Sep 26;Volume 10:3083–98.
48. Hay ED. The mesenchymal cell, its role in the embryo, and the remarkable signaling mechanisms that create it. *Dev Dyn*. 2005 Jul;233(3):706–20.
49. Kontoyiannis D, Kollias G. Fibroblast biology. Synovial fibroblasts in rheumatoid arthritis: leading role or chorus line? *Arthritis Res*. 2(5):342–3.
50. Pap T, Müller-Ladner U, Gay RE, Gay S. Fibroblast biology. Role of synovial fibroblasts in the pathogenesis of rheumatoid arthritis. *Arthritis Res*. 2000;2(5):361–7.
51. Lefèvre S, Knedla A, Tennie C, Kampmann A, Wunrau C, Dinser R, Korb A, Schnäker E-M, Tarner IH, Robbins PD, Evans CH, Stürz H, Steinmeyer J, Gay S, Schölmerich J, Pap T, Müller-Ladner U, Neumann E. Synovial fibroblasts spread rheumatoid arthritis to unaffected joints. *Nat Med*. 2009 Dec 8;15(12):1414–20.
52. Bartok B, Firestein GS. Fibroblast-like synoviocytes: key effector cells in rheumatoid arthritis. *Immunol Rev*. 2010 Jan;233(1):233–55.
53. Dakin SG, Coles M, Sherlock JP, Powrie F, Carr AJ, Buckley CD. Pathogenic stromal cells as therapeutic targets in joint inflammation. *Nat Rev Rheumatol*. 2018 Dec 12;14(12):714–26.
54. Karouzakis E, Gay RE, Gay S, Neidhart M. Epigenetic control in rheumatoid arthritis synovial fibroblasts. *Nat Rev Rheumatol*. 2009 May;5(5):266–72.
55. Frank-Bertoncelj M, Trenkmann M, Klein K, Karouzakis E, Rehrauer H, Bratus A, Kolling C, Armaka M, Filer A, Michel BA, Gay RE, Buckley CD, Kollias G, Gay S, Ospelt C. Epigenetically-driven anatomical diversity of synovial fibroblasts guides joint-specific fibroblast functions. *Nat Commun*. 2017;8:14852.
56. Croft AP, Campos J, Jansen K, Turner JD, Marshall J, Attar M, … Buckley CD. Distinct fibroblast subsets drive inflammation and damage in arthritis. Vol. 570, Nature. Nature Publishing Group; 2019. p. 246–51.
57. Neumann E, Lefèvre S, Zimmermann B, Gay S, Müller-Ladner U. Rheumatoid arthritis progression mediated by activated synovial fibroblasts. *Trends Mol Med*. 2010 Oct 1;16(10):458–68.
58. Han Z, Boyle DL, Manning AM, Firestein GS. AP-1 and NF-κB regulation in rheumatoid arthritis and murine collagen-induced arthritis. *Autoimmunity*. 1998;28(4):197–208.
59. Ospelt C. Synovial fibroblasts in 2017. *RMD Open*. 2017 Oct 15;3(2):e000471.
60. Kollias G, Papadaki P, Apparailly F, Vervoordeldonk MJ, Holmdahl R, Baumans V, … Gay S. Animal models for arthritis: innovative tools for prevention and treatment. *Ann Rheum Dis*. 2011 Aug 1;70(8):1357–62.
61. Caplazi P, Baca M, Barck K, Carano RAD, DeVoss J, Lee WP, Bolon B, Diehl L. Mouse Models of Rheumatoid Arthritis. *Vet Pathol*. 2015 Sep 10;52(5):819–26.
62. van den Berg WB. Lessons from animal models of arthritis over the past decade. *Arthritis Res Ther*. 2009;11(5):250.
63. Asquith DL, Miller AM, McInnes IB, Liew FY. Animal models of rheumatoid arthritis. *Eur J Immunol*. 2009 Aug;39(8):2040–4.

64. Trentham DE, Townes AS, Kang AH. Autoimmunity to type II collagen an experimental model of arthritis. *J Exp Med*. 1977 Sep 1;146(3):857–68.
65. Holmdahl R, Malmström V, Vuorio E. Autoimmune recognition of cartilage collagens. *Ann Med*. 1993 Jun;25(3):251–64.
66. Terato K, Hasty KA, Reife RA, Cremer MA, Kang AH, Stuart JM. Induction of arthritis with monoclonal antibodies to collagen. *J Immunol*. 1992 Apr 1;148(7):2103–8.
67. Nandakumar KS, Svensson L, Holmdahl R. Collagen Type II-Specific Monoclonal Antibody-Induced Arthritis in Mice. *Am J Pathol*. 2003 Nov;163(5):1827–37.
68. Keystone EC, Schorlemmer HU, Pope C, Allison AC. Zymosan-induced arthritis: a model of chronic proliferative arthritis following activation of the alternative pathway of complement. *Arthritis Rheum*. 20(7):1396–401.
69. Frasnelli ME, Tarussio D, Chobaz-Péclat V, Busso N, So A. TLR2 modulates inflammation in zymosan-induced arthritis in mice. *Arthritis Res Ther*. 2005;7(2):R370-9.
70. Maffia P, Brewer JM, Gracie JA, Ianaro A, Leung BP, Mitchell PJ, Smith KM, McInnes IB, Garside P. Inducing experimental arthritis and breaking self-tolerance to joint-specific antigens with trackable, ovalbumin-specific T cells. *J Immunol*. 2004 Jul 1;173(1):151–6.
71. Brackertz D, Mitchell GF, Mackay IR. Antigen-induced arthritis in mice. I. Induction of arthritis in various strains of mice. *Arthritis Rheum*. 1977 Apr;20(3):841–50.
72. Wooley PH, Seibold JR, Whalen JD, Chapdelaine JM. Pristane-induced arthritis. The immunologic and genetic features of an experimental murine model of autoimmune disease. *Arthritis Rheum*. 1989 Aug;32(8):1022–30.
73. Holmdahl R, Lorentzen JC, Lu S, Olofsson P, Wester L, Holmberg J, Pettersson U. Arthritis induced in rats with nonimmunogenic adjuvants as models for rheumatoid arthritis. *Immunol Rev*. 2001 Dec;184:184–202.
74. Christensen AD, Haase C, Cook AD, Hamilton JA. K/BxN Serum-Transfer Arthritis as a Model for Human Inflammatory Arthritis. *Front Immunol*. 2016;7:213.
75. Christianson CA, Corr M, Yaksh TL, Svensson CI. K/BxN Serum Transfer Arthritis as a Model of Inflammatory Joint Pain. *Methods Mol Biol*. 2012;851:249.
76. Geiler T, Kriegsmann J, Keyszer GM, Gay RE, Gay S. A new model for rheumatoid arthritis generated by engraftment of rheumatoid synovial tissue and normal human cartilage into SCID mice. *Arthritis Rheum*. 1994 Nov;37(11):1664–71.
77. Kontoyiannis D, Pasparakis M, Pizarro T. Impaired on/off regulation of TNF biosynthesis in mice lacking TNF AU-rich elements: implications for joint and gut-associated immunopathologies. *Immunity*. 1999;10(3):387–98.
78. Hayward MD, Jones BK, Saparov A, Hain HS, Trillat AC, Bunzel MM, … Buiakova O. An extensive phenotypic characterization of the hTNFα transgenic mice. *BMC Physiol*. 2007;7.
79. Horai R, Saijo S, Tanioka H, Nakae S, Sudo K, Okahara A, Ikuse T, Asano M, Iwakura Y. Development of Chronic Inflammatory Arthropathy Resembling Rheumatoid Arthritis in Interleukin 1 Receptor Antagonist-Deficient Mice. *J Exp Med*. 2000 Jan 17;191(2):313–20.
80. Maccioni M, Zeder-Lutz G, Huang H, Ebel C, Gerber P, Hergueux J, Marchal P, Duchatelle V, Degott C, van Regenmortel M, Benoist C, Mathis D. Arthritogenic Monoclonal Antibodies from K/BxN Mice. *J Exp Med*. 2002 Apr 15;195(8):1071–7.
81. Korganow AS, Ji H, Mangialaio S, Duchatelle V, Pelanda R, Martin T, Degott C, Kikutani H, Rajewsky K, Pasquali JL, Benoist C, Mathis D. From systemic T cell self-reactivity to organ-specific autoimmune disease via immunoglobulins. *Immunity*. 1999 Apr;10(4):451–61.
82. Hata H, Sakaguchi N, Yoshitomi H, Iwakura Y, Sekikawa K, Azuma Y, Kanai C, Moriizumi E, Nomura T, Nakamura T, Sakaguchi S. Distinct contribution of IL-6, TNF-α, IL-1, and IL-10 to T cell–mediated spontaneous autoimmune arthritis in mice. *J Clin Invest*. 2004 Aug 16;114(4):582–8.
83. Kawane K, Ohtani M, Miwa K, Kizawa T, Kanbara Y, Yoshioka Y, Yoshikawa H, Nagata S. Chronic polyarthritis caused by mammalian DNA that escapes from degradation in macrophages. *Nature*. 2006 Oct 26;443(7114):998–1002.
84. Sieper J, Poddubnyy D. New evidence on the management of spondyloarthritis. *Nat Rev Rheumatol*. 2016 May 7;12(5):282–95.

85. Karagianni N, Kranidioti K, Fikas N, Tsochatzidou M, Chouvardas P, Denis MC, Kollias G, Nikolaou C. An integrative transcriptome analysis framework for drug efficacy and similarity reveals drug-specific signatures of anti-TNF treatment in a mouse model of inflammatory polyarthritis. Cantacessi C, editor. *PLOS Comput Biol*. 2019 May 9;15(5):e1006933.
86. Vasilopoulos Y, Gkretsi V, Armaka M. Actin cytoskeleton dynamics linked to synovial fibroblast activation as a novel pathogenic principle in TNF-driven arthritis. *Ann Rheum Dis*. 2007;66(Suppl 3):iii23–8.
87. Aidinis V, Plows D, Haralambous S, Armaka M, Papadopoulos P, Kanaki MZ, Koczan D, Thiesen HJ, Kollias G. Functional analysis of an arthritogenic synovial fibroblast. *Arthritis Res Ther*. 2003;5(3):R140-57.
88. Aidinis V, Carninci P, Armaka M, Witke W, Harokopos V, Pavelka N, Koczan D, Argyropoulos C, Thwin M-M, Möller S, Kazunori W, Gopalakrishnakone P, Ricciardi-Castagnoli P, Thiesen H-J, Hayashizaki Y, Kollias G, Kollias G. Cytoskeletal Rearrangements in Synovial Fibroblasts as a Novel Pathophysiological Determinant of Modeled Rheumatoid Arthritis. *PLoS Genet*. 2005 Oct;1(4):e48.
89. Kollias G, Douni E, Kassiotis G, Kontoyiannis D. On the role of tumor necrosis factor and receptors in models of multiorgan failure, rheumatoid arthritis, multiple sclerosis and inflammatory bowel disease. *Immunol Rev*. 1999 Jun;169:175–94.
90. Ntougkos E, Chouvardas P, Roumelioti F, Ospelt C, Frank-Bertoncelj M, Filer A, Buckley CD, Gay S, Nikolaou C, Kollias G. Genomic Responses of Mouse Synovial Fibroblasts During Tumor Necrosis Factor–Driven Arthritogenesis Greatly Mimic Those in Human Rheumatoid Arthritis. *Arthritis Rheumatol*. 2017;
91. Sauer B, Henderson N. Site-specific DNA recombination in mammalian cells by the Cre recombinase of bacteriophage P1. *Proc Natl Acad Sci*. 1988 Jul 1;85(14):5166–70.
92. Prados A, Kollias G, Koliaraki V. CollagenVI-Cre mice: A new tool to target stromal cells in secondary lymphoid organs. *Sci Rep*. 2016 Dec 8;6(1):33027.
93. Victoratos P, Lagnel J, Tzima S, Alimzhanov MB, Rajewsky K, Pasparakis M, Kollias G. FDC-specific functions of p55TNFR and IKK2 in the development of FDC networks and of antibody responses. *Immunity*. 2006 Jan;24(1):65–77.
94. Van Hauwermeiren F, Armaka M, Karagianni N, Kranidioti K, Vandenbroucke RE, Loges S, Van Roy M, Staelens J, Puimège L, Palagani A, Berghe W Vanden, Victoratos P, Carmeliet P, Libert C, Kollias G. Safe TNF-based antitumor therapy following p55TNFR reduction in intestinal epithelium. *J Clin Invest*. 2013 Jun;123(6):2590–603.
95. Armaka M, Ospelt C, Pasparakis M, Kollias G. The p55TNFR-IKK2-Ripk3 axis orchestrates arthritis by regulating death and inflammatory pathways in synovial fibroblasts. *Nat Commun*. 2018 Dec 12;9(1):618.
96. Muzumdar MD, Tasic B, Miyamichi K, Li L, Luo L. A global double-fluorescent Cre reporter mouse. *Genesis*. 2007 Sep;45(9):593–605.
97. Dougados M, Soubrier M, Antunez A, Balint P, Balsa A, Buch MH, … Kay J. Prevalence of comorbidities in rheumatoid arthritis and evaluation of their monitoring: results of an international, cross-sectional study (COMORA). *Ann Rheum Dis*. 2014 Jan;73(1):62–8.
98. Gabriel SE, Michaud K. Epidemiological studies in incidence, prevalence, mortality, and comorbidity of the rheumatic diseases. *Arthritis Res Ther*. 2009;11(3):229.
99. Gabriel SE. Why do people with rheumatoid arthritis still die prematurely? *Ann Rheum Dis*. 2008 Dec;67 Suppl 3(Suppl 3):iii30-4.
100. Gullick NJ, Scott DL. Co-morbidities in established rheumatoid arthritis. *Best Pract Res Clin Rheumatol*. 2011 Aug;25(4):469–83.
101. Nurmohamed M, Heslinga M, Kitas G. Cardiovascular comorbidity in rheumatic diseases. *Nat Rev Rheumatol*. 2015;11:693–704.
102. Biesbroek PS, Heslinga SC, Konings TC, van der Horst-Bruinsma IE, Hofman MBM, van de Ven PM, Kamp O, van Halm VP, Peters MJL, Smulders YM, van Rossum AC, Nurmohamed MT, Nijveldt R. Insights into cardiac involvement in ankylosing spondylitis from cardiovascular magnetic resonance. *Heart*. 2017;103(10):745–52.
103. Corrao S, Messina S, Pistone G. Heart involvement in rheumatoid arthritis: systematic review and meta-analysis. *Int J Cardiol*. 2013;167:2031–8.

104. Symmons DPM, Gabriel SE. Epidemiology of CVD in rheumatic disease, with a focus on RA and SLE. *Nat Rev Rheumatol*. 2011 Jul 31;7(7):399–408.
105. Rudominer RL, Roman MJ, Devereux RB, Paget SA, Schwartz JE, Lockshin MD, Crow MK, Sammaritano L, Levine DM, Salmon JE. Independent association of rheumatoid arthritis with increased left ventricular mass but not with reduced ejection fraction. *Arthritis Rheum*. 2009 Jan;60(1):22–9.
106. Cassar A, Holmes DR, Rihal CS, Gersh BJ, Gersh BJ. Chronic coronary artery disease: diagnosis and management. *Mayo Clin Proc*. 2009 Dec;84(12):1130–46.
107. Karpouzas GA, Malpeso J, Choi T-Y, Li D, Munoz S, Budoff MJ. Prevalence, extent and composition of coronary plaque in patients with rheumatoid arthritis without symptoms or prior diagnosis of coronary artery disease. *Ann Rheum Dis*. 2014 Oct;73(10):1797–804.
108. Sattar N, McCarey DW, Capell H, McInnes IB. Explaining How “High-Grade” Systemic Inflammation Accelerates Vascular Risk in Rheumatoid Arthritis. *Circulation*. 2003 Dec 16;108(24):2957–63.
109. Nicola PJ, Maradit-Kremers H, Roger VL, Jacobsen SJ, Crowson CS, Ballman K V., Gabriel SE. The risk of congestive heart failure in rheumatoid arthritis: A population-based study over 46 years. *Arthritis Rheum*. 2005 Feb;52(2):412–20.
110. Mavrogeni S, Dimitroulas T, Kitas GD. Multimodality imaging and the emerging role of cardiac magnetic resonance in autoimmune myocarditis. *Autoimmun Rev*. 2012 Dec;12(2):305–12.
111. Davis JM, Roger VL, Crowson CS, Kremers HM, Therneau TM, Gabriel SE. The presentation and outcome of heart failure in patients with rheumatoid arthritis differs from that in the general population. *Arthritis Rheum*. 2008 Sep;58(9):2603–11.
112. Voskuyl AE. The heart and cardiovascular manifestations in rheumatoid arthritis. *Rheumatology (Oxford)*. 2006 Oct;45 Suppl 4(Suppl 4):iv4-7.
113. Corrao S, Sallì L, Arnone S, Scaglione R, Amato V, Cecala M, Licata A, Licata G. Cardiac involvement in rheumatoid arthritis: evidence of silent heart disease. *Eur Heart J*. 1995 Feb;16(2):253–6.
114. Baumgartner H, Hung J, Bermejo J, Chambers JB, Evangelista A, Griffin BP, Iung B, Otto CM, Pellikka PA, Quiñones M, American Society of Echocardiography, European Association of Echocardiography. Echocardiographic Assessment of Valve Stenosis: EAE/ASE Recommendations for Clinical Practice. *J Am Soc Echocardiogr*. 2009 Jan;22(1):1–23.
115. Marwick TH. The Role of Echocardiography in Heart Failure. *J Nucl Med*. 2015 Jun 1;56(Supplement_4):31S-38S.
116. Yndestad A, Damås JK, Øie E, Ueland T, Gullestad L, Aukrust P. Role of inflammation in the progression of heart failure. *Curr Cardiol Rep*. 2007 May;9(3):236–41.
117. Levine B, Kalman J, Mayer L, Fillit HM, Packer M. Elevated Circulating Levels of Tumor Necrosis Factor in Severe Chronic Heart Failure. *N Engl J Med*. 1990 Jul 26;323(4):236–41.
118. Torre-Amione G, Kapadia S, Lee J, Durand JB, Bies RD, Young JB, Mann DL. Tumor necrosis factor-alpha and tumor necrosis factor receptors in the failing human heart. *Circulation*. 1996 Feb 15;93(4):704–11.
119. Cesari M, Penninx BWJH, Newman AB, Kritchevsky SB, Nicklas BJ, Sutton-Tyrrell K, Rubin SM, Ding J, Simonsick EM, Harris TB, Pahor M. Inflammatory Markers and Onset of Cardiovascular Events. *Circulation*. 2003 Nov 11;108(19):2317–22.
120. Cicha I, Urschel K. TNF-α in the cardiovascular system: from physiology to therapy. *Int J Interf Cytokine Mediat Res*. 2015 Jul 9;7:9.
121. Pantos C, Xinaris C, Mourouzis I, Kokkinos AD, Cokkinos D V. TNF-alpha administration in neonatal cardiomyocytes is associated with differential expression of thyroid hormone receptors: a response prevented by T3. *Horm Metab Res*. 2008 Oct 6;40(10):731–4.
122. Kubota T, McTiernan CF, Frye CS, Slawson SE, Lemster BH, Koretsky AP, Demetris AJ, Feldman AM. Dilated cardiomyopathy in transgenic mice with cardiac-specific overexpression of tumor necrosis factor-alpha. *Circ Res*. 1997 Oct;81(4):627–35.
123. Sivasubramanian N, Coker ML, Kurrelmeyer KM, MacLellan WR, DeMayo FJ, Spinale FG, Mann DL. Left ventricular remodeling in transgenic mice with cardiac restricted overexpression of tumor necrosis factor. *Circulation*. 2001 Aug 14;104(7):826–31.

124. Bryant D, Becker L, Richardson J, Shelton J, Franco F, Peshock R, Thompson M, Giroir B. Cardiac failure in transgenic mice with myocardial expression of tumor necrosis factor-alpha. *Circulation*. 1998 Apr 14;97(14):1375–81.
125. Li YY, Feng YQ, Kadokami T, McTiernan CF, Draviam R, Watkins SC, Feldman AM. Myocardial extracellular matrix remodeling in transgenic mice overexpressing tumor necrosis factor alpha can be modulated by anti-tumor necrosis factor alpha therapy. *Proc Natl Acad Sci*. 2000 Nov 7;97(23):12746–51.
126. Bozkurt B, Torre-Amione G, Warren MS, Whitmore J, Soran OZ, Feldman AM, Mann DL. Results of targeted anti-tumor necrosis factor therapy with etanercept (ENBREL) in patients with advanced heart failure. *Circulation*. 2001 Feb 27;103(8):1044–7.
127. Sinagra E, Perricone G, Romano C, Cottone M. Heart failure and anti tumor necrosis factor-alpha in systemic chronic inflammatory diseases. *Eur J Intern Med*. 2013 Jul 1;24(5):385–92.
128. Kosmas CE, Silverio D, Sourlas A, Montan PD, Guzman E, Garcia MJ. Anti-inflammatory therapy for cardiovascular disease. *Ann Transl Med*. 2019;7(7).
129. Sarzi-Puttini P, Atzeni F, Shoenfeld Y, Ferraccioli G. TNF-α, rheumatoid arthritis, and heart failure: a rheumatological dilemma. *Autoimmun Rev*. 2005 Mar 1;4(3):153–61.
130. Galeone A, Paparella D, Colucci S, Grano M, Brunetti G. The role of TNF-α and TNF superfamily members in the pathogenesis of calcific aortic valvular disease. *ScientificWorldJournal*. 2013 Nov 6;2013:875363.
131. Galeone A, Brunetti G, Oranger A, Greco G, Di Benedetto A, Mori G, Colucci S, Zallone A, Paparella D, Grano M. Aortic valvular interstitial cells apoptosis and calcification are mediated by TNF-related apoptosis-inducing ligand. *Int J Cardiol*. 2013 Nov 15;169(4):296–304.
132. Kapadia SR, Yakoob K, Nader S, Thomas JD, Mann DL, Griffin BP. Elevated circulating levels of serum tumor necrosis factor-alpha in patients with hemodynamically significant pressure and volume overload. *J Am Coll Cardiol*. 2000 Jul 1;36(1):208–12.
133. Lacey D, Hickey P, Arhatari BD, O'Reilly LA, Rohrbeck L, Kiriazis H, Du X-J, Bouillet P. Spontaneous retrotransposon insertion into *TNF* 3′UTR causes heart valve disease and chronic polyarthritis. *Proc Natl Acad Sci*. 2015 Aug 4;112(31):9698–703.
134. Isoda K, Matsuki T, Kondo H, Iwakura Y, Ohsuzu F. Deficiency of interleukin-1 receptor antagonist induces aortic valve disease in BALB/c Mice. *Arterioscler Thromb Vasc Biol*. 2010;30(4):708–15.
135. Ghosh S, Hoenerhoff MJ, Clayton N, Myers P, Stumpo DJ, Maronpot RR, Blackshear PJ. Left-sided cardiac valvulitis in tristetraprolin-deficient mice: The role of tumor necrosis factor α. *Am J Pathol*. 2010;176(3):1484–93.
136. Roubille C, Richer V, Starnino T, McCourt C, McFarlane A, Fleming P, Siu S, Kraft J, Lynde C, Pope J, Gulliver W, Keeling S, Dutz J, Bessette L, Bissonnette R, Haraoui B. The effects of tumour necrosis factor inhibitors, methotrexate, non-steroidal anti-inflammatory drugs and corticosteroids on cardiovascular events in rheumatoid arthritis, psoriasis and psoriatic arthritis: a systematic review and meta-analysis. *Ann Rheum Dis*. 2015 Mar;74(3):480–9.
137. Wang H, Leinwand LA, Anseth KS. Cardiac valve cells and their microenvironment—insights from in vitro studies. *Nat Rev Cardiol*. 2014 Dec 14;11(12):715–27.
138. Taylor PM, Allen SP, Yacoub MH. Phenotypic and functional characterization of interstitial cells from human heart valves, pericardium and skin. *J Heart Valve Dis*. 2000 Jan;9(1):150–8.
139. Nomura A, Seya K, Yu Z, Daitoku K, Motomura S, Murakami M, Fukuda I, Furukawa KI. CD34-negative mesenchymal stem-like cells may act as the cellular origin of human aortic valve calcification. *Biochem Biophys Res Commun*. 2013;
140. Li X, Lim J, Lu J, Pedego TM, Demer L, Tintut Y. Protective Role of Smad6 in Inflammation-Induced Valvular Cell Calcification. *J Cell Biochem*. 2015 Oct;116(10):2354–64.
141. Pinto AR, Ilinykh A, Ivey MJ, Kuwabara JT, D'Antoni ML, Debuque R, Chandran A, Wang L, Arora K, Rosenthal NA, Tallquist MD. Revisiting Cardiac Cellular Composition. *Circ Res*. 2016 Feb 5;118(3):400–9.
142. Liu AC, Joag VR, Gotlieb AI. The emerging role of valve interstitial cell phenotypes in regulating heart valve pathobiology. *Am J Pathol*. 2007 Nov;171(5):1407–18.

143. Hjortnaes J, Shapero K, Goettsch C, Hutcheson JD, Keegan J, Kluin J, Mayer JE, Bischoff J, Aikawa E. Valvular interstitial cells suppress calcification of valvular endothelial cells. *Atherosclerosis*. 2015 Sep;242(1):251–60.
144. Yu Z, Seya K, Daitoku K, Motomura S, Fukuda I, Furukawa K-I. Tumor necrosis factor-α accelerates the calcification of human aortic valve interstitial cells obtained from patients with calcific aortic valve stenosis via the BMP2-Dlx5 pathway. *J Pharmacol Exp Ther*. 2011 Apr;337(1):16–23.
145. Chester A, Taylor P. Molecular and functional characteristics of heart-valve interstitial cells. *Philos Trans R Soc B Biol Sci*. 2007;362(1484):1437–43.
146. López-Otín C, Blasco MA, Partridge L, Serrano M, Kroemer G. The hallmarks of aging. *Cell*. 2013 Jun 6;153(6):1194–217.
147. Regulski MJ. Cellular Senescence: What, Why, and How. *Wounds a Compend Clin Res Pract*. 2017 Jun;29(6):168–74.
148. Kirkwood TBL. Understanding the Odd Science of Aging. *Cell*. 2005 Feb 25;120(4):437–47.
149. Hoeijmakers JH. DNA repair mechanisms. *Maturitas*. 2001 Feb 28;38(1):17–22; discussion 22-3.
150. Xi H, Li C, Ren F, Zhang H, Zhang L. Telomere, aging and age-related diseases. *Aging Clin Exp Res*. 2013 May 3;25(2):139–46.
151. von Zglinicki T. Oxidative stress shortens telomeres. *Trends Biochem Sci*. 2002 Jul;27(7):339–44.
152. Armanios M, Blackburn EH. The telomere syndromes. *Nat Rev Genet*. 2012 Oct 11;13(10):693–704.
153. Powers ET, Morimoto RI, Dillin A, Kelly JW, Balch WE. Biological and Chemical Approaches to Diseases of Proteostasis Deficiency. *Annu Rev Biochem*. 2009 Jun;78(1):959–91.
154. Rubinsztein DC, Mariño G, Kroemer G. Autophagy and Aging. *Cell*. 2011 Sep;146(5):682–95.
155. Barzilai N, Huffman DM, Muzumdar RH, Bartke A. The Critical Role of Metabolic Pathways in Aging. *Diabetes*. 2012 Jun 1;61(6):1315–22.
156. Vermeij WP, Dollé MET, Reiling E, Jaarsma D, Payan-Gomez C, Bombardieri CR, … Hoeijmakers JHJ. Restricted diet delays accelerated ageing and genomic stress in DNA-repair-deficient mice. *Nature*. 2016 Sep 24;537(7620):427–31.
157. Palikaras K, Lionaki E, Tavernarakis N. Coordination of mitophagy and mitochondrial biogenesis during ageing in C. elegans. *Nature*. 2015 May 28;521(7553):525–8.
158. Campisi J, D'Adda Di Fagagna F. Cellular senescence: When bad things happen to good cells. Vol. 8, Nature Reviews Molecular Cell Biology. 2007. p. 729–40.
159. Coppé J-P, Desprez P-Y, Krtolica A, Campisi J. The Senescence-Associated Secretory Phenotype: The Dark Side of Tumor Suppression. *Annu Rev Pathol Mech Dis*. 2010 Jan;5(1):99–118.
160. Rando TA, Chang HY. Aging, rejuvenation, and epigenetic reprogramming: resetting the aging clock. *Cell*. 2012 Jan 20;148(1–2):46–57.
161. Salminen A, Kaarniranta K, Kauppinen A. Inflammaging: disturbed interplay between autophagy and inflammasomes. *Aging (Albany NY)*. 2012 Mar 7;4(3):166–75.
162. Rothwell PM, Fowkes FGR, Belch JF, Ogawa H, Warlow CP, Meade TW. Effect of daily aspirin on long-term risk of death due to cancer: analysis of individual patient data from randomised trials. *Lancet*. 2011 Jan 1;377(9759):31–41.
163. Nelson G, Wordsworth J, Wang C, Jurk D, Lawless C, Martin-Ruiz C, von Zglinicki T. A senescent cell bystander effect: senescence-induced senescence. *Aging Cell*. 2012 Apr;11(2):345–9.
164. Giglia-Mari G, Zotter A, Vermeulen W. DNA damage response. *Cold Spring Harb Perspect Biol*. 2011 Jan;3(1):1–19.
165. Lindahl T. Instability and decay of the primary structure of DNA. Vol. 362, Nature. 1993. p. 709–15.
166. Akbari M, Krokan HE. Cytotoxicity and mutagenicity of endogenous DNA base lesions as potential cause of human aging. *Mech Ageing Dev*. 2008 Jul;129(7–8):353–65.
167. Hoeijmakers JHJ. DNA damage, aging, and cancer. Vol. 361, New England Journal of Medicine. Massachussetts Medical Society; 2009. p. 1475–85.
168. Jiricny J. The multifaceted mismatch-repair system. Vol. 7, Nature Reviews Molecular

Cell Biology. 2006. p. 335–46.
169. David SS, O'Shea VL, Kundu S. Base-excision repair of oxidative DNA damage. Vol. 447, Nature. Nature Publishing Group; 2007. p. 941–50.
170. Caldecott KW. DNA single-strand break repair and spinocerebellar ataxia. Vol. 112, Cell. Cell Press; 2003. p. 7–10.
171. Mao Z, Bozzella M, Seluanov A, Gorbunova V. Compare NHEJ & HR in human cells. *DNA Repair (Amst)*. 2008;7(10):1765–71.
172. Jackson SP, Bartek J. The DNA-damage response in human biology and disease. Vol. 461, Nature. 2009. p. 1071–8.
173. Postel-Vinay S, Vanhecke E, Olaussen KA, Lord CJ, Ashworth A, Soria JC. The potential of exploiting DNA-repair defects for optimizing lung cancer treatment. Vol. 9, Nature Reviews Clinical Oncology. 2012. p. 144–55.
174. Liakos A, Lavigne MD, Fousteri M. Nucleotide excision repair: From neurodegeneration to cancer. In: Advances in Experimental Medicine and Biology. Springer New York LLC; 2017. p. 17–39.
175. Spivak G. Nucleotide excision repair in humans. *DNA Repair (Amst)*. 2015 Dec;36:13–8.
176. Hanawalt PC, Spivak G. Transcription-coupled DNA repair: two decades of progress and surprises. *Nat Rev Mol Cell Biol*. 2008 Dec;9(12):958–70.
177. Marteijn JA, Lans H, Vermeulen W, Hoeijmakers JHJ. Understanding nucleotide excision repair and its roles in cancer and ageing. *Nat Rev Mol Cell Biol*. 2014 Jul;15(7):465–81.
178. Hoeijmakers JHJ. Genome maintenance mechanisms for preventing cancer. Vol. 411, Nature. 2001. p. 366–74.
179. Cleaver JE, Lam ET, Revet I. Disorders of nucleotide excision repair: the genetic and molecular basis of heterogeneity. *Nat Rev Genet*. 2009 Nov;10(11):756–68.
180. Kraemer KH, Patronas NJ, Schiffmann R, Brooks BP, Tamura D, DiGiovanna JJ. Xeroderma pigmentosum, trichothiodystrophy and Cockayne syndrome: a complex genotype-phenotype relationship. *Neuroscience*. 2007 Apr 14;145(4):1388–96.
181. Cleaver JE. Defective Repair Replication of DNA in Xeroderma Pigmentosum. *Nature*. 1968 May;218(5142):652–6.
182. Kraemer KH, Lee MM, Andrews AD, Lambert WC. The role of sunlight and DNA repair in melanoma and nonmelanoma skin cancer. The xeroderma pigmentosum paradigm. *Arch Dermatol*. 1994 Aug;130(8):1018–21.
183. Nance MA, Berry SA. Cockayne syndrome: review of 140 cases. *Am J Med Genet*. 1992 Jan 1;42(1):68–84.
184. Rapin I, Weidenheim K, Lindenbaum Y, Rosenbaum P, Merchant S, Krishna S, Dickson DW. Cockayne syndrome in adults: Review with clinical and pathologic study of a new case. *J Child Neurol*. 2006 Nov;21(11):991–1006.
185. Chang HR, Ishizaki K, Ikenaga M, Asada Y. Cockayne syndrome in two adult siblings. *J Am Acad Dermatol*. 1994;30(2):329–35.
186. Jaspers NGJ, Raams A, Silengo MC, Wijgers N, Niedernhofer LJ, Robinson AR, Giglia-Mari G, Hoogstraten D, Kleijer WJ, Hoeijmakers JHJ, Vermeulen W. First reported patient with human ERCC1 deficiency has cerebro-oculo-facio-skeletal syndrome with a mild defect in nucleotide excision repair and severe developmental failure. *Am J Hum Genet*. 2007 Mar;80(3):457–66.
187. Houtsmuller AB, Rademakers S, Nigg AL, Hoogstraten D, Hoeijmakers JH, Vermeulen W. Action of DNA Repair Endonuclease ERCC1/XPF in Living Cells. *Science (80-)*. 1999 May 7;284(5416):958–61.
188. Tripsianes K, Folkers G, Ab E, Das D, Odijk H, Jaspers NGJ, Hoeijmakers JHJ, Kaptein R, Boelens R. The structure of the human ERCC1/XPF interaction domains reveals a complementary role for the two proteins in nucleotide excision repair. *Structure*. 2005 Dec;13(12):1849–58.
189. Petit C, Sancar A. Nucleotide excision repair: From E. coli to man. *Biochimie*. 1999;81(1–2):15–25.
190. Zhu X-D, de Lange T, Niedernhofer L, Kuster B, Mann M, Hoeijmakers JHJ. ERCC1/XPF removes the 3' overhang from uncapped telomeres and represses formation of telomeric DNA-containing double minute chromosomes. *Mol Cell*. 2003;12(6):1489–98.

191. Gregg SQ, Robinson AR, Niedernhofer LJ. Physiological consequences of defects in ERCC1-XPF DNA repair endonuclease. *DNA Repair (Amst)*. 2011 Jul 15;10(7):781–91.
192. Niedernhofer LJ, Garinis GA, Raams A, Lalai AS, Robinson AR, Appeldoorn E, Odijk H, Oostendorp R, Ahmad A, van Leeuwen W, Theil AF, Vermeulen W, van der Horst GTJ, Meinecke P, Kleijer WJ, Vijg J, Jaspers NGJ, Hoeijmakers JHJ. A new progeroid syndrome reveals that genotoxic stress suppresses the somatotroph axis. *Nature*. 2006 Dec 21;444(7122):1038–43.
193. Jaarsma D, van der Pluijm I, van der Horst GTJ, Hoeijmakers JHJ. Cockayne syndrome pathogenesis: Lessons from mouse models. *Mech Ageing Dev*. 2013 May;134(5–6):180–95.
194. Weeda G, Donker I, De Wit J, Morreau H, Janssens R, Vissers CJ, Nigg A, Van Steeg H, Bootsma D, Hoeijmakers JHJ. Disruption of mouse ERCC1 results in a novel repair syndrome with growth failure, nuclear abnormalities and senescence. *Curr Biol*. 1997 Jun 1;7(6):427–39.
195. McWhir J, Selfridge J, Harrison DJ, Squires S, Melton DW. Mice with DNA repair gene (ERCC-1) deficiency have elevated levels of p53, liver nuclear abnormalities and die before weaning. *Nat Genet*. 1993;5(3):217–24.
196. Selfridge J, Hsia KT, Redhead NJ, Melton DW. Correction of liver dysfunction in DNA repair-deficient mice with an ERCC1 transgene. *Nucleic Acids Res*. 2001 Nov 15;29(22):4541–50.
197. De Waard MC, Van Der Pluijm I, Zuiderveen Borgesius N, Comley LH, Haasdijk ED, Rijksen Y, Ridwan Y, Zondag G, Hoeijmakers JHJ, Elgersma Y, Gillingwater TH, Jaarsma D. Age-related motor neuron degeneration in DNA repair-deficient Ercc1 mice. *Acta Neuropathol*. 2010 Oct;120(4):461–75.
198. Vo N, Seo H-Y, Robinson A, Sowa G, Bentley D, Taylor L, Studer R, Usas A, Huard J, Alber S, Watkins SC, Lee J, Coehlo P, Wang D, Loppini M, Robbins PD, Niedernhofer LJ, Kang J. Accelerated aging of intervertebral discs in a mouse model of progeria. *J Orthop Res*. 2010 Dec;28(12):1600–7.
199. Chen Q, Liu K, Robinson AR, Clauson CL, Blair HC, Robbins PD, Niedernhofer LJ, Ouyang H. DNA damage drives accelerated bone aging via an NF- κ B-dependent mechanism. *J Bone Miner Res*. 2013 May;28(5):1214–28.
200. Takayama K, Kawakami Y, Lee S, Greco N, Lavasani M, Mifune Y, Cummins JH, Yurube T, Kuroda R, Kurosaka M, Fu FH, Huard J. Involvement of ERCC1 in the pathogenesis of osteoarthritis through the modulation of apoptosis and cellular senescence. *J Orthop Res*. 2014 Oct;32(10):1326–32.
201. Doig J, Anderson C, Lawrence NJ, Selfridge J, Brownstein DG, Melton DW. Mice with skin-specific DNA repair gene (Ercc1) inactivation are hypersensitive to ultraviolet irradiation-induced skin cancer and show more rapid actinic progression. *Oncogene*. 2006 Oct 12;25(47):6229–38.
202. Kirschner K, Singh R, Prost S, Melton DW. Characterisation of Ercc1 deficiency in the liver and in conditional Ercc1-deficient primary hepatocytes in vitro. *DNA Repair (Amst)*. 2007 Mar 1;6(3):304–16.
203. Lawrence NJ, Sacco JJ, Brownstein DG, Gillingwater TH, Melton DW. A neurological phenotype in mice with DNA repair gene Ercc1 deficiency. *DNA Repair (Amst)*. 2008 Feb 1;7(2):281–91.
204. Selfridge J, Song L, Brownstein DG, Melton DW. Mice with DNA repair gene Ercc1 deficiency in a neural crest lineage are a model for late-onset Hirschsprung disease. *DNA Repair (Amst)*. 2010 Jun 4;9(6):653–60.
205. Borgesius NZ, de Waard MC, van der Pluijm I, Omrani A, Zondag GCM, van der Horst GTJ, Melton DW, Hoeijmakers JHJ, Jaarsma D, Elgersma Y. Accelerated age-related cognitive decline and neurodegeneration, caused by deficient DNA repair. *J Neurosci*. 2011 Aug 31;31(35):12543–53.
206. Verhagen-Oldenampsen JHE, Haanstra JR, Van Strien PMH, Valkhof M, Touw IP, Von Lindern M. Loss of Ercc1 results in a time- and dose-dependent reduction of proliferating early hematopoietic progenitors. *Anemia*. 2012;
207. Karakasilioti I, Kamileri I, Chatzinikolaou G, Kosteas T, Vergadi E, Robinson AR, Tsamardinos I, Rozgaja TA, Siakouli S, Tsatsanis C, Niedernhofer LJ, Garinis GA. DNA Damage Triggers a Chronic Autoinflammatory Response, Leading to Fat

Depletion in NER Progeria. *Cell Metab*. 2013 Sep 3;18(3):403–15.
208. Weyand CM, Goronzy JJ. Aging of the Immune System. Mechanisms and Therapeutic Targets. *Ann Am Thorac Soc*. 2016;13 Suppl 5:S422–8.
209. Hager K, Machein U, Krieger S, Platt D, Seefried G, Bauer J. Interleukin-6 and selected plasma proteins in healthy persons of different ages. *Neurobiol Aging*. 1994;15(6):771–2.
210. Bruunsgaard H. A high plasma concentration of tnf-α is associated with dementia in centenarians. *Journals Gerontol - Ser A Biol Sci Med Sci*. 1999;54(7).
211. Bruunsgaard H, Andersen-Ranberg K, Hjelmborg JVB, Pedersen BK, Jeune B. Elevated levels of tumor necrosis factor alpha and mortality in centenarians. *Am J Med*. 2003;115(4):278–83.
212. Krabbe KS, Pedersen M, Bruunsgaard H. Inflammatory mediators in the elderly. *Exp Gerontol*. 2004 May;39(5):687–99.
213. Bruunsgaard H, Pedersen M, Pedersen BK. Aging and proinflammatory cytokines. Vol. 8, Current Opinion in Hematology. 2001. p. 131–6.
214. Chung HY, Kim HJ, Kim KW, Choi JS, Yu BP. Molecular inflammation hypothesis of aging based on the anti-aging mechanism of calorie restriction. *Microsc Res Tech*. 2002 Nov 15;59(4):264–72.
215. Tilstra JS, Robinson AR, Wang J, Gregg SQ, Clauson CL, Reay DP, … Robbins PD. NF-κB inhibition delays DNA damage - Induced senescence and aging in mice. *J Clin Invest*. 2012 Jul 2;122(7):2601–12.
216. Majka SM, Barak Y, Klemm DJ. Concise review: Adipocyte origins: Weighing the possibilities. Vol. 29, Stem Cells. 2011. p. 1034–40.
217. Shao L. DNA Damage Response Signals Transduce Stress From Rheumatoid Arthritis Risk Factors Into T Cell Dysfunction. *Front Immunol*. 2018 Dec 20;9:3055.
218. Fujii H, Shao L, Colmegna I, Goronzy JJ, Yand CM. Telomerase insufficiency in rheumatoid arthritis. *Proc Natl Acad Sci U S A*. 2009 Mar 17;106(11):4360–5.
219. Weyand CM, Fujii H, Shao L, Goronzy JJ. Rejuvenating the immune system in rheumatoid arthritis. Vol. 5, Nature Reviews Rheumatology. 2009. p. 583–8.
220. Yang Z, Shen Y, Oishi H, Matteson EL, Tian L, Goronzy JJ, Weyand CM. Restoring oxidant signaling suppresses proarthritogenic T cell effector functions in rheumatoid arthritis. *Sci Transl Med*. 2016 Mar 23;8(331).
221. Prelog M. Aging of the immune system: a risk factor for autoimmunity? *Autoimmun Rev*. 2006 Feb;5(2):136–9.
222. Sethe S, Scutt A, Stolzing A. Aging of mesenchymal stem cells. *Ageing Res Rev*. 2006 Feb;5(1):91–116.
223. Baxter MA, Wynn RF, Jowitt SN, Wraith JE, Fairbairn LJ, Bellantuono I. Study of Telomere Length Reveals Rapid Aging of Human Marrow Stromal Cells following In Vitro Expansion. *Stem Cells*. 2004 Sep 1;22(5):675–82.
224. Armstrong L, Lako M, Lincoln J, Cairns PM, Hole N. mTert expression correlates with telomerase activity during the differentiation of murine embryonic stem cells. *Mech Dev*. 2000 Oct;97(1–2):109–16.
225. Alexopoulou L, Pasparakis M, Kollias G. A murine transmembrane tumor necrosis factor (TNF) transgene induces arthritis by cooperative p55/p75 TNF receptor signaling. *Eur J Immunol*. 1997 Oct;27(10):2588–92.
226. Douni E, Sfikakis PP, Haralambous S, Fernandes P, Kollias G. Attenuation of inflammatory polyarthritis in TNF transgenic mice by diacerein: comparative analysis with dexamethasone, methotrexate and anti-TNF protocols. *Arthritis Res Ther*. 2004;6(1):R65–72.
227. Khachigian LM. Collagen antibody-induced arthritis. *Nat Protoc*. 2006 Dec 29;1(5):2512–6.
228. Mourouzis I, Kostakou E, Galanopoulos G, Mantzouratou P, Pantos C. Inhibition of thyroid hormone receptor α1 impairs post-ischemic cardiac performance after myocardial infarction in mice. *Mol Cell Biochem*. 2013 Jul;379(1–2):97–105.
229. Armaka M, Gkretsi V, Kontoyiannis D, Kollias G. A standardized protocol for the isolation and culture of normal and arthritogenic murine synovial fibroblasts. *Protoc Exch*. 2009 May 1;
230. Rodriguez LG, Wu X, Guan J-L. Wound-healing assay. *Methods Mol Biol*. 2005;294:23–9.

231. Lawrence M, Huber W, Pagès H, Aboyoun P, Carlson M, Gentleman R, Morgan MT, Carey VJ. Software for Computing and Annotating Genomic Ranges. *PLoS Comput Biol*. 2013 Aug;9(8).
232. Anders S, Huber W. Differential expression analysis for sequence count data. *Genome Biol*. 2010 Oct 27;11(10).
233. Moulos P, Hatzis P. Systematic integration of RNA-Seq statistical algorithms for accurate detection of differential gene expression patterns. *Nucleic Acids Res*. 2015 Feb 27;43(4).
234. R Core Team. R: A language and environment for statistical computing. *Vienna R Foudation Stat Comput*. 2013;
235. Kanehisa M, Goto S. KEGG: kyoto encyclopedia of genes and genomes. *Nucleic Acids Res*. 2000 Jan 1;28(1):27–30.
236. Chen EY, Tan CM, Kou Y, Duan Q, Wang Z, Meirelles G V., Clark NR, Ma'ayan A. Enrichr: Interactive and collaborative HTML5 gene list enrichment analysis tool. *BMC Bioinformatics*. 2013 Apr 15;14.
237. Chouvardas P, Kollias G, Nikolaou C. Inferring active regulatory networks from gene expression data using a combination of prior knowledge and enrichment analysis. *BMC Bioinformatics*. 2016 Jun 6;17(S5):181.
238. Shannon P, Markiel A, Ozier O, Baliga NS, Wang JT, Ramage D, Amin N, Schwikowski B, Ideker T. Cytoscape: A software Environment for integrated models of biomolecular interaction networks. *Genome Res*. 2003 Nov;13(11):2498–504.
239. Koliaraki V, Pasparakis M, Kollias G. IKKβ in intestinal mesenchymal cells promotes initiation of colitis-associated cancer. *J Exp Med*. 2015;212(13):2235–51.
240. Bentzinger C, Lin S, Romanino K, Castets P, Guridi M, Summermatter S, Handschin C, Tintignac LA, Hall MN, Rüegg MA. Differential response of skeletal muscles to mTORC1 signaling during atrophy and hypertrophy. *Skelet Muscle*. 2013;3(1):6.
241. Moskalewski S, Hyc A, Jankowska-Steifer E, Osiecka-Iwan A. Formation of synovial joints and articular cartilage. *Folia Morphol (Warsz)*. 2013 Aug;72(3):181–7.
242. Crisan M, Yap S, Casteilla L, Chen C-W, Corselli M, Park TS, … Péault B. A Perivascular Origin for Mesenchymal Stem Cells in Multiple Human Organs. *Cell Stem Cell*. 2008 Sep 11;3(3):301–13.
243. Rabkin-Aikawa E, Farber M, Aikawa M, Schoen FJ. Dynamic and reversible changes of interstitial cell phenotype during remodeling of cardiac valves. *J Heart Valve Dis*. 2004 Sep;13(5):841–7.
244. Ritchlin C. Fibroblast biology. Effector signals released by the synovial fibroblast in arthritis. Vol. 2, Arthritis Research. 2000. p. 356–60.
245. El Bakry SA, Fayez D, Morad CS, Abdel-salam AM, Abdel-Salam Z, ElKabarity RH, El Dakrony AHM. Ischemic heart disease and rheumatoid arthritis: Do inflammatory cytokines have a role? *Cytokine*. 2017 Aug;96:228–33.
246. Janckila AJ, Nakasato YR, Neustadt DH, Yam LT. Disease-Specific Expression of Tartrate-Resistant Acid Phosphatase Isoforms. *J Bone Miner Res*. 2003 Oct 1;18(10):1916–9.
247. Ozkan Y. Cardiac Involvement in Ankylosing Spondylitis. *J Clin Med Res*. 2016 Jun;8(6):427–30.
248. Roldan CA, DeLong C, Qualls CR, Crawford MH. Characterization of valvular heart disease in rheumatoid arthritis by transesophageal echocardiography and clinical correlates. *Am J Cardiol*. 2007 Aug 1;100(3):496–502.
249. Vieira-Sousa E, van Duivenvoorde LM, Fonseca JE, Lories RJ, Baeten DL. Review: Animal Models as a Tool to Dissect Pivotal Pathways Driving Spondyloarthritis. *Arthritis Rheumatol*. 2015 Nov;67(11):2813–27.
250. Chandrasekhar J, Dangas G, Mehran R. Valvular Heart Disease in Women, Differential Remodeling, and Response to New Therapies. *Curr Treat Options Cardiovasc Med*. 2017 Sep 11;19(9):74.
251. Lazúrová I, Tomáš Ľ. Cardiac Impairment in Rheumatoid Arthritis and Influence of Anti-TNFα Treatment. Vol. 52, Clinical Reviews in Allergy and Immunology. Humana Press Inc.; 2017. p. 323–32.
252. Kaźmierczak J, Peregud-Pogorzelska M, Biernawska J, Przepiera-Będzak H, Gorący J, Brzosko I, Plonska E, Brzosko M. Cardiac Arrhythmias and Conduction Disturbances in Patients With Ankylosing Spondylitis. *Angiology*. 2008 Dec

7;58(6):751–6.
253. Lazzerini PE, Capecchi PL, Acampa M, Galeazzi M, Laghi-Pasini F. Arrhythmic risk in rheumatoid arthritis: The driving role of systemic inflammation. Vol. 13, Autoimmunity Reviews. Elsevier; 2014. p. 936–44.
254. Glass AM, Coombs W, Taffet SM. Spontaneous cardiac calcinosis in BALB/cByJ mice. *Comp Med*. 2013 Feb;63(1):29–37.
255. Binstadt BA, Hebert JL, Ortiz-Lopez A, Bronson R, Benoista C, Mathisa D. The same systemic autoimmune disease provokes arthritis and endocarditis via distinct mechanisms. *Proc Natl Acad Sci U S A*. 2009 Sep 29;106(39):16758–63.
256. Haimovici A, Humbert M, Federzoni EA, Shan-Krauer D, Brunner T, Frese S, Kaufmann T, Torbett BE, Tschan MP. PU.1 supports TRAIL-induced cell death by inhibiting NF-κB-mediated cell survival and inducing DR5 expression. *Cell Death Differ*. 2017 May 31;24(5):866–77.
257. Rosenbauer F, Wagner K, Kutok JL, Iwasaki H, Le Beau MM, Okuno Y, Akashi K, Fiering S, Tenen DG. Acute myeloid leukemia induced by graded reduction of a lineage-specific transcription factor, PU.1. *Nat Genet*. 2004 Jun;36(6):624–30.
258. Itoh K, Nagatani K. Rheumatoid arthritis fibroblast-like synoviocytes show the upregulation of myeloid cell specific transcription factor PU.1 and B cell specific transcriptional co-activator OBF-1, and express functional BCMA. *Arthritis Res Ther*. 2012;14(Suppl 1):P28.
259. Tang Y, Yu S, Liu Y, Zhang J, Han L, Xu Z. MicroRNA-124 controls human vascular smooth muscle cell phenotypic switch via Sp1. *Am J Physiol Heart Circ Physiol*. 2017 Sep 1;313(3):H641–9.
260. Michopoulos F, Karagianni N, Whalley NM, Firth MA, Nikolaou C, Wilson ID, Critchlow SE, Kollias G, Theodoridis GA. Targeted Metabolic Profiling of the Tg197 Mouse Model Reveals Itaconic Acid as a Marker of Rheumatoid Arthritis. *J Proteome Res*. 2016 Dec 2;15(12):4579–90.
261. Kim S, Hwang J, Xuan J, Jung YH, Cha H-S, Kim KH. Global Metabolite Profiling of Synovial Fluid for the Specific Diagnosis of Rheumatoid Arthritis from Other Inflammatory Arthritis. Bahn Y-S, editor. *PLoS One*. 2014 Jun 2;9(6):e97501.
262. Shirai T, Nazarewicz RR, Wallis BB, Yanes RE, Watanabe R, Hilhorst M, Tian L, Harrison DG, Giacomini JC, Assimes TL, Goronzy JJ, Weyand CM. The glycolytic enzyme PKM2 bridges metabolic and inflammatory dysfunction in coronary artery disease. *J Exp Med*. 2016 Mar 7;213(3):337–54.
263. Durik M, Kavousi M, van der Pluijm I, Isaacs A, Cheng C, Verdonk K, … Roks AJM. Nucleotide Excision DNA Repair Is Associated With Age-Related Vascular Dysfunction. *Circulation*. 2012 Jul 24;126(4):468–78.
264. Zhang S, Wang X-B, Han Y, Xiong C-L, Zhou Y, Wang C, Liu Z-J, Yang N, Zheng F. Polymorphism in ERCC1 confers susceptibility of coronary artery disease and severity of coronary artery atherosclerosis in a Chinese Han population. *Sci Rep*. 2017;7(1):6407.

Appendix (Publication)

Ntari, L., M. Sakkou, P. Chouvardas, I. Mourouzis, A. Prados, M.C. Denis, N. Karagianni, C. Pantos, and G. Kollias. 2018. Comorbid TNF-mediated heart valve disease and chronic polyarthritis share common mesenchymal cell-mediated aetiopathogenesis. *Ann. Rheum. Dis.* 77:926–934. doi:10.1136/ANNRHEUMDIS-2017-212597.

EXTENDED REPORT

Comorbid TNF-mediated heart valve disease and chronic polyarthritis share common mesenchymal cell-mediated aetiopathogenesis

Lydia Ntari,[1,2] Maria Sakkou,[1] Panagiotis Chouvardas,[1,3] Iordanis Mourouzis,[4] Alejandro Prados,[1] Maria C Denis,[5] Niki Karagianni,[5] Constantinos Pantos,[4] George Kollias[1,3]

Handling editor Josef S Smolen

► Additional material is published online only. To view please visit the journal online (http://dx.doi.org/10.1136/annrheumdis-2017-212597)

[1]Institute of Immunology, Biomedical Sciences Research Center (BSRC), 'Alexander Fleming', Vari, Greece
[2]Faculty of Medicine, University of Crete, Heraklion, Greece
[3]Department of Physiology, School of Medicine, National Kapodistrian University, Athens, Greece
[4]Department of Pharmacology, School of Medicine, National Kapodistrian University, Athens, Greece
[5]Biomedcode Hellas SA, Vari, Greece

Correspondence to
Professor George Kollias, Institute of Immunology, Biomedical Sciences Research Center (BSRC), "Alexander Fleming", Vari 16672, Greece; kollias@fleming.gr

LN and MS contributed equally.

Received 25 October 2017
Revised 29 December 2017
Accepted 25 January 2018
Published Online First 23 February 2018

► http://dx.doi.org/10.1136/annrheumdis-2018-213118

To cite: Ntari L, Sakkou M, Chouvardas P, *et al*. *Ann Rheum Dis* 2018;**77**:926–934.

ABSTRACT

Objectives Patients with rheumatoid arthritis and spondyloarthritisshow higher mortality rates, mainly caused by cardiac comorbidities. The TghuTNF (Tg197) arthritis model develops tumour necrosis factor (TNF)-driven and mesenchymalsynovial fibroblast (SF)-dependent polyarthritis. Here, we investigate whether this model develops, similarly to human patients, comorbid heart pathology and explore cellular and molecular mechanisms linking arthritis to cardiac comorbidities.

Methods Histopathological analysis and echocardiographic evaluation of cardiac function were performed in the Tg197 model. Valve interstitial cells (VICs) were targeted by mice carrying the *ColVI-Cre*transgene. Tg197 *ColVI-Cre Tnfr1*$^{fl/fl}$ and Tg197 *ColVI-Cre Tnfr1*$^{cneo/cneo}$ mutant mice were used to explore the role of mesenchymal TNF signalling in the development of heart valve disease. Pathogenic VICs and SFs were further analysed by comparative RNA-sequencing analysis.

Results Tg197 mice develop left-sided heart valve disease, characterised by valvular fibrosis with minimal signs of inflammation. Thickened valve areas consist almost entirely of hyperproliferative *ColVI*-expressing mesenchymal VICs. Development of pathology results in valve stenosis and left ventricular dysfunction, accompanied by arrhythmic episodes and, occasionally, valvular regurgitation. TNF dependency of the pathology was indicated by disease modulation following pharmacological inhibition or mesenchymal-specific genetic ablation or activation of TNF/TNFR1 signalling. Tg197-derived VICs exhibited an activated phenotype *ex vivo*, reminiscent of the activated pathogenic phenotype of Tg197-derived SFs. Significant functional similarities between SFs and VICs were revealed by RNA-seq analysis, demonstrating common cellular mechanisms underlying TNF-mediated arthritides and cardiac comorbidities.

Conclusions Comorbidheart valve disease and chronic polyarthritis are efficiently modelled in the Tg197 arthritis model and share common TNF/TNFR1-mediated, mesenchymal cell-specific aetiopathogenic mechanisms.

INTRODUCTION

Chronic inflammatory joint diseases are associated with articular inflammation leading to joint damage and increased mortality rates, which are mainly attributed to cardiovascular comorbidities.[1 2] Cardiac disease manifestations are detected in 70%–80% of patients with rheumatoid arthritis (RA) and spondyloarthritis (SpA) and symptoms can vary greatly, including arrhythmias, ischaemic heart failure as well as valvular diseases, such as valve insufficiency and stenosis.[3 4] The mechanisms mediating the co-occurrence of cardiac comorbidities in patients with chronic inflammatory joint diseases remain unknown.

The critical role of tumour necrosis factor (TNF) in RA and SpA pathologies is now well established both in transgenic animal models[5–8] and by the highly positive clinical responses of human patients to anti-TNF therapies.[9 10] Interestingly, recent studies in mice with deregulated TNF expression indicated a pivotal role of TNF also in cardiovascular diseases.[11–15] It, therefore, appears that TNF may commonly underlie arthritis and arthritis-related cardiac manifestations in human patients, which could also explain the amelioration of both of these comorbidities in patients treated with anti-TNF biologics.[16]

Mesenchymal cells are active participants in the structure and function of almost all tissues and contribute to their homeostasis.[17] The mesenchymal cells of the joint are the synovial fibroblasts (SFs).[18 19] Several studies have implicated SFs as key pathogenic cells, capable of initiating and driving the development of joint pathologies both in mouse models and human patients.[8 20 21] Interestingly, using TNF-driven models of comorbid arthritis and inflammatory bowel disease (IBD), we have previously established that TNF signals, uniquely operating in SFs or intestinal mesenchymal cells (IMCs), are sufficient to orchestrate the full pathogenic process of these two complex pathologies.[8] Yet another mesenchymal cell type, which is known to form the heart valves and is responsible for the maintenance of valve extracellular matrix structures, is the valve interstitial cells (VICs).[22–24] Recent *in vitro* studies have suggested that TNF can activate quiescent VICs into myofibroblasts inducing their pathogenic contribution to heart valve diseases (HVDs).[23 25] We have therefore hypothesised that the huTNF-driven, Tg197 model of arthritis[5] may exhibit heart valve pathology and that a common mesenchymal cell-specific TNF-mediated mechanism, operating on VICs, could explain the comorbidity.

We show here that Tg197 mice develop spontaneous left-sided heart valve pathology, characterised by extensive fibrosis and thickening of the aortic valve (AV) and mitral valve (MV) and associated with activated and hyperproliferating VICs. Valvular stenosis was associated with deterioration of cardiac function due to valvular degeneration and left ventricular (LV) dysfunction, simulating comorbid valvular diseases detected in patients with RA/SpA. Moreover, we show that this cardiac phenotype is ameliorated on Ab-mediated inhibition of TNF or by genetic mesenchymal-specific ablation of TNFR1. We further demonstrate that Tg197 VICs cultured *ex vivo* exhibit an activated phenotype characterised by increased huTNF production as well as increased proliferative and migratory capacities, similar to the one exhibited by arthritogenic SFs. Comparison of RNA-sequencing profiles between Tg197-derived SFs and VICs revealed similar pathogenic genes and pathways being activated in the two cell types. Overall, our studies establish a common TNF-driven mesenchymal cell-specific mechanism that may underlie aetiopathogenesis of comorbid joint and HVDs also in human patients.

MATERIALS AND METHODS

Mice

Tg197,[5] *ColVI-Cre*,[8] *Tnfr1*$^{fl/fl}$[26] and *Tnfr1*$^{cneo/cneo}$[27] mice were previously described; *Rosa26*$^{mT/mG}$ mice[28] were purchased from the Jackson Laboratories. Mice were maintained on a C57BL/6J or C57BL/6×CBA genetic background in the animal facilities of Biomedical Sciences Research Center (BSRC) 'Alexander Fleming' under SPF conditions. All animals were sacrificed at 11–12 weeks of age. Further details can be seen online in supplementary methods.

Antibodies

Antibodies used for immunohistochemistry, fluorescence-activated cell sorting (FACS) and immunofluorescence can be found in online supplementary methods.

Immunohistochemistry and immunofluorescence

Paraffin-embedded tissue sections and heart transverse optimal cutting temperature (OCT) cryosections were stained and evaluated according to protocols found in online supplementary methods.

Echocardiography and ECG

Echocardiography assessment and ECG were performed in the Department of Pharmacology, Medical School NKUA, Greece. Further details can be seen in online supplementary methods.

Isolation and culturing of SFs and VICs

SFs and VICs were isolated and cultured up to the third or fourth passage when they were used for cellular assays and sequencing. Detailed protocol is described in online supplementary methods.

FACS

See details in online supplementary methods.

Proliferation assay

To determine cellular proliferation, the Cell Proliferation ELISA, BrdU kit (Sigma-Aldrich) was used.

ELISA

Detection of hTNF was performed using the hTNF Quantikine Elisa (R&D Systems).

Wound-healing assay

To determine the migratory capacity of the cells, we used the wound-healing assay as described in online supplementary methods.

3′ RNA-sequencing and analysis

RNA-seq was performed in three biological replicates of cultured VICs and SFs isolated from Tg197 mice and WT littermates at their eighth week of age. Further analysis is found in online supplementary methods.

Statistical analysis

Data are presented as mean±SEM, and Student's t test was used for the evaluation of statistical significance, with P values <0.05 being considered statistically significant. Analysis was performed using the GraphPad Prism V.6.

RESULTS

TNF-dependent left-sided heart valve pathology develops as a comorbid condition in the Tg197 arthritis model

Histopathological evaluation of heart tissue from Tg197 animals revealed pathological alterations localised in the left side of the heart, affecting specifically the AV (figure 1A) and MV area (figure 1B), while the pulmonary valve as well as the blood arteries and vessels appeared unaffected (online supplementary figure S1,4). Pathology was associated with AV and MV thickening (figure 1C) mainly due to fibrosis, which extended to the root of the valve, as shown by the intense Masson's staining (figure 1A,B). Inflammation appeared to have only a minimal contribution, as indicated by the limited number of infiltrating inflammatory cells in the valves at 12 weeks of age (online supplementary figure S3).

Signs of heart valve pathology were detected in the Tg197 mice already from 4 weeks of age and became progressively worse as animals aged (online supplementary figure S4) in parallel to their arthritis pathology. By 8 weeks of age, when Tg197 mice had established arthritis, pathology in both valves was manifested with 100% penetrance and without a gender bias. Treatment of Tg197 animals with the anti-TNF infliximab (Remicade), from 4 to 11 weeks of age, resulted in the amelioration of the HVD, demonstrated by the decrease in valvular thickening and fibrosis (figure 1C and supplementary figure S2)

Heart valve pathology leads to LV dysfunction in the Tg197 animals

To assess whether the valvular thickening and fibrosis observed in Tg197 animals also affect their cardiac function, we performed echocardiography and ECG analysis in 12-week-old mice. Tg197 mice displayed increased AV and MV velocities (figure 1D), indicative of valvular stenosis. Moreover, in approximately 15% of the transgenic mice examined, aortic and/or mitral regurgitation was detected (online supplementary figure S5), suggesting valvular insufficiency. An additional consequence of the MV dysfunction was the observed increased atrial pressure leading to dilation of the left atrium (LA) (table 1). Echocardiography data analysis consistently showed that Tg197 animals displayed LV dilation with some degree of hypertrophy, indicated by the increased LV dimensions (LV end-diastolic diameter (LVEDd), LV end-systolic diameter (LVEDs), LV length in diastole (LVLd),

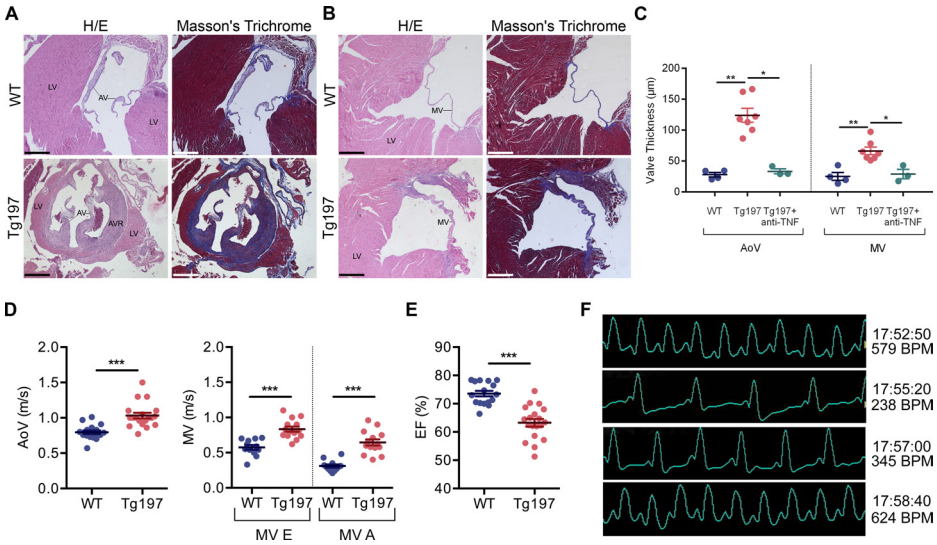

Figure 1 Tg197 arthritis model develops tumour necrosis factor (TNF)-dependent left-sided heart valve disease which leads to left ventricle (LV) dysfunction. (A, B) Representative images of H&E and Masson's trichrome-stained transverse heart sections showing the aortic valve (AV) (A) and the mitral valve (MV) (B) leaflets of Tg197 and WT littermate animals at 12 weeks old of age;(scale bar, 400 µm) (C) Comparison of the AoV and MV thickness between WT, Tg197 and Tg197 treated with anti-TNF infliximab (Remicade) animals at 11–12 weeks of age (data are presented as individual values, with mean±SEM; *P<0.02; **P<0.01). (D) Blood aortic (AoV) and mitral velocities (MV E and A) acquired by Doppler analysis of Tg197 mice and WT littermates at their 12 weeks of age (left and right panels, respectively; data are presented as individual values, with mean±SEM; ***P<0.0001). (E) Ejection fraction (EF%) of Tg197 mice and WT littermates at their 12 weeks of age, calculated by the modified Simpson equation, using 2D images in echocardiography analysis (data are presented as individual values, with mean±SEM; ***P<0.0001). (F) Representative ECGs of Tg197 animals with few minutes interval (four consecutive time points with ~1 min interval, starting from the upper panel), at their 12 weeks of age. AVR, aortic valve root; WT, wild type.

LV end-diastolic posterior wall thickness (LVPWd), end-diastolic interventricular septal thickness (IVSd)) and the significant increase of heart-to-body weight ratio compared to WT mice (table 1). Tg197 mice also exhibited significant reduction of the global cardiac function, as indicated by their reduced ejection fraction (EF%) (figure 1E) and, more importantly, by their reduced regional contractile function reflected in the lower systolic velocity of the posterior wall (SVPW) (table 1).

Interestingly, we have observed that Tg197 animals exhibit increased premature mortality of unknown aetiology starting at 10 weeks of age, reaching an ~50% incidence at 13 weeks of age (online supplementary figure S6). Notably, assessment of cardiac function of Tg197 animals showed that they were prone to exhibit fatal episodes of arrhythmias in advanced disease stages (12 weeks), mainly switching from bradycardia (~200 bpm) to tachycardia (~500–650 bpm) in a few minutes interval during ECG (figure 1F). Therefore, arrhythmic episodes could be associated with the premature deaths observed in Tg197 animals.

Collectively, our data show that the histopathological findings in Tg197 heart valves are associated with left-sided valvular degeneration and dysfunction and are accompanied by echocardiographic findings of LV cardiomyopathy.

Table 1 Echocardiographic parameters in Tg197 and WT mice at 12 weeks of age

	WT (n=16)	Tg197 (n=19)	P value
Body weight (g)	26.25±1.06	16.73±0.091	<0.0001
Heart weight (mg)	107.10±3.39	83.00±5.31	<0.0001
HW/BW (mg/g)	4.11±0.08	5.05±0.27	0.0054
LVEDd (mm/BW)	0.14±0.01	0.22±0.01	<0.0001
LVEDs (mm/BW)	0.08±0.01	0.14±0.01	<0.0001
LVLd (mm/BW)	0.28±0.01	0.38±0.01	<0.0001
LVPWd (mm/BW)	0.026±0.001	0.038±0.002	<0.0001
IVSd (mm/BW)	0.026±0.001	0.038±0.002	<0.0001
LA (mm/BW)	0.083±0.003	0.132±0.006	<0.0001
SVPW (cm/s)	3.02±0.08	2.14±0.07	<0.0001
E/A ratio	1.87±0.13	1.33±0.09	0.0009

Values were normalised with the body weight (except for SVPW), as indicated in the table. Data were expressed as mean±SEM.
E/A ratio, ratio between E (peak early diastolic flow) and A (peak late diastolic flow); HW/BW, heart weight-to-body weight ratio; IVSd, end-diastolic interventricular septal thickness; LA, left atrium; LVEDd, left ventricular end-diastolic diameter; LVEDs, left ventricular end-systolic diameter; LVLd, left ventricular length in diastole; LVPWd, left ventricular end-diastolic posterior wall thickness; SVPW: systolic velocity of the posterior wall.

Hypertrophic valves of Tg197 mice consist mainly of activated VICs

Since SFs have been previously established as drivers of arthritogenesis in the Tg197 model,[8] we investigated whether VICs play also a pathogenic role in the observed Tg197 heart valve pathology. To this end, we first crossed the reporter mouse *Rosa26*$^{mT/mG}$ which expresses green fluorescent protein (GFP) upon recombination, with the *ColVI-Cre* mouse, which has been previously used to target mesenchymal cells in the joints, small intestine,[8] colon[29] and other organs.[30] Examination of the heart valves of *ColVI-Cre-Rosa26*$^{mT/mG}$ mice revealed co-localisation of GFP expression with vimentin (figure 2A), a known marker of fibroblasts and VICs,[23 31] indicating efficient targeting of VICs by *ColVI-Cre*, and confirming their mesenchymal origin.[22] Efficient recombination was confirmed by further characterisation of GFP$^+$ cells derived from dissociated heart valve tissue from *ColVI-Cre-Rosa26*$^{mT/mG}$ mice using FACS analysis. GFP$^+$ cells strongly expressed VIC and mesenchymal cell markers (vimentin, CD29 and podoplanin), while displaying no expression of haematopoietic (CD45) and endothelial (CD31) markers

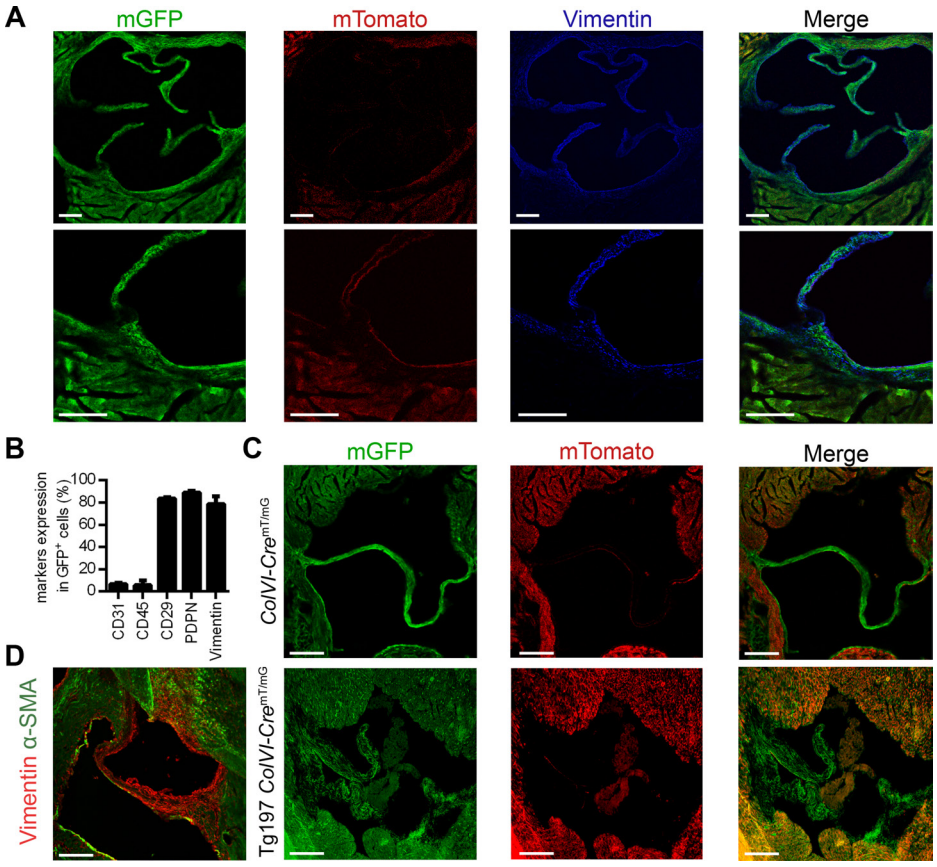

Figure 2 Heart valve disease of Tg197 mice is caused by accumulation of activated mesenchymal valve interstitial cells (VICs). (A) Representative images of transverse heart cryosections of *ColVI-Cre-Rosa26*$^{mT/mG}$ mice, at their 8 weeks of age, and colocalisation of GFP expression with vimentin expression in the heart valve (lower panel: higher magnification of the upper panel) (scale bar: 100 µm). (B) Fluorescence-activated cell sorting (FACS) analysis of ColVI-expressing cells (GFP$^+$) with markers for endothelial (CD31), haematopoietic (CD45) and fibroblast/mesenchymal cells (CD29, podoplanin [PDPN], vimentin) from dissociated heart valves of *ColVI-Cre-Rosa26*$^{mT/mG}$ mice, at their 8 weeks of age (data are presented as mean±SEM, n=3 from three individual experiments). (C) Representative images of transverse heart cryosections of *ColVI-Cre*$^{mT/mG}$ and Tg197 *ColVI-Cre*$^{mT/mG}$ mice at their 12 weeks of age (scale bar: 100 µm). (D) Representative image of transverse heart cryosections of Tg197 mice at their 12 weeks of age and colocalisation of smooth muscle actin (α-SMA) expression with vimentin expression in the heart valve and root (scale bar: 100 µm).

(figure 2B). These results suggest that the *ColVI-Cre* mouse effectively targets mainly vimentin$^+$, CD29$^+$ and podoplanin$^+$ mesenchymal-like VICs in the heart valve.

To explore the role of VICs in the Tg197 heart valve pathology, we crossed the *ColVI-Cre-Rosa26*$^{mT/mG}$ mice with Tg197 mice. The thickened fibrotic heart valves of these mice were mainly populated by GFP$^+$ VICs (figure 2C), supporting their central role in the heart valve phenotype. The pathogenic potential of VICs in Tg197 animals was further assessed by the expression of α-SMA, a well-established marker of activated myofibroblastic VICs.[32] Interestingly, α-SMA-expressing VICs were detected in the thickened valvular area and root of Tg197 mice (figure 2D), indicating that the pathology observed is mainly characterised by accumulation of activated VICs.

TNFR1 signalling in mesenchymal cells is necessary and sufficient for the development of Tg197 heart valve pathology

Having established the contribution of activated mesenchymal VICs and TNF dependency of the valvular hyperplasia in Tg197 mice, we further explored the role of mesenchyme-specific TNF signalling in the development of this pathology. To address whether TNF signalling in mesenchymal VICs is required for the development of heart valve pathology, Tg197 animals were crossed with *ColVI-Cre Tnfr1*$^{fl/fl}$ animals.[26] Tg197 *ColVI-Cre Tnfr1*$^{fl/fl}$ mice exhibited ameliorated heart valve pathology, as indicated by the lack of heart valve thickening and fibrosis (figure 3A, C). This finding suggests that TNF signalling, through TNFR1 in mesenchymal cells, is essential for the pathogenesis of HVD in the Tg197 model.

Next, we examined whether TNF signalling in mesenchymal cells was also sufficient to induce heart valve pathology in Tg197 mice. To this end, we crossed Tg197 with *ColVI-Cre Tnfr1*$^{cneo/cneo}$ mice to achieve specific reactivation of TNFR1 signalling only in mesenchymal cells.[27] Tg197 *ColVI-Cre Tnfr1*$^{cneo/cneo}$ mice developed valvular thickening and extensive fibrosis, while control Tg197 *Tnfr1*$^{cneo/cneo}$ did not show any signs of heart valve thickening and fibrosis (figure 3B,D), demonstrating that TNF signalling through TNFR1 in mesenchymal cells is sufficient to trigger heart valve pathology in Tg197 mice. Consequently, TNF signalling in the mesenchyme is both necessary and sufficient for the development of heart valve pathology in Tg197 animals.

Ex vivo-derived Tg197 VICs exhibit an activated phenotype

It is known that *ex vivo* human RA and mouse arthritogenic SFs exhibit increased proliferative and migratory capacities.[33–35] To investigate whether pathogenic VICs display a similar phenotype, we isolated VICs from Tg197 and WT animals at 8 weeks of age, when HVD is well established.

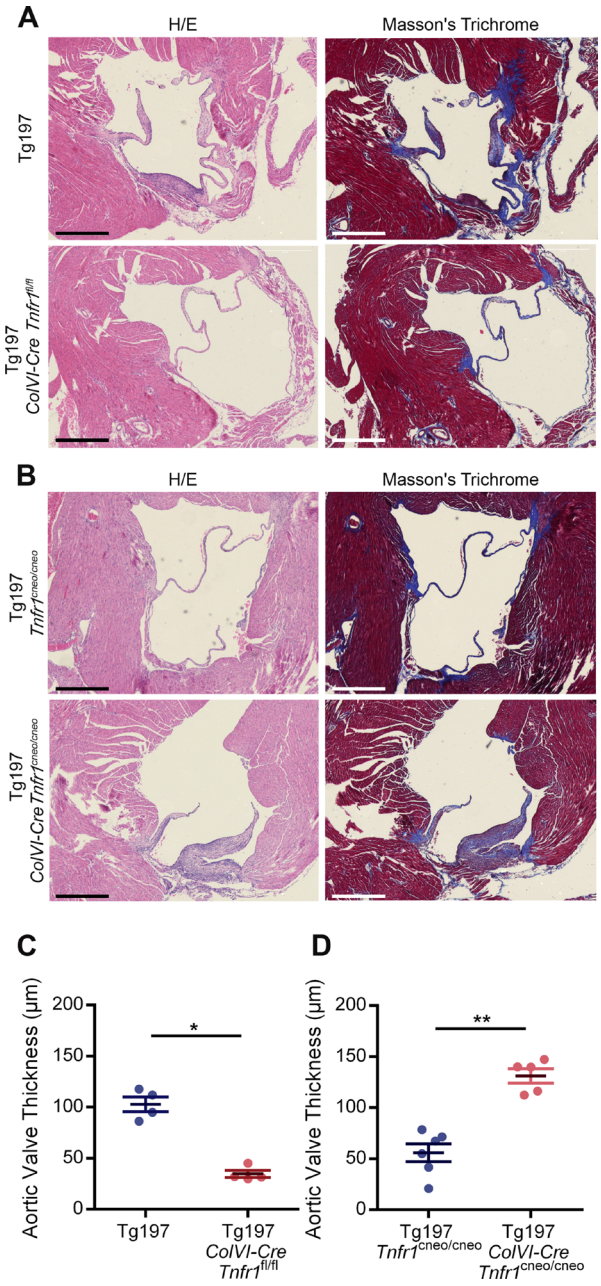

Figure 3 TNF signalling on valve interstitial cells (VICs) is required and sufficient for the development of heart valve disease of Tg197 animals. (A) Representative images of H&E and Masson's trichrome-stained transverse heart sections of Tg197 and Tg197 *ColVI-Cre Tnfr1*$^{fl/fl}$ and animals at 12 weeks of age (scale bar, 500 µm). (B) Representative images of H&E and Masson's trichrome-stained transverse heart sections of Tg197 *Tnfr1*$^{cneo/cneo}$ and Tg197 *ColVI-Cre Tnfr1*$^{cneo/cneo}$ and at 12 weeks of age (scale bar, 500 µm). (C) Comparison of the aortic valve thickness between Tg197 and Tg197 *ColVI-Cre Tnfr1*$^{fl/fl}$ animals at 12 weeks of age (data are presented as individual values, with mean± SEM; *P<0.03). (D) Comparison of the aortic valve thickness between Tg197 *Tnfr1*$^{cneo/cneo}$ and Tg197 *Tnfr1*$^{cneo/cneo}$ at 12 weeks of age (data are presented as individual values, with mean± SEM; **P<0.005).

We first confirmed the homogeneity of VICs cultures by characterising cultured VICs isolated from *ColVI-Cre-Rosa26*$^{mT/mG}$ animals. FACS analysis confirmed that approximately 80% of the isolated VICs were GFP^{+} and displayed high expression of known fibroblast and mesenchymal cell markers including CD29, vimentin, podoplanin, CD140a, CD90.2, CD105, vascular cell adhesion protein 1 (VCAM-1) and intercellular adhesion molecular 1 (ICAM-1) (figure 4A), while they lacked expression of haematopoietic (CD45) and endothelial (CD31) markers, thus preserving the observed *in vivo* expression marker profile (figure 2B).

We further assessed the activation status of Tg197-derived VICs. These cells were found to overexpress hTNF (figure 4B) and displayed increased proliferative and migratory capacities (figure 4C,D), similarly to Tg197-derived SFs.[34] Therefore, VICs are shown to exhibit an activated phenotype with similar characteristics to the one exhibited by the arthritogenic Tg197 SFs *ex vivo*.[33 34]

Tg197 VICs express common pathogenic signatures with Tg197 SFs

Arthritogenic SFs have been recently found to exhibit a distinct expression profile, characterised by pathogenic deregulation of genes affecting key pathways for the development of polyarthritis symptoms.[36] We, therefore, explored the commonalities of pathogenic Tg197 VICs and SFs at the gene expression, pathway and transcriptional regulation level. For this purpose, we isolated SFs and VICs from 8-week-old Tg197 animals, with established arthritis and HVD, and compared their expression profiles to those of SFs and VICs isolated from WT littermates by using RNA-sequencing.

Both Tg197 SFs and VICs displayed >500 significant differentially expressed genes (DEGs) compared to their WT controls (figure 5A). More specifically, a total of 408 and 381 genes were upregulated in Tg197 VICs and SFs, respectively, with almost 30% of them commonly upregulated in both cell types (figure 5B), while a total of 327 and 160 genes were downregulated in Tg197 VICs and SFs, respectively, with approximately 10% of them commonly downregulated in both cell types (figure 5B). Further functional enrichment analysis of the common upregulated genes placed immune and inflammatory responses, as well as nuclear factor (NF)-κB signalling at the top enriched pathways. Pathways enriched in the overlapping downregulated genes included extracellular matrix organisation and regulation of growth, indicating extracellular matrix (ECM) remodelling and deregulated cell growth (online supplementary figure S7).

To further explore the similarities of these two pathogenic cell types at the pathway level, functional enrichment analysis was performed for all DEGs in SFs and VICs. Interestingly, KEGG pathways enriched in SFs' and VICs' upregulated genes show a great overlap (60%) (figure 5C). These pathways were subsequently clustered into broader KEGG pathway categories. The most pronounced category was immune response, which included pathways such as chemokine and TLR signalling, while the most prominent correlation was to human 'rheumatoid arthritis' term, with known RA-related and cardiovascular disease-related genes (*Tnf*, *Il1b*[37] and *Acp5*[38]) being upregulated in both cell types. Other categories include cancer and infectious diseases, such as tuberculosis and pertussis which have also been associated with inflammation and TNF signalling. TNF and NF-κB signalling were also enriched in both cell types, with a distinct set of genes such as *Mmp9, Tnf, Il1b, Cxcl2;3;12, Ccl4 and Cd14* being upregulated in both Tg197 SFs and VICs (figure 5D). Interestingly, some of the functions enriched only in VICs' DEGs involve cardiovascular diseases, indicating the differences between VICs and SFs due to their different tissue of origin (online supplementary figure S7).

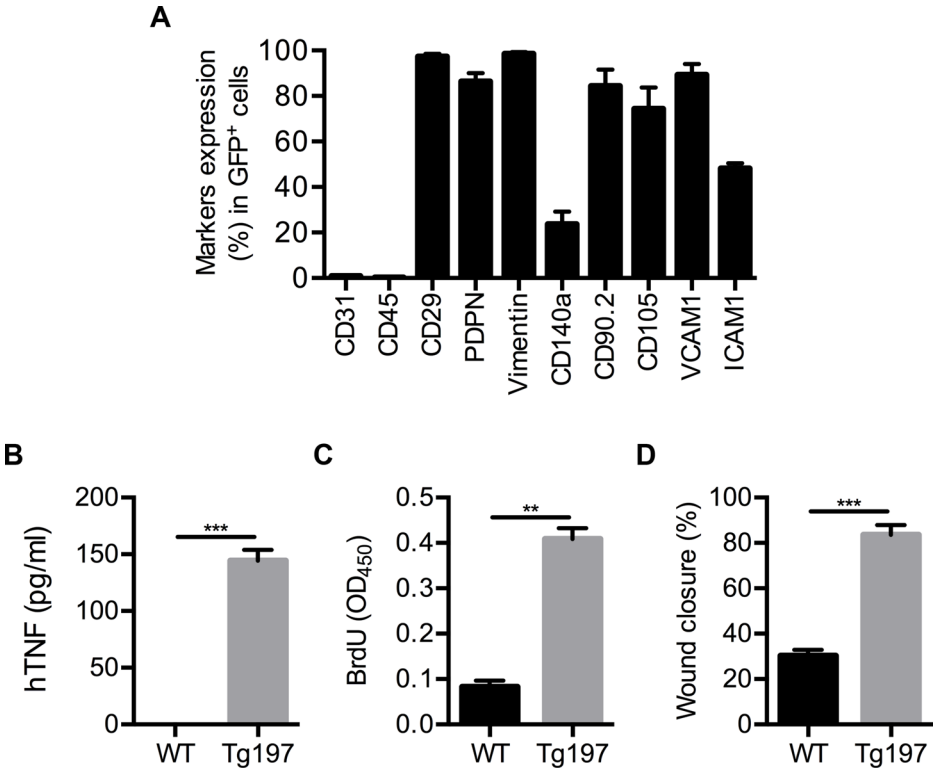

Figure 4 Activated phenotype of Tg197-derived valve interstitial cells (VICs) *ex vivo*. (A) Fluorescence-activated cell sorting (FACS) analysis of *ColVI*-expressing cells (GFP$^+$) with markers for endothelial (CD31), haematopoietic (CD45) and fibroblast/mesenchymal cells (CD29, podoplanin [PDPN], vimentin, CD140a, CD90.2, CD105, VCAM-1, ICAM-1) in isolated VICs from *ColVI-Cre-Rosa26*$^{mT/mG}$ mice at 8 weeks of age. (B–D) Levels of secreted hTNF in the supernatants (B), BrdU incorporation (C) and wound healing ability calculated by percentage of wound closure (D) of VICs isolated from WT and Tg197 mice at 8 weeks of age (data are presented as mean±SEM, n=3 from three individual experiments; **P<0.001; ***P<0.0005).

Furthermore, the RNEA tool,[39] which infers regulatory networks by predicting interactions between transcription factors and their target genes, was used to explore the similarities between VICs and SFs at the transcriptional regulation level. Regulatory networks were extracted from both cells' gene expression profile and their intersection is reported in figure 5E. Interestingly, *Sfpi1* and *Pparg*, which are known to regulate mesenchymal activation,[36] were revealed by this analysis as the two main common regulators of the two networks; *Tnf* was also found to be a central regulator. These findings strongly suggest that Tg197 VICs share a commonly altered expression profile with Tg197 SFs at the gene expression, functional pathways and transcriptional regulation circuit levels.

DISCUSSION

Patients with RA and SpA show a higher risk of developing associated cardiac diseases, which highly contribute to their increased mortality rates.[2] More specifically, they exhibit a 30% increased incidence of valvular pathologies, including non-specific valvular thickening and mild valve regurgitation.[3 40] Recent studies using sensitive imaging methods, such as transesophageal echocardiography, report an even greater prevalence of left-sided HVD in RA patients with valve thickening in half of the cases involving both mitral (47%) and aortic valves (32%) and valve regurgitation (21%).[41] The involvement of TNF in the pathogenesis of RA and SpA is well established; however, its role in the development of arthritis-related cardiac comorbidities remains unknown.

We demonstrate here that overexpression of TNF, in the TghuTNF (Tg197) arthritis model, in addition to the chronic polyarthritis[5] drives also the development of spontaneous left-sided HVD, which mainly leads to valvular thickening with some degree of stenosis and occasionally to valve insufficiency, comorbid pathologies often observed in patients with RA/SpA.[3 42] Interestingly, a similar left-sided heart valve pathology, exhibiting valvular thickening and fibrosis, was also observed in the TgA86, transmembrane TNF overexpressing, mouse model of SpA[6 43] (supplementary figure S8), further strengthening the pathogenic role of TNF in the development of arthritis-related cardiac comorbidities. The greater mechanical stress and haemodynamic pressures imposed on the left side of the heart is a likely explanation for the discrepancy between the diseased left-sided and unaffected right-sided valves, also observed in patients with RA/SpA.

AV stenosis and MV and/or AV regurgitation have been shown to result in LV hypertrophy with preserved EF and occasionally in LV dilation with some degree of contractile dysfunction.[44] Similarly, in the Tg197 model, valvular pathology contributes to the observed extensive LV dilation with some degree of LV hypertrophy as well as to the concomitant contractile dysfunction. However, additional mechanisms that have been proposed as contributing factors in the increased prevalence of global heart failure in patients with RA/SpA, such as myocardial fibrosis and oedema as well as arterial blood pressure, coronary heart disease and myocardial remodeling[45] remain to be studied for their contribution in the global heart impairment observed in Tg197 animals. We have also detected repeated arrhythmic episodes in Tg197 mice which could explain the premature sudden deaths observed in this model recapitulating the increased risk of sudden cardiac death experienced by patients with RA/SpA, due to atrial fibrillation and other types of tachyarrhythmias which suggest diffuse myocardial electrical instability.[46 47] Overall, our

Figure 5 Tg197 valve interstitial cells (VICs) exhibit common pathogenic molecular signatures with Tg197 synovial fibroblasts (SFs) at 8 weeks of age. (A) Volcano plots with the number of differentially expressed genes (DEGs) of Tg197 VICs and SFs compared to WT. (B) Venn diagram showing the overlap of DEGs in Tg197 VICs and SFs. (C) Venn diagram showing overlap of enriched KEGG pathways derived from functional enrichment analysis of upregulated DEGs in Tg1917 VICs and SFs. (D) Alluvial diagram illustrating overlapping KEGG pathways in Tg197 VICs and SFs, grouped according to their KEGG broader categories. (E) Intersection of regulatory networks of Tg197 VICs and SFs.

data demonstrate that the Tg197 arthritis model develops HVD and cardiac arrhythmias that closely mimic the cardiac clinical findings and premature mortality observed in patients with arthritis, supporting the value of this model in providing mechanistic insights into the pathogenesis of these comorbidities. The reversal of the cardiac phenotype by pharmacological inhibition of TNF in this model supports the vital role of TNF in the development of RA/SpA-related cardiac valvular comorbidities and suggests that anti-TNF therapy could also prevent cardiac comorbidities and avoid adverse cardiovascular side effects caused by other drugs, such as DMARDs.[2] Our findings also highlight the importance of regular echocardiographic screening on patients with RA and SpA.

The association between elevated TNF levels and valvular pathology has been previously suggested in other mutant mice.[14 15] Notably, these mice exhibit an inflammatory valvulitis, in contrast to the hypertrophic valves of Tg197 mice, which consist mainly of activated mesenchymal VICs. This discrepancy could be attributed to various factors, such as differences in the genetic background or in the cytokine imbalances driving the pathology. More specifically, the inflammatory phenotype of IL1Ra-deficient mice[14] has been observed in the inflammation-susceptible[48] BALB/c genetic background whereas in the C57 background they show milder pathology.[14] Additionally, pathology in the IL1Ra-[14] as well as in the TTP-deficient[15] and K/BxN transgenic[49] mice could be driven by diverse upstream mechanisms providing additional pathogenic cytokine disbalances apart from TNF.

Extensive characterisation and comparison of the transcriptional profiles of pathogenic Tg197 VICs and SFs, compared with their healthy counterparts, revealed a shared altered and pathogenic profile of these two cell types. Inflammatory and immune responses were among the commonly enriched KEGG pathways in both Tg197 SFs and VICs, supporting their activated and pathogenic status. Our analysis further supports the central role of *Tnf* in both cell types and pathologies. Interestingly, *Sfpi1*, an NF-κB modulator,[50] emerged as a common transcriptional regulator of both activated VICs and SFs, highlighting the importance of NF-κB signalling in this process, as was also confirmed by the enrichment of the NF-κB signalling pathway in both cell types. Moreover, *Sfpi1*, encoding the myeloid-specific transcription factor PU.1,[51] has been found to be upregulated in RA-FLS,[52] while being also implicated in the pathogenesis of heart hypertrophy.[53] Collectively, the centrality of *Sfpi1*, in combination with the enriched immune and TLR signalling, as well as NF-κB signalling pathways, in both Tg197 VICs and SFs could support their conversion to activated mesenchymal cells possessing pathogenic innate immune properties. This hypothesis is further supported by recent findings suggesting that Tg197 SFs undergo a metabolic reprogramming,[54] similar to the metabolic alterations reported in both inflammatory heart diseases and RA.[55 56] Therefore, we hypothesise that VICs and SFs become pathogenic on common TNF-induced metabolic reprogramming acquiring a detrimental innate phenotype, which should be further explored.

We finally show here that mesenchymal-specific TNF signalling, through TNFR1, is both required and sufficient for the development of heart valve pathology. Notably, SF-specific and IMC-specific TNFR1 signalling has been previously demonstrated to be causal in orchestrating comorbid polyarthritis and Crohn's-like IBD in a TNF overexpressing mouse model.[8] It may, therefore, be strongly postulated that mesenchymal cell responses to TNF explain complex chronic inflammatory disease comorbidities involving joint, intestinal and, as shown in the

present study, also cardiac pathologies. Future detailed insights into the molecular and cellular mechanisms commonly underlying aetiopathogenesis of mesenchymal cell-driven comorbidities, such as those expressed under the RA/SpA paradigm, may also offer novel approaches to therapeutically target common pathogenic processes.

Acknowledgements The authors are grateful to Dr Branko Simic, Professor Thomas F Lüscher and Dr Stelios Psarras for their scientific input and advice, as well as Dr Vaggelis Harokopos, Dr Panagiotis Moulos and the personnel of BSRC "Alexander Fleming" Genomics Facility for performing RNA-sequencing and and raw data analysis, Anna Katevaini and Christina Geka for histology, Michalis Meletiou for technical assistance and Ana Henriques for help in figure preparation.

Contributors GK, LN, MS, NK and MCD designed the study and interpreted the experimental results. LN, MS, PC and IM performed the experiments and data analysis. AP contributed to the data analysis. LN and MCD wrote the first draft of the manuscript and all authors were involved in critically revising its final preparation. All authors approved the final version to be published.

Funding This work has been funded by the IMI project BTCure (GA no. 115142-2), the Advanced ERC grant MCs-inTEST (340217), and a 'Research Project for Excellence IKY/Siemens' (GA no. 3288) to GK, an 'IKY fellowship of Excellence for postgraduate studies in Greece – Siemens program' to MS, the Operational Program "Competitiveness, Entrepreneurship and Innovation 2014-2020", co-financed by Greece and the European Union (European Regional Development Fund) (MIS 5002562-KRIPIS II) as well the grant GA 31354 (CodeAge) FP7 -PEOPLE-2011-ITN to LN. The authors also wish to thank the InfrafrontierGR Infrastructure (co-funded by the ERDF and Greek NSRF 2007-2013) for providing mouse hosting and phenotyping facilities, including histopathology, flow cytometry and advanced microscopy.

Competing interests None declared.

Provenance and peer review Not commissioned; externally peer reviewed.

REFERENCES

1 Dougados M, Soubrier M, Antunez A, *et al*. Prevalence of comorbidities in rheumatoid arthritis and evaluation of their monitoring: results of an international, cross-sectional study (COMORA). *Ann Rheum Dis* 2014;73:62–8.
2 Nurmohamed MT, Heslinga M, Kitas GD. Cardiovascular comorbidity in rheumatic diseases. *Nat Rev Rheumatol* 2015;11:693–704.
3 Corrao S, Messina S, Pistone G, *et al*. Heart involvement in rheumatoid arthritis: systematic review and meta-analysis. *Int J Cardiol* 2013;167:2031–8.
4 Biesbroek PS, Heslinga SC, Konings TC, *et al*. Insights into cardiac involvement in ankylosing spondylitis from cardiovascular magnetic resonance. *Heart* 2017;103:745–52.
5 Keffer J, Probert L, Cazlaris H, *et al*. Transgenic mice expressing human tumour necrosis factor: a predictive genetic model of arthritis. *Embo J* 1991;10:4025–31.
6 Alexopoulou L, Pasparakis M, Kollias G. A murine transmembrane tumor necrosis factor (TNF) transgene induces arthritis by cooperative p55/p75 TNF receptor signaling. *Eur J Immunol* 1997;27:2588–92.
7 Kontoyiannis D, Pasparakis M, Pizarro TT, *et al*. Impaired on/off regulation of TNF biosynthesis in mice lacking TNF AU-rich elements: implications for joint and gut-associated immunopathologies. *Immunity* 1999;10:387–98.
8 Armaka M, Apostolaki M, Jacques P, *et al*. Mesenchymal cell targeting by TNF as a common pathogenic principle in chronic inflammatory joint and intestinal diseases. *J Exp Med* 2008;205:331–7.
9 Smolen JS, Landewé R, Bijlsma J, *et al*. EULAR recommendations for the management of rheumatoid arthritis with synthetic and biological disease-modifying antirheumatic drugs: 2016 update. *Ann Rheum Dis* 2017;76:960–77.
10 Sieper J, Poddubnyy D. New evidence on the management of spondyloarthritis. *Nat Rev Rheumatol* 2016;12:282–95.
11 Kubota T, McTiernan CF, Frye CS, *et al*. Dilated cardiomyopathy in transgenic mice with cardiac-specific overexpression of tumor necrosis factor-alpha. *Circ Res* 1997;81:627–35.
12 Bryant D, Becker L, Richardson J, *et al*. Cardiac failure in transgenic mice with myocardial expression of tumor necrosis factor-alpha. *Circulation* 1998;97:1375–81.
13 Sivasubramanian N, Coker ML, Kurrelmeyer KM, *et al*. Left ventricular remodeling in transgenic mice with cardiac restricted overexpression of tumor necrosis factor. *Circulation* 2001;104:826–31.
14 Isoda K, Matsuki T, Kondo H, *et al*. Deficiency of interleukin-1 receptor antagonist induces aortic valve disease in BALB/c mice. *Arterioscler Thromb Vasc Biol* 2010;30:708–15.
15 Ghosh S, Hoenerhoff MJ, Clayton N, *et al*. Left-sided cardiac valvulitis in tristetraprolin-deficient mice: the role of tumor necrosis factor alpha. *Am J Pathol* 2010;176:1484–93.
16 Roubille C, Richer V, Starnino T, *et al*. The effects of tumour necrosis factor inhibitors, methotrexate, non-steroidal anti-inflammatory drugs and corticosteroids on cardiovascular events in rheumatoid arthritis, psoriasis and psoriatic arthritis: a systematic review and meta-analysis. *Ann Rheum Dis* 2015;74:480–9.
17 Hay ED. The mesenchymal cell, its role in the embryo, and the remarkable signaling mechanisms that create it. *Dev Dyn* 2005;233:706–20.
18 Kontoyiannis D, Kollias G. Fibroblast biology. Synovial fibroblasts in rheumatoid arthritis: leading role or chorus line? *Arthritis Res* 2000;2:342–3.
19 Pap T, Müller-Ladner U, Gay RE, *et al*. Fibroblast biology. Role of synovial fibroblasts in the pathogenesis of rheumatoid arthritis. *Arthritis Res* 2000;2:361–7.
20 Bottini N, Firestein GS. Duality of fibroblast-like synoviocytes in RA: passive responders and imprinted aggressors. *Nat Rev Rheumatol* 2013;9:24–33.
21 Karouzakis E, Gay RE, Gay S, *et al*. Epigenetic control in rheumatoid arthritis synovial fibroblasts. *Nat Rev Rheumatol* 2009;5:266–72.
22 Nomura A, Seya K, Yu Z, *et al*. CD34-negative mesenchymal stem-like cells may act as the cellular origin of human aortic valve calcification. *Biochem Biophys Res Commun* 2013;440:780–5.
23 Liu AC, Joag VR, Gotlieb AI. The emerging role of valve interstitial cell phenotypes in regulating heart valve pathobiology. *Am J Pathol* 2007;171:1407–18.
24 Wang H, Sridhar B, Leinwand LA, *et al*. Characterization of cell subpopulations expressing progenitor cell markers in porcine cardiac valves. *PLoS One* 2013;8:e69667.
25 Yu Z, Seya K, Daitoku K, *et al*. Tumor necrosis factor-α accelerates the calcification of human aortic valve interstitial cells obtained from patients with calcific aortic valve stenosis via the BMP2-Dlx5 pathway. *J Pharmacol Exp Ther* 2011;337:16–23.
26 Van Hauwermeiren F, Armaka M, Karagianni N, *et al*. Safe TNF-based antitumor therapy following p55TNFR reduction in intestinal epithelium. *J Clin Invest* 2013;123:2590–603.
27 Victoratos P, Lagnel J, Tzima S, *et al*. FDC-specific functions of p55TNFR and IKK2 in the development of FDC networks and of antibody responses. *Immunity* 2006;24:65–77.
28 Muzumdar MD, Tasic B, Miyamichi K, *et al*. A global double-fluorescent Cre reporter mouse. *Genesis* 2007;45:593–605.
29 Koliaraki V, Pasparakis M, Kollias G. IKKβ in intestinal mesenchymal cells promotes initiation of colitis-associated cancer. *J Exp Med* 2015;212:2235–51.
30 Prados A, Kollias G, Koliaraki V. CollagenVI-Cre mice: a new tool to target stromal cells in secondary lymphoid organs. *Sci Rep* 2016;6:33027.
31 Rabkin-Aikawa E, Farber M, Aikawa M, *et al*. Dynamic and reversible changes of interstitial cell phenotype during remodeling of cardiac valves. *J Heart Valve Dis* 2004;13:841–7.
32 Chester AH, Taylor PM. Molecular and functional characteristics of heart-valve interstitial cells. *Philos Trans R Soc Lond B Biol Sci* 2007;362:1437–43.
33 Vasilopoulos Y, Gkretsi V, Armaka M, *et al*. Actin cytoskeleton dynamics linked to synovial fibroblast activation as a novel pathogenic principle in TNF-driven arthritis. *Ann Rheum Dis* 2007;66(Suppl 3):iii23–iii28.
34 Aidinis V, Plows D, Haralambous S, *et al*. Functional analysis of an arthritogenic synovial fibroblast. *Arthritis Res Ther* 2003;5:R140–R157.
35 Ritchlin C. Fibroblast biology. Effector signals released by the synovial fibroblast in arthritis. *Arthritis Res* 2000;2:356–60.
36 Ntougkos E, Chouvardas P, Roumelioti F, *et al*. Genomic responses of mouse synovial fibroblasts during tumor necrosis factor-driven arthritogenesis greatly mimic those in human rheumatoid arthritis. *Arthritis Rheumatol* 2017;69:1588–600.
37 El Bakry SA, Fayez D, Morad CS, *et al*. Ischemic heart disease and rheumatoid arthritis: Do inflammatory cytokines have a role? *Cytokine* 2017;96:228–33.
38 Janckila AJ, Nakasato YR, Neustadt DH, *et al*. Disease-specific expression of tartrate-resistant acid phosphatase isoforms. *J Bone Miner Res* 2003;18:1916–9.
39 Chouvardas P, Kollias G, Nikolaou C. Inferring active regulatory networks from gene expression data using a combination of prior knowledge and enrichment analysis. *BMC Bioinformatics* 2016;17(Suppl 5):181.
40 Ozkan Y. Cardiac Involvement in ankylosing spondylitis. *J Clin Med Res* 2016;8:427–30.
41 Roldan CA, DeLong C, Qualls CR, *et al*. Characterization of valvular heart disease in rheumatoid arthritis by transesophageal echocardiography and clinical correlates. *Am J Cardiol* 2007;100:496–502.
42 Voskuyl AE. The heart and cardiovascular manifestations in rheumatoid arthritis. *Rheumatology* 2006;45(Suppl 4):iv4–iv7.
43 Vieira-Sousa E, van Duivenvoorde LM, Fonseca JE, *et al*. Review: animal models as a tool to dissect pivotal pathways driving spondyloarthritis. *Arthritis Rheumatol* 2015;67:2813–27.

44 Chandrasekhar J, Dangas G, Mehran R. Valvular heart disease in women, differential remodeling, and response to new therapies. *Curr Treat Options Cardiovasc Med* 2017;19:74.
45 Lazúrová I, Tomáš Ľ. Cardiac impairment in rheumatoid arthritis and influence of anti-TNFα treatment. *Clin Rev Allergy Immunol* 2017;52:323–32.
46 Lazzerini PE, Capecchi PL, Acampa M, *et al*. Arrhythmic risk in rheumatoid arthritis: the driving role of systemic inflammation. *Autoimmun Rev* 2014;13:936–44.
47 Kazmierczak J, Peregud-Pogorzelska M, Biernawska J, *et al*. Cardiac arrhythmias and conduction disturbances in patients with ankylosing spondylitis. *Angiology* 2007;58:751–6.
48 Glass AM, Coombs W, Taffet SM. Spontaneous cardiac calcinosis in BALB/cByJ mice. *Comp Med* 2013;63:29–37.
49 Binstadt BA, Hebert JL, Ortiz-Lopez A, *et al*. The same systemic autoimmune disease provokes arthritis and endocarditis via distinct mechanisms. *Proc Natl Acad Sci U S A* 2009;106:16758–63.
50 Haimovici A, Humbert M, Federzoni EA, *et al*. PU.1 supports TRAIL-induced cell death by inhibiting NF-κB-mediated cell survival and inducing DR5 expression. *Cell Death Differ* 2017;24:866–77.
51 Rosenbauer F, Wagner K, Kutok JL, *et al*. Acute myeloid leukemia induced by graded reduction of a lineage-specific transcription factor, PU.1. *Nat Genet* 2004;36:624–30.
52 Itoh K, Nagatani K. Rheumatoid arthritis fibroblast-like synoviocytes show the upregulation of myeloid cell specific transcription factor PU.1 and B cell specific transcriptional co-activator OBF-1, and express functional BCMA. *Arthritis Res Ther* 2012;14:P28.
53 Tang Y, Yu S, Liu Y, *et al*. MicroRNA-124 controls human vascular smooth muscle cell phenotypic switch via Sp1. *Am J Physiol Heart Circ Physiol* 2017;313:H64 1–H649.
54 Michopoulos F, Karagianni N, Whalley NM, *et al*. Targeted metabolic profiling of the Tg197 mouse model reveals itaconic acid as a marker of rheumatoid arthritis. *J Proteome Res* 2016;15:4579–90.
55 Shirai T, Nazarewicz RR, Wallis BB, *et al*. The glycolytic enzyme PKM2 bridges metabolic and inflammatory dysfunction in coronary artery disease. *J Exp Med* 2016;213:337–54.
56 Kim S, Hwang J, Xuan J, *et al*. Global metabolite profiling of synovial fluid for the specific diagnosis of rheumatoid arthritis from other inflammatory arthritis. *PLoS One* 2014;9:e97501.